CHAPTER 2 TDIP SURVEY

2-1 Objectives

The TDIP (Time Domain Induced Polarization) survey was carried out in order to extract mineralized zones in the potential area delineated by geological and airborne magnetic survey in Phase I and II of this project.

2-2 Survey Locations and Specifications

The survey areas were Khujiriin gol area, Zuukhiin gol area, Danbatseren east area and Tsagaan chuluut west area located respectively to the west-northwest, north, southwest and northwest of Erdenet Mine. The distance from Erdenet Mine is about 45km to Khujiriin gol area, about 25km to Zuukhiin gol area and about 20km to Tsagaan chuluut west area. In Danbatseren east area, the potential area was narrowed down to three small areas(Danbatseren east 1, 3 and 4 areas) based on the result of airborne magnetic survey. Table II-2-1 shows the coordinates of the survey areas.

Table II-2-1 Coordinate of the survey area

Area	UTM coordinate of the corners		Area	UTM coordinate of the corners	
	East	North		East	North
Khujiriin gol	390860	5445450	Danbatseren east-4	415340	5414120
	396250	5445450		417300	5414120
	396250	5438150		417300	5412640
	390860	5438150		420230	5412640
Zuukhiin gol	440550	5454660		420230	5409000
	447050	5454660		416320	5409000
	447050	5448150		416320	5407690
	440550	5448150		414235	5407690
Danbatseren east-1	425580	5402440		414235	5410000
	427780	5402440		415340	5410000
	427780	5399620	Tsagaan chuluut west	417040	5439730
	425580	5399620		423520	5439730
Danbatseren east-3	412210	5412650		423520	5435730
	414240	5412650		417040	5435730
	414240	5410450			
	412210	5410450			

The IP data were taken along lines by keeping a potential dipole of 200m with a separation factor from 1 to 5. Table II-2-2 shows amounts of TDIP survey.

Table II-2-2 Amounts of TDIP survey

Area	Number of lines	Total length	Number of points
Khujiriin gol	3.0km × 4 lines	12.0km	220
Zuukhiin gol	3.0km × 9 lines 4.0km × 3 lines	39.0km	735
Danbatseren east-1	3.0km × 2 lines	6.0km	110
Danbatseren east-3	5.0km × 1 lines	5.0km	105
Danbatseren east-4	3.0km × 2 lines	6.0km	110
Tsagaan chuluut west	2.4km × 1 lines	2.4km	40
Total	22 lines	70.4km	1320

Resistivity as well as chargeability values of rocks and core samples were also measured in the laboratory

2-3 Survey Method

2-3-1 Procedures

The Induced Polarization survey was carried out by using a time-domain method with a dipole-dipole electrode configuration. The electrode configuration was arranged so that the measurements were taken every 200m along the lines by using a separation factor from 1 to 5. In the measurement, the current was injected into the earth through current electrodes and the resulting voltage was measured across potential electrodes. Fig. Ⅱ-2-1 shows the array utilized as well as the location of the plotting points.

In the TDIP surveys, the current is turned on for a certain length of time (on-time) then turned off (off-time). The transmitted waveform is then repeated with current flow in opposite direction. The pair of positive and negative on-off waveforms constitutes a cycle, which in this survey lasted 8 seconds, as indicated in Fig. Ⅱ-2-2. According to Fig. Ⅱ-2-3, the polarization of the target creates a transient decay voltage and its corresponding changing response is observed in the received waveform.

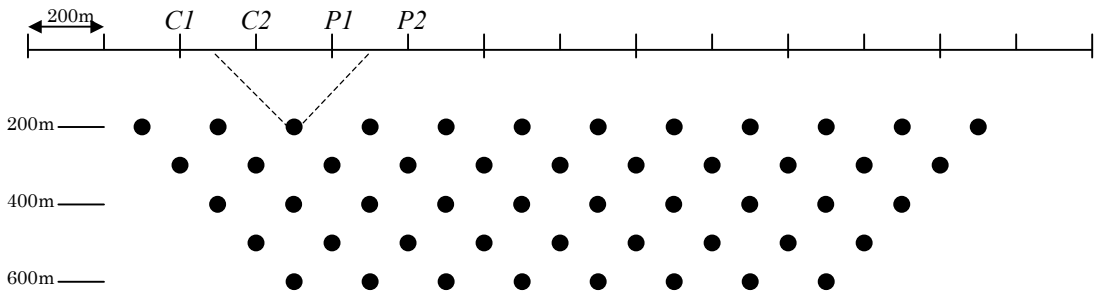

Fig. II-2-1　Dipole-dipole array and plotting procedure

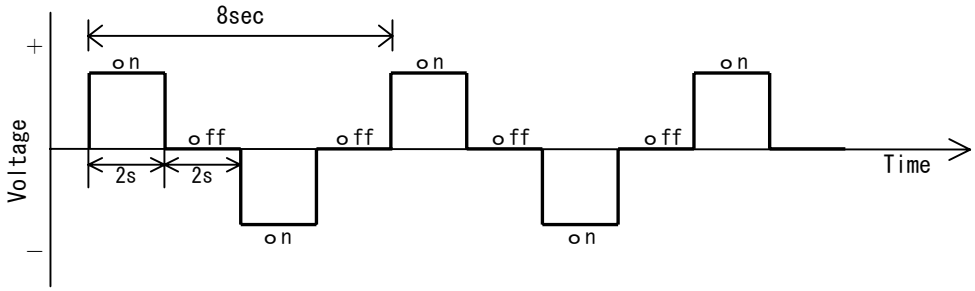

Fig. II-2-2　Waveform produced by the transmitter

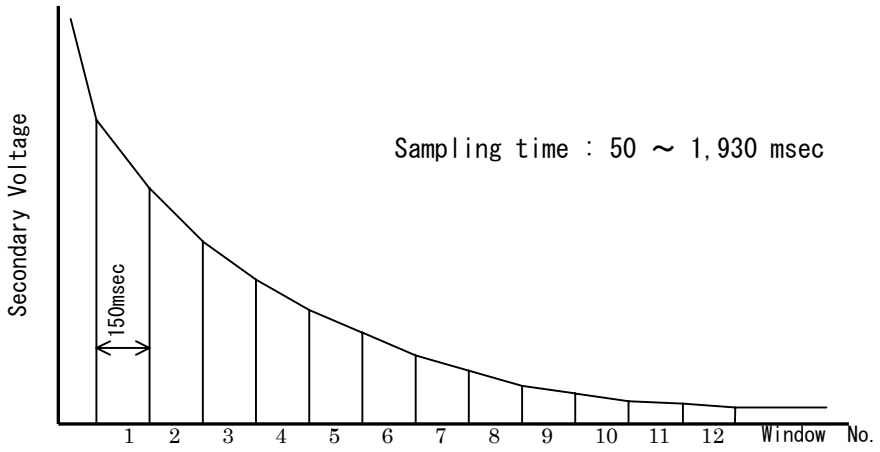

Fig. II-2-3　Sampling interval of the TDIP

2-3-2 Instrumentation

The instrumentation used for the time-domain IP survey is described in the Table Ⅱ - 2-3.

Table II-2-3 Specifications of TDIP survey instruments

Receiver	**Zonge GDP-16**
Frequency range	DC to 8KHz
Number of channels	8
Maximum input voltage	±32V
Detectable signal	1μV
Transmitter	**CH-95A**
Output Power	2Kw,800v,12A
Maximum Current	10A
Generator	**Geonics GPU2000**
Maximum output	2Kw
Output Voltage	200V
Output Frequency	400Hz

2-4 Analysis Method

2-4-1 Data processing

The TDIP data processing involves the determination of 3 parameters, i.e., apparent resistivity, chargeability as well as metal factor. The first 2 parameters are calculated directly by the receiver unit during data acquisition. The third one is calculated as a simple relation between the first 2 parameters. These 3 parameters are calculated as follows:

a) Apparent resistivity (ρ)

$$\rho = K\frac{V_P}{I},$$

where $K = \pi an(n+1)(n+2)$, Vp is the received voltage in volts, a is the A-spacing in meters, n is the separation factor and I is the transmitted current in amperes.

b) Chargeability (M)

$$M = \frac{1.87}{V_P}\int_{t_1}^{t_2} V_s dt,$$

where Vp is the primary voltage in volts and Vs is the secondary voltage in millivolts. Here, the secondary voltage is calculated from 450msec. to 1,100msec.

c) Metal factor (*MF*)

$$MF = \frac{M}{\rho} \times 100,$$

where ***M*** is the chargeability (mV/V) and ρ the apparent resistivity (Ωm)

2-4-2 Topographic corrections

Since the apparent resistivity is calculated here as a function of the location of the current and potential electrodes on a half-infinite plane, and is affected by topography depending on the location of the electrodes. For the case of a dipole-dipole configuration, the apparent resistivity appears to be high beneath a hill and low beneath a valley. On the other hand, the chargeability values are less affected by topography.

In order to make the appropriate corrections for the present survey, the topographic correction is calculated for each survey line by using 2D finite element method (FEM). The corrected apparent resistivity values are then used to construct the related sections and plane maps.

2-4-3 Pseudo-sections and plane maps

After topographic corrections, apparent resistivity, chargeability and metal factor pseudo-sections are made for every line of the survey. Plane maps of the above mentioned 3 parameters are also made for every separation factor.

It is normal to plot the measured results as conventional pseudo-sections so that preliminary interpretations can be made. This is also important for assessing data quality. Anomalies having high chargeability are easily observed but caution should be taken to directly infer the location and depth by simple inspection of the pseudo-section.

2-4-4 Two-dimensional analysis

The pseudo-sections do not show the real image of subsurface structure. In order to estimate the subsurface structure from TDIP data, we applied a 2-D quantitative analysis method to the measured data, consisting of forward calculations using FEM and inversion calculations using non-linear least square method.

In order to make the model calculations, the subsurface structure is divided into many small blocks, each of them having initially assigned their own chargeability and resistivity value. The size of the blocks are relatively small at the shallower part, but large at the deeper part.

Theoretical values are calculated from the block models using FEM, and the parameter of each block is made to change until the difference between the theoretical value and measured value is sufficiently small.

2-5 Survey Results

2-5-1 Khujiriin gol area

(1) Lines location

Fig.II-2-4 shows the location of the TDIP lines in Khujiriin gol area. 4 lines of 3.0km long each were set up along N0°E. Total line length is 12.0km.

(2) Results

Figs.II-2-5 ~ II-2-7 show the pseudo-sections, while Figs.II-2-8 ~ II-2-10 indicate the plane maps from n=1 to 5.

In this area, the apparent resistivity value ranges between 217 ~ 3050Ωm, and average is 836Ωm. Low resistivity zones are distributed along the direction of E-W, and are corresponds to the area underlain by Quaternary sediments. High resistivity above 1000Ωm is distributed widely from n=2 to 5 on the north side of the station 14 and on the south side of the station 8 on the line B and is also recognized at the north part of the other lines. According to the plane maps, high resistivity zone is distributed in the mountain area on the east side of the stream running through the eastern part of the area from north to south. The plane maps from n=3 to 5 show that this high resistivity zone extends westward in the north part of this area.

The chargeability value ranges between 1.4 and 10.6mV/V, and average is 5.4mV/V. No remarkable high chargeability anomaly such as to indicate existence of porphyry copper deposit is detected. Slightly high chargeability above 10mV/V is recognized at deeper part on the lines A and C.

The maximum value of metal factor is 2.1, and no remarkable anomaly is recognized.

(3) 2-D analysis

Figs.II-2-11 ~ II.2-14 show the 2-D analysis sections and plane maps.

The analyzed resistivity value ranges between 82 ~ 11kΩm, and average is 1270Ωm. According to the plane map at the depth of 50m, low resistivity under 500Ωm is distributed at the area underlain by Quaternary sediments, and high resistivity is distributed at the mountain area. The plane maps below the depth of 150m show high resistivity distributed widely in the east part of the area. The resistivity structure changes greatly on the east and west of the stream running through the eastern part of the area from north to south. Below the depth of 300m, the high resistivity extends westward around the stations 14 to 16 on each line. The section of the line A shows high resistivity zone inclining to north.

The analyzed chargeability value ranges between 1.6 ~ 16.7mV/V and, average is 6.2mV/V. In

the western part of the area, high chargeability anomaly zone inclining to north is distributed continuously to deeper part below the depth of 200m around the stations 12 to 16 on the lines A and E. This high chargeability zone is seemed to continue eastward, but on the lines C and B, the center of high chargeability is located at the depth of 300 to 400m around the stations 14 to 18, and continuity to deeper part is not recognized. High chargeability is also distributed at the deep part of the stations 24 to 26 on the line A.

Metal factor value is almost under 4, and no remarkable anomaly is recognized.

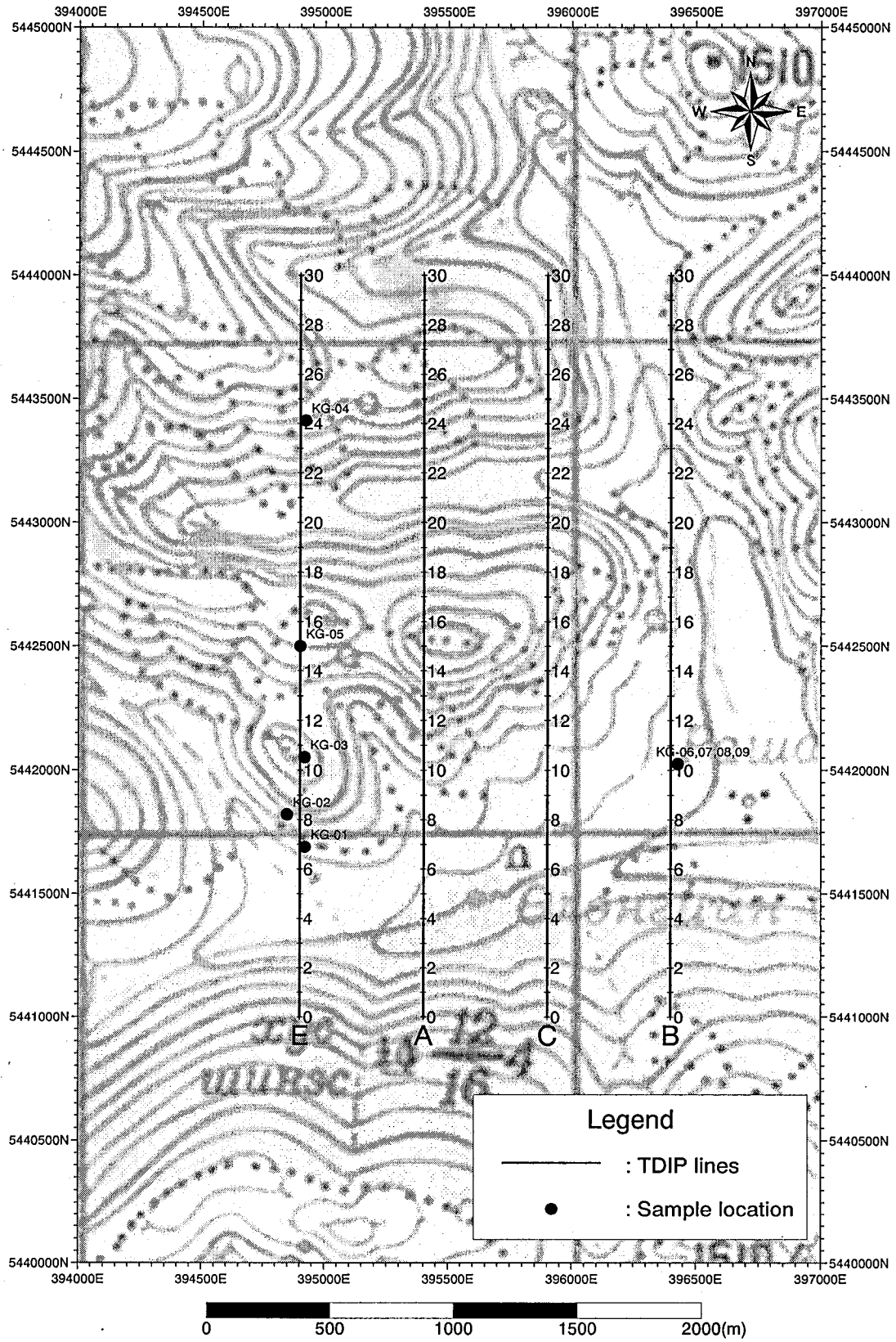

Fig. II-2-4 Geophysical survey location in Khujiriin gol area

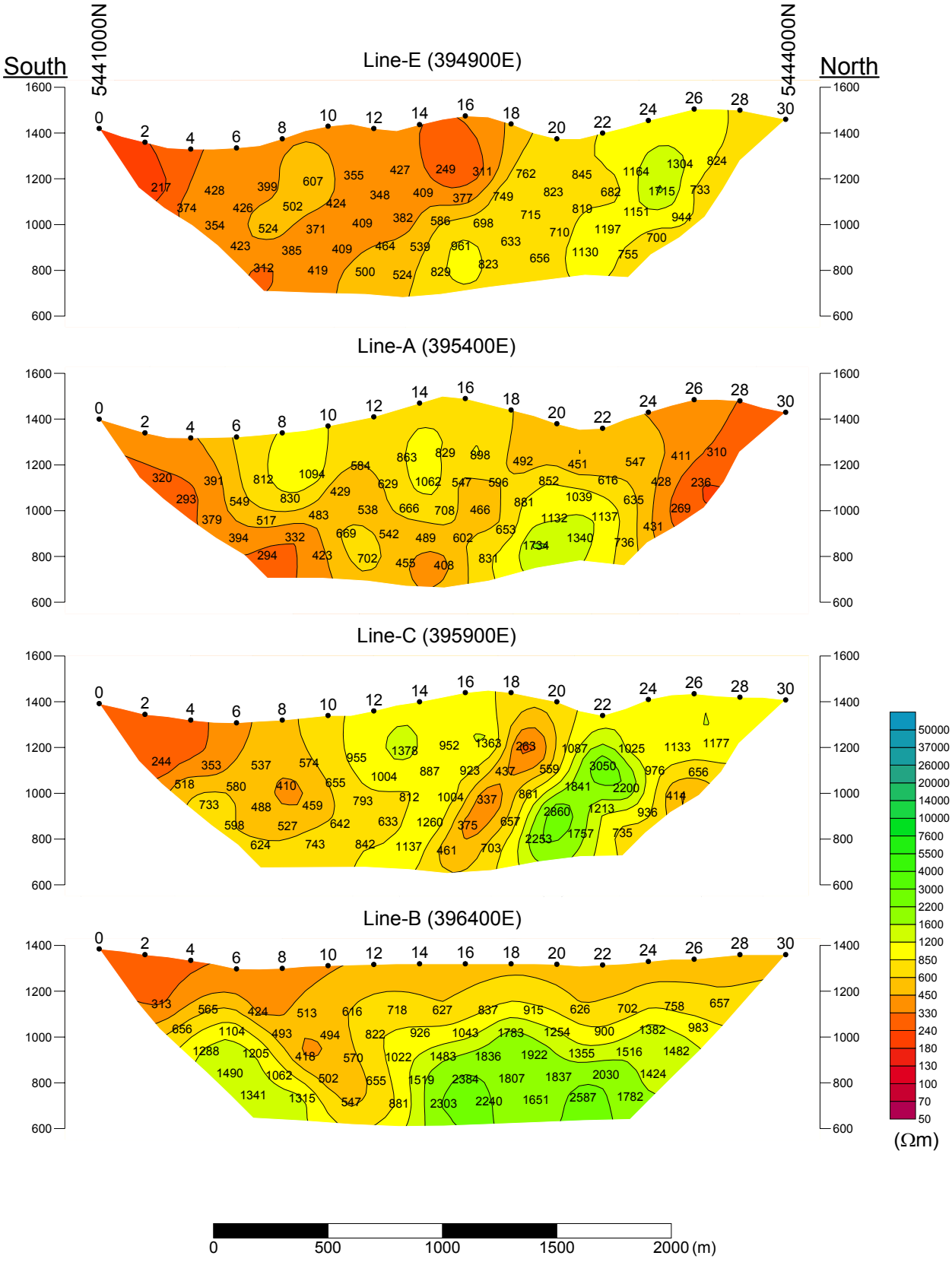

Fig. II-2-5 Apparent resistivity pseudo-sections in Khujiriin gol area

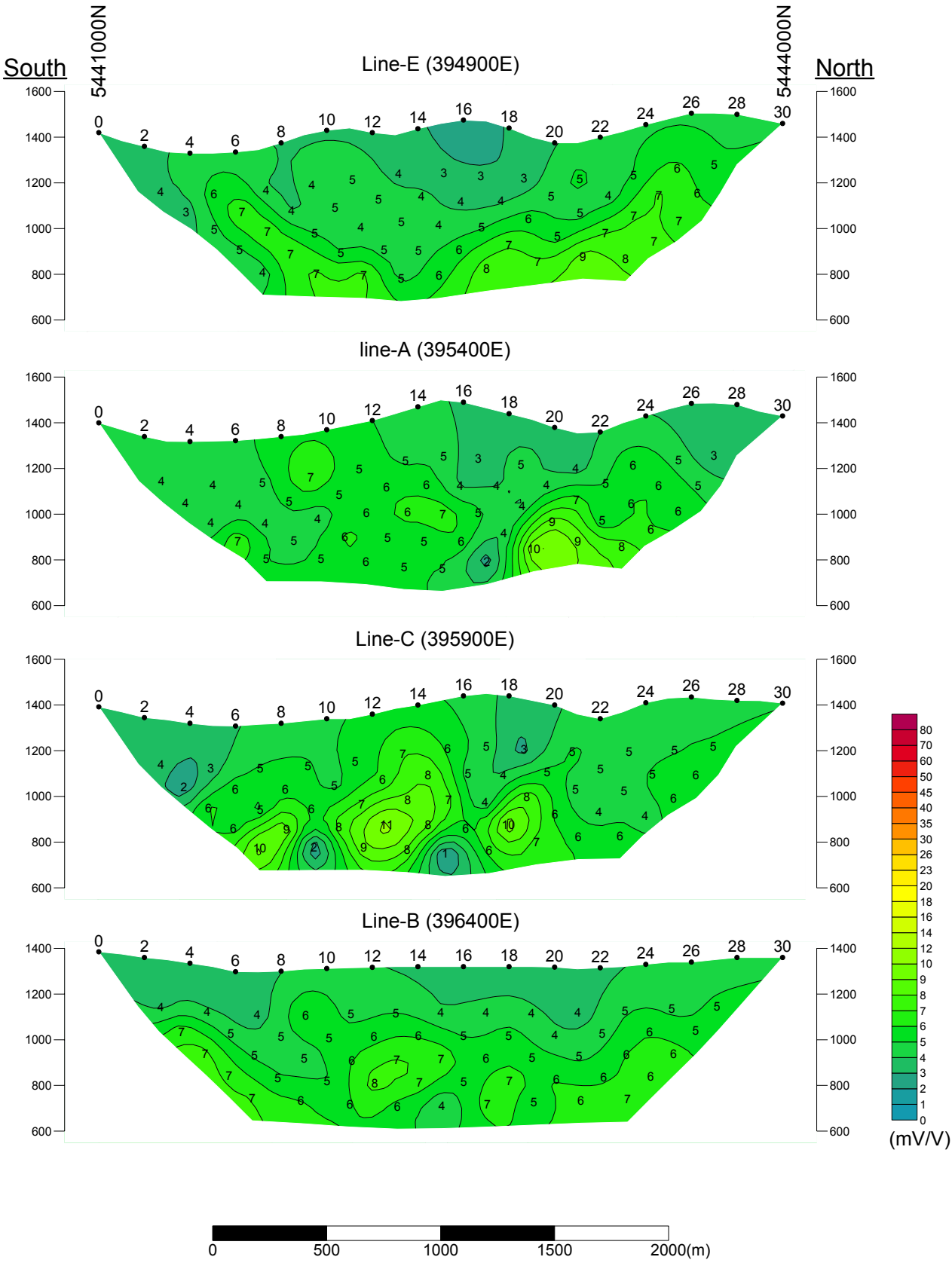

Fig. II-2-6 Chargeability pseudo-sections in Khujiriin gol area

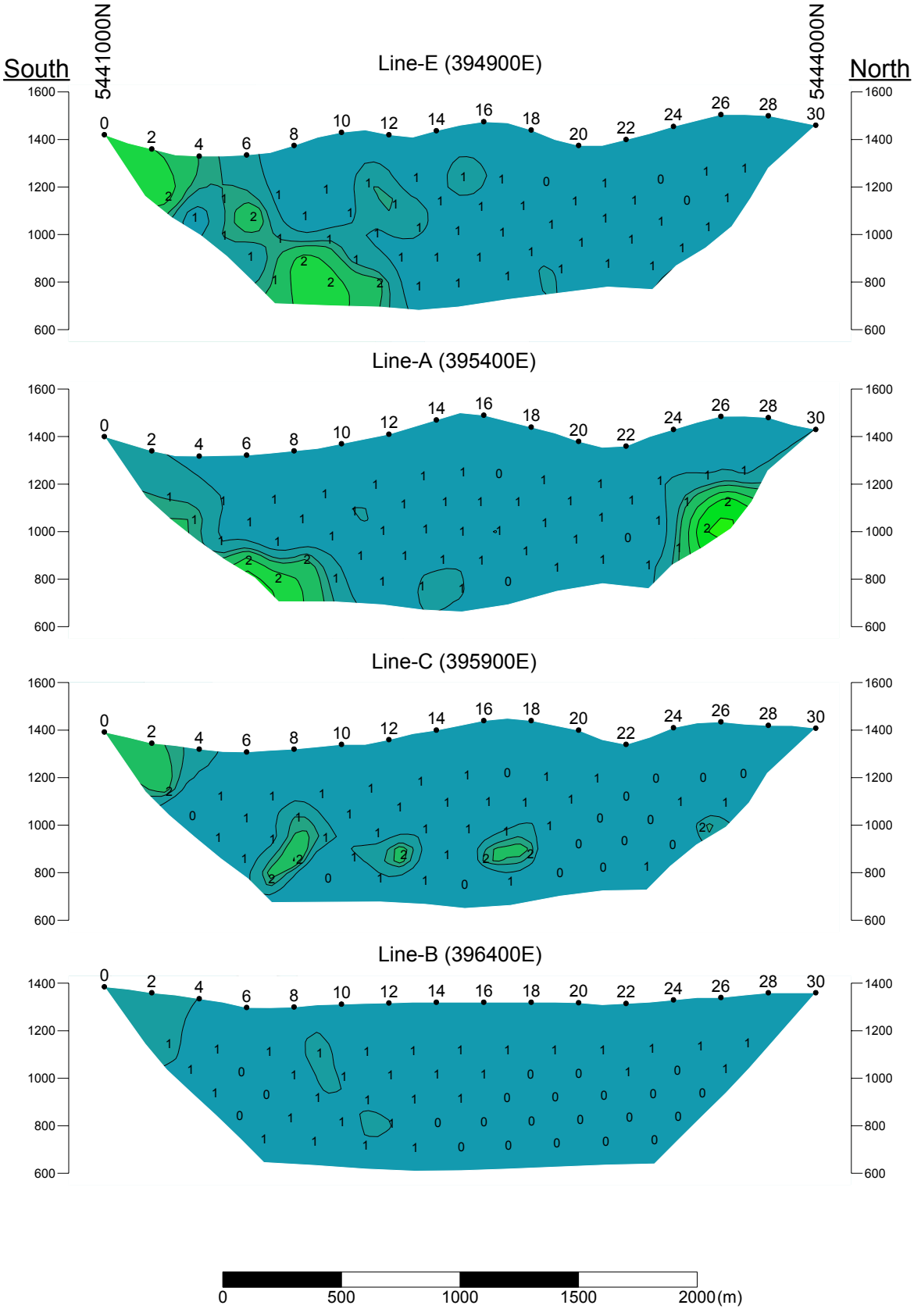

Fig. II-2-7 Metal factor pseudo-sections in Khujiriin gol area

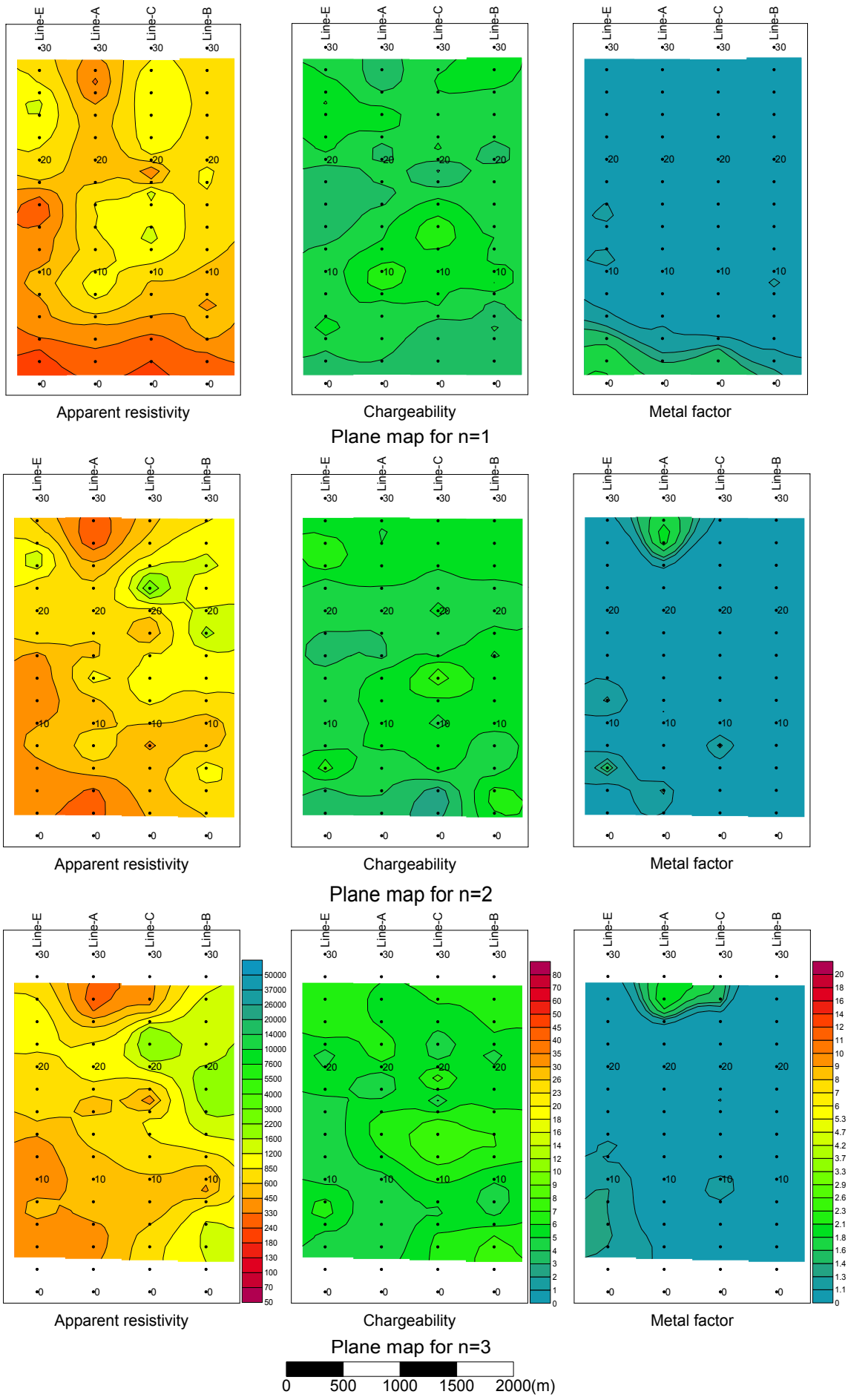

Fig. II-2-8 TDIP plane map for n=1, 2 and 3 in Khujiriin gol area

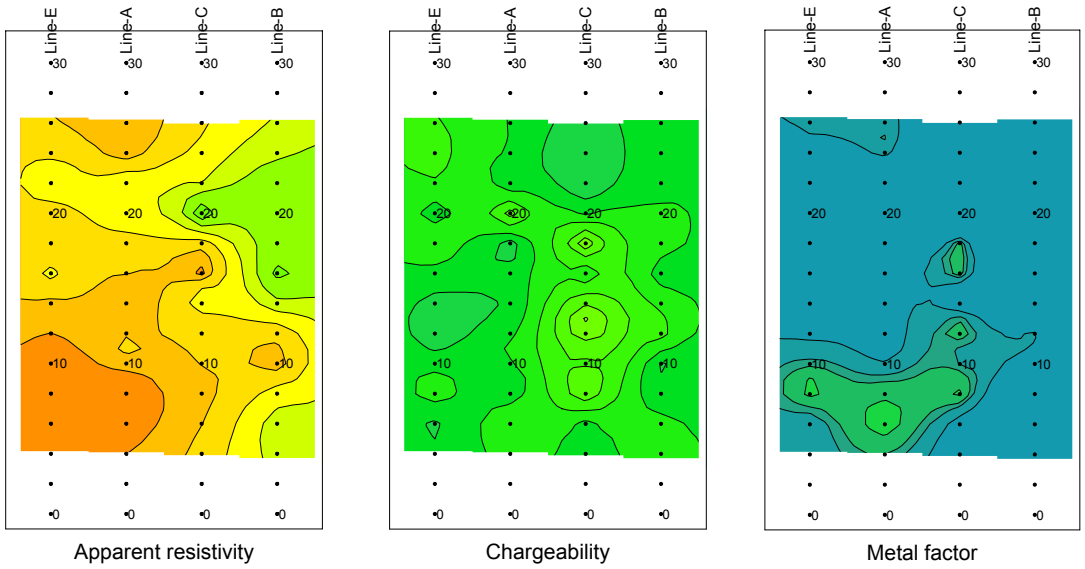

Plane map for n=4

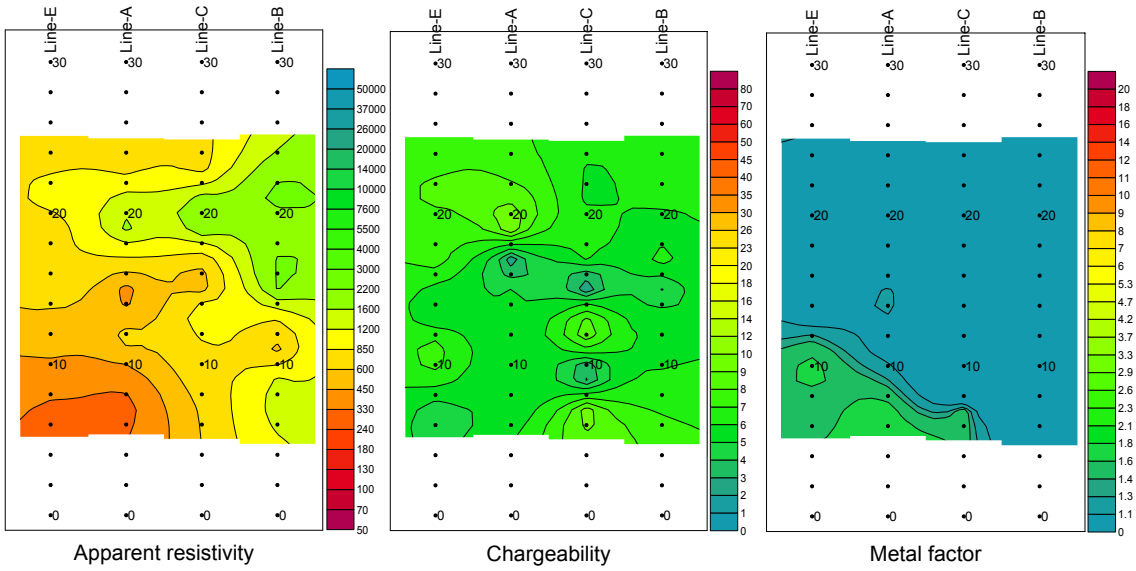

Plane map for n=5

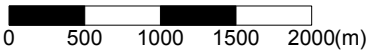

Fig. II-2-9 TDIP plane map for n=4 and 5 in Khujiriin gol area

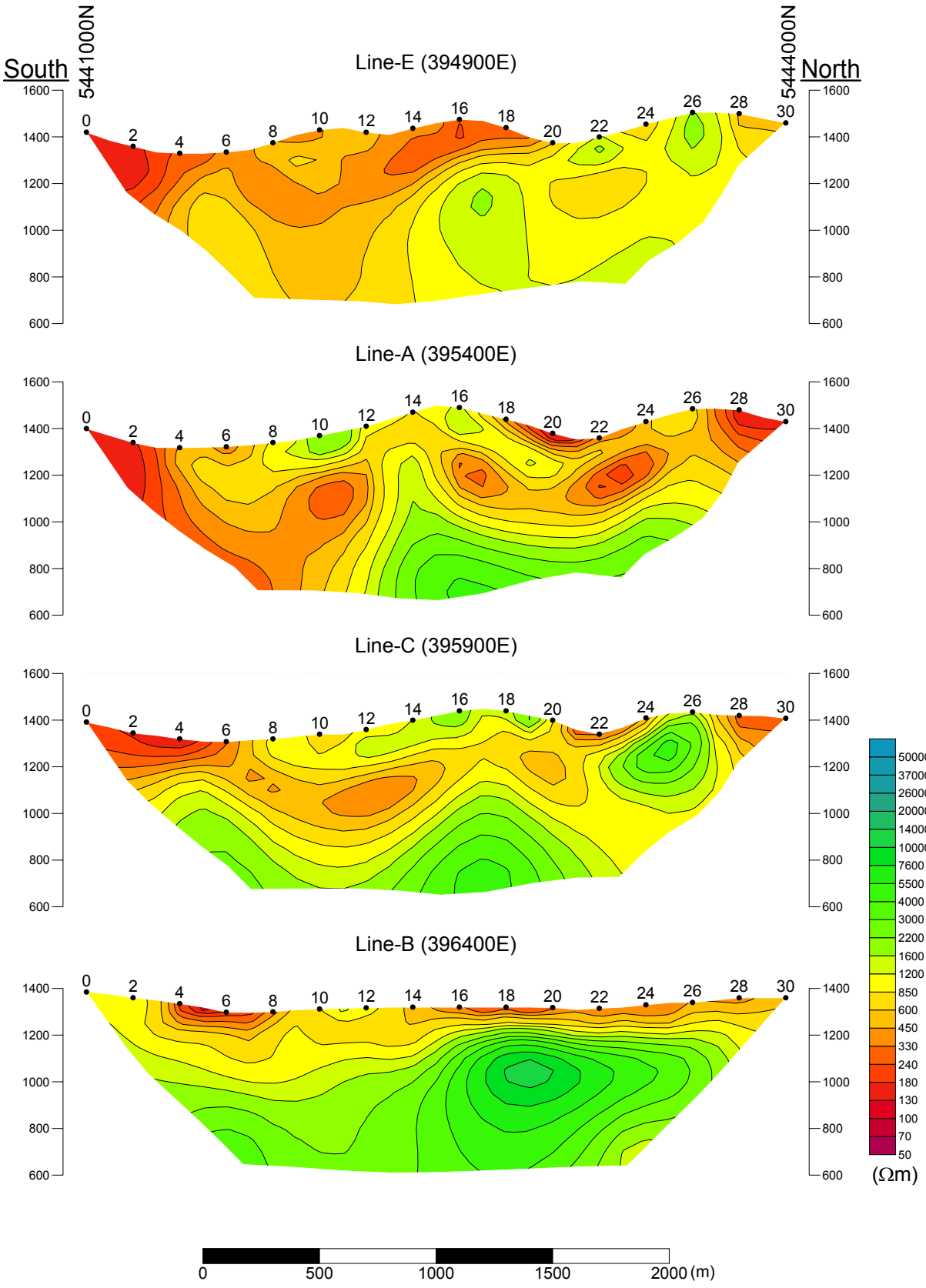

Fig. II-2-10　2D analysis sections for resistivity in Khujiriin gol area

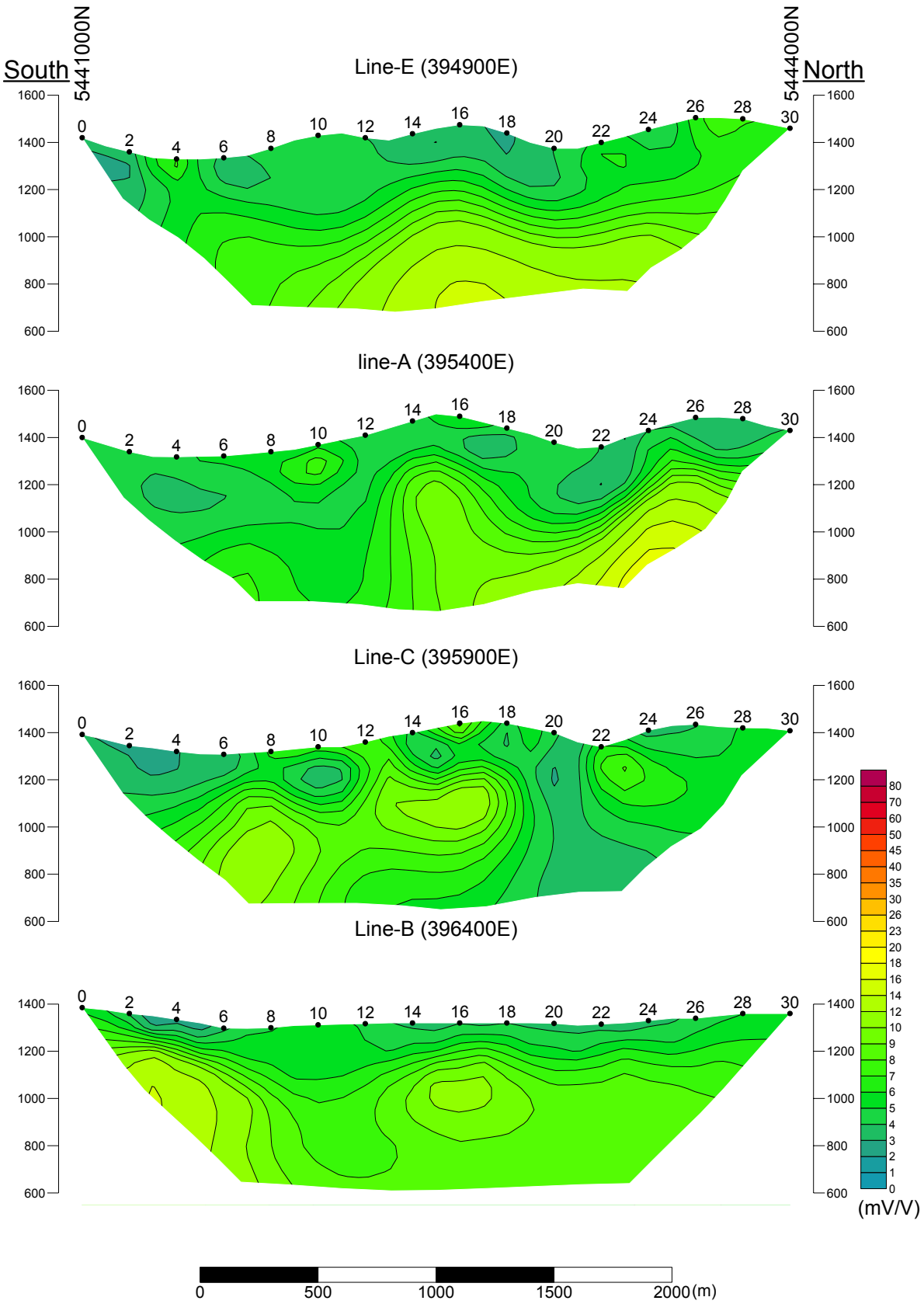

Fig. II-2-11　2D analysis sections for chargeability in Khujiriin gol area

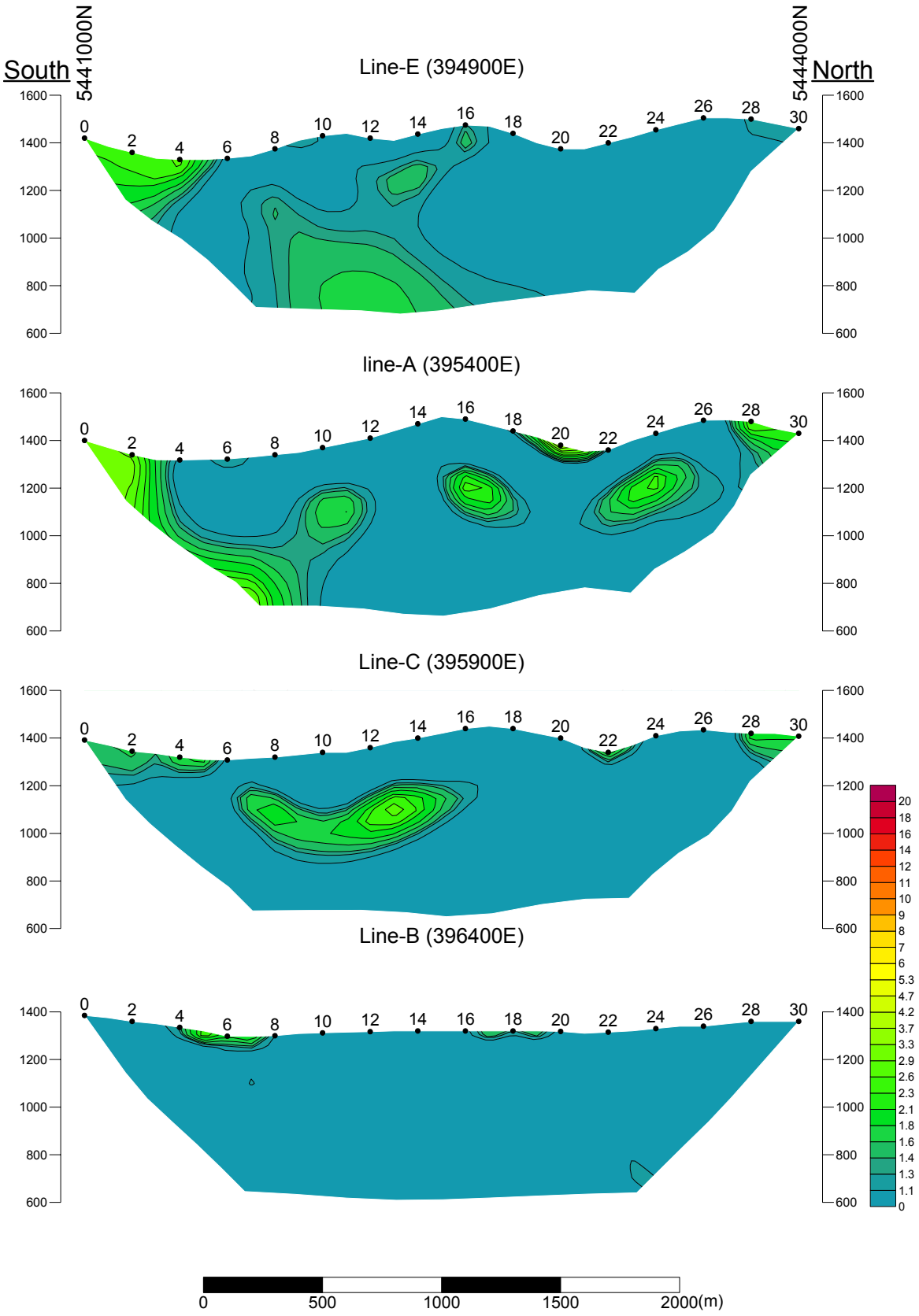

Fig. II-2-12　2D analysis sections for metal factor in Khujiriin gol area

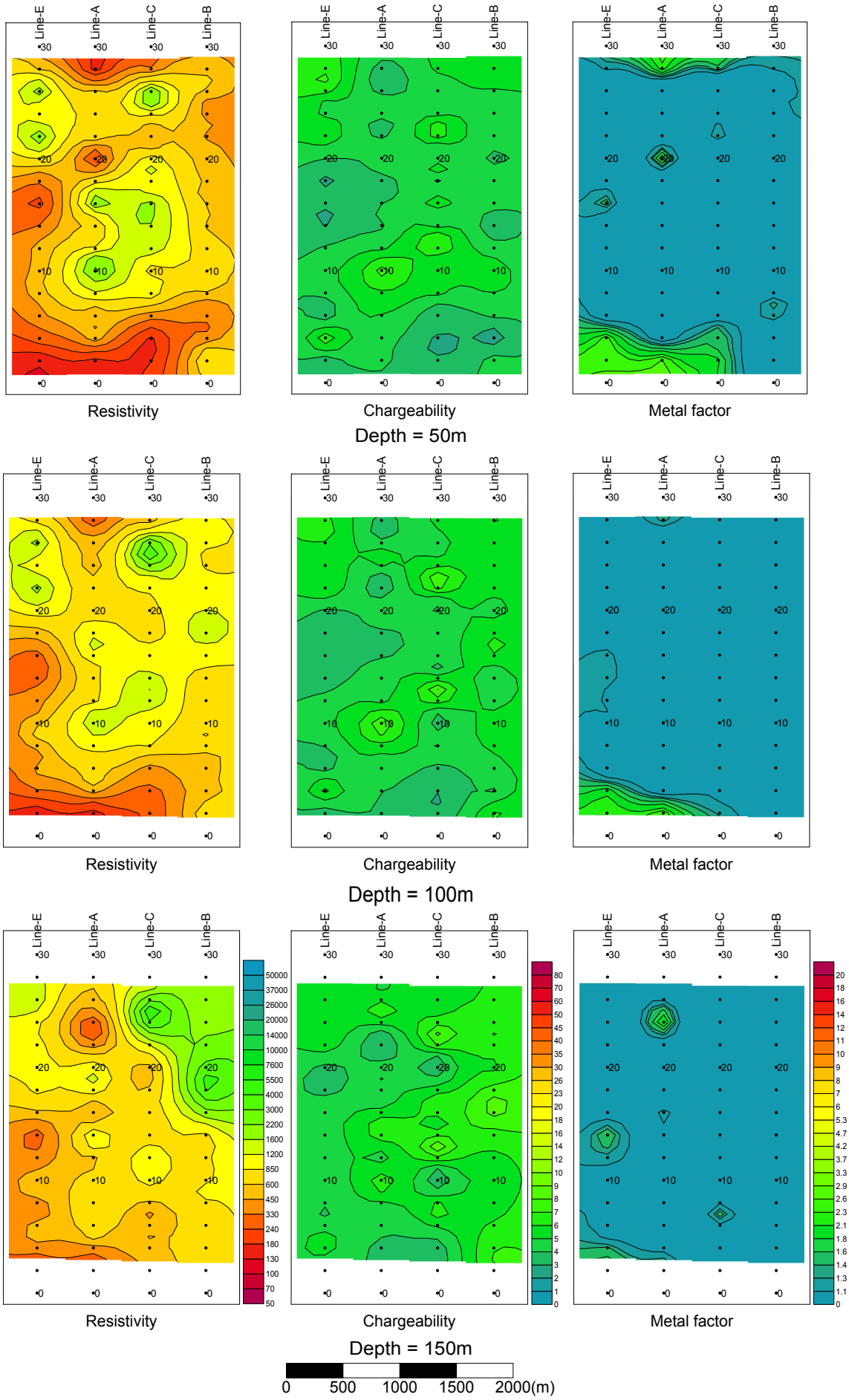

Fig. II-2-13　2D analysis plane map at the depth of 50, 100 and 150m in Khujiriin gol area

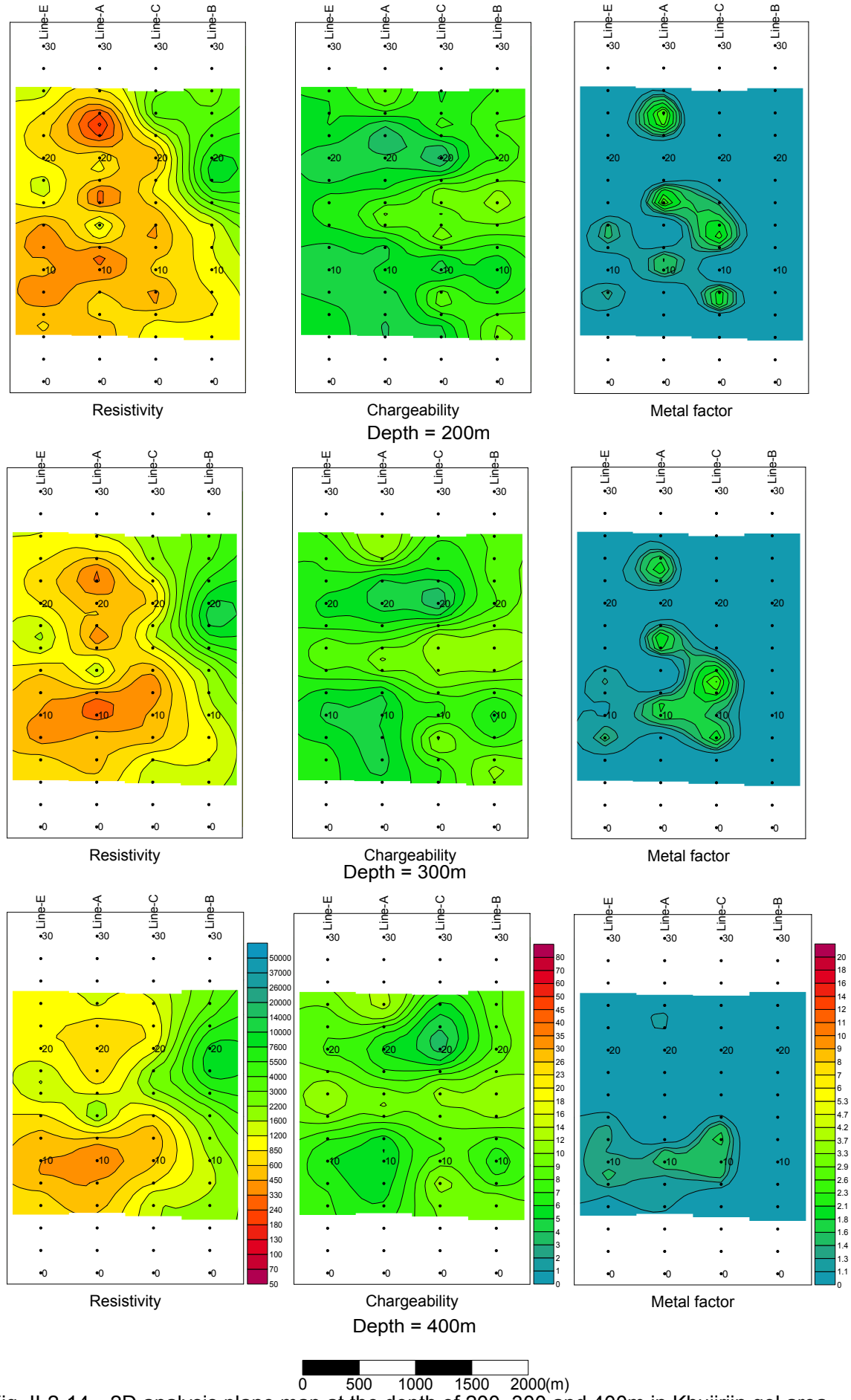

Fig. II-2-14 2D analysis plane map at the depth of 200, 300 and 400m in Khujiriin gol area

2-5-2 Zuukhiin gol area

(1) Lines location

Fig.II-2-15 shows the location of TDIP lines. 9 lines of 3.0km and 3 lines of 4.0km were set up along N0°E. Total line length is 39.0km.

(2) Results

Figs.II-2-16 ~ II-2-18 show the pseudo-sections, while Figs.II-2-19 ~ II-2-23 indicate the plane maps from n=1 to 5.

In this area, the apparent resistivity value ranges between 237 ~ 6581Ωm, and average is 1480Ωm. According to the plane maps for n=1 and 2, low resistivity is distributed at the area underlain by Quaternary sediments, and high resistivity is distributed in the mountain area. Low resistivity is distributed exceptionally at the ridge around the stations 16 to 20 on the lines F and K. This low resistivity zone continues from shallow to deep part.

The chargeability value ranges between 1.5 ~ 46.2mV/V, and average is 13.0mV/V. High chargeability over 20mV/V is distributed widely from shallow to deep part around the stations 10 to 30 on all lines located in the western half of this area (from line H to I). This anomaly indicates a large scale mineralization. Within this high chargeability zone, highest value over 40mV/V is recognized at n=2 and 3 around the stations 14 to 16 on the line J and at n=1 and 2 around the stations 14 to 16 on the line A. On the east of the line I, chargeability show high value over 10mV/V, and it is considered that sulfide exists all over the area.

The maximum value of metal factor is 11. High metal factor zone is distributed along the direction of EW in the western part of the area corresponding to the high chargeability zone.

(3) 2-D analysis

Figs.II-2-24 ~ II.2-32 show the 2-D analysis sections and plane maps.

The analyzed resistivity value ranges between 85 ~ 18kΩm, and average is 2032Ωm. According to the plane maps at the depth of 50m and 100m, low resistivity is distributed at the area underlain by Quaternary sediments, and high resistivity is distributed in the mountain area. Low resistivity is distributed exceptionally at the ridge around the station 16 to 20 on the lines F and K. Below the depth of 150m, low resistivity caused by Quaternary sediments disappear. At the depth from 200m to 400m, low resistivity zone extends from the station 10 on the line L to the station 20 on the line J along the direction of WSW-ENE.

The analyzed chargeability value ranges between 0.4 ~ 70.6mV/V and average is 14.3mV/V. High chargeability zone is distributed widely in the western part of the area. The area of this high chargeability zone becomes broader at the deeper part, and high chargeability zone over 20mV/V

ranges 4km in E-W, and 2km in N-S at the depth of 200m. It seems that the high chargeability zone consists three parts. According to the plane map at the depth of 200m, high chargeability zones over 30mV/V are recognized around the stations 10 to 18 on the lines F to I, the stations 20 to 28 on the lines G to F and the stations 12 to 18 on the lines L to K. The low resistivity zone above mentioned is surrounded by these three high chargeability zones.

The maximum value of metal factor is 17. High metal factor zone is distributed in the direction of E-W in the western part of the area corresponding to the high chargeability zone.

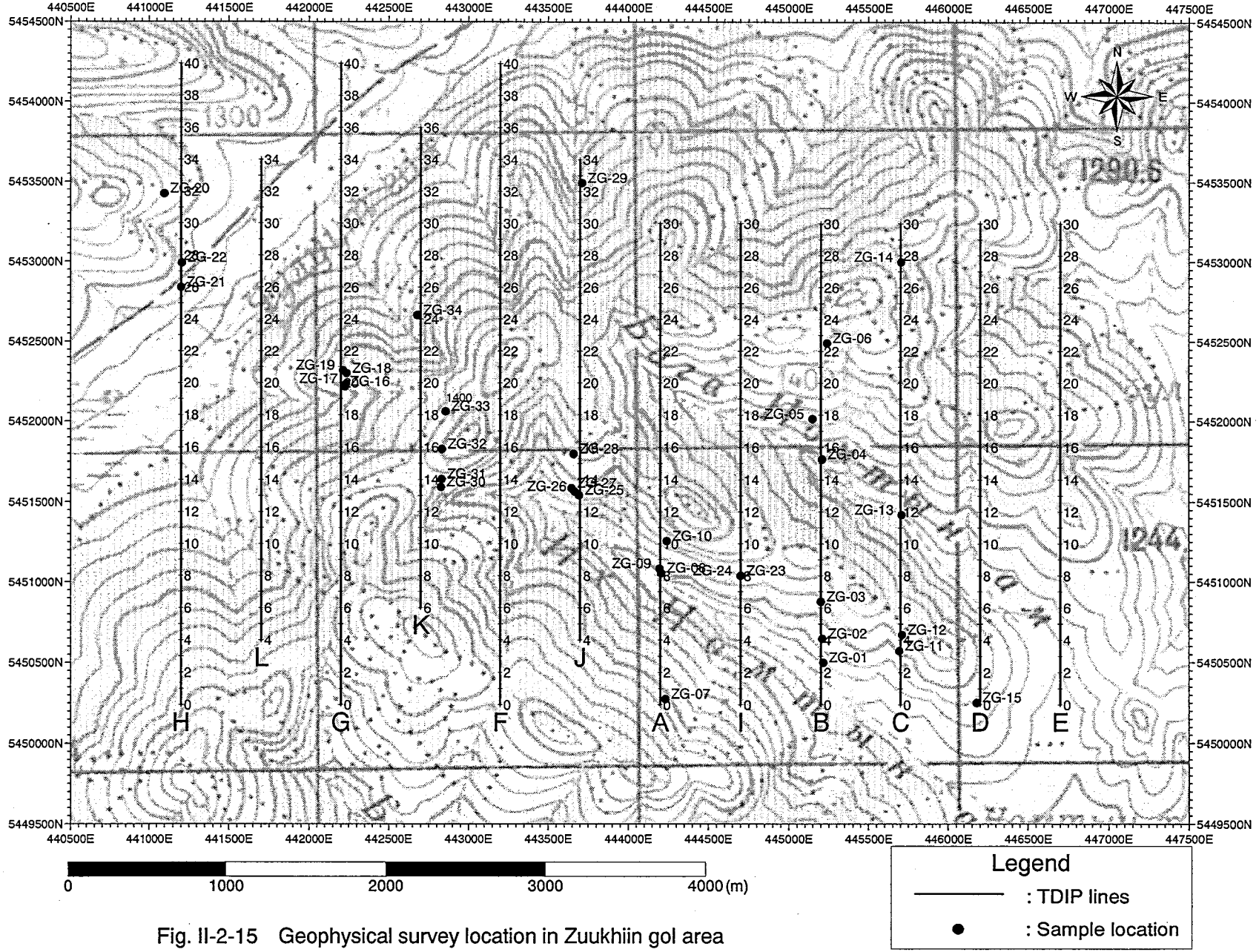

Fig. II-2-15 Geophysical survey location in Zuukhiin gol area

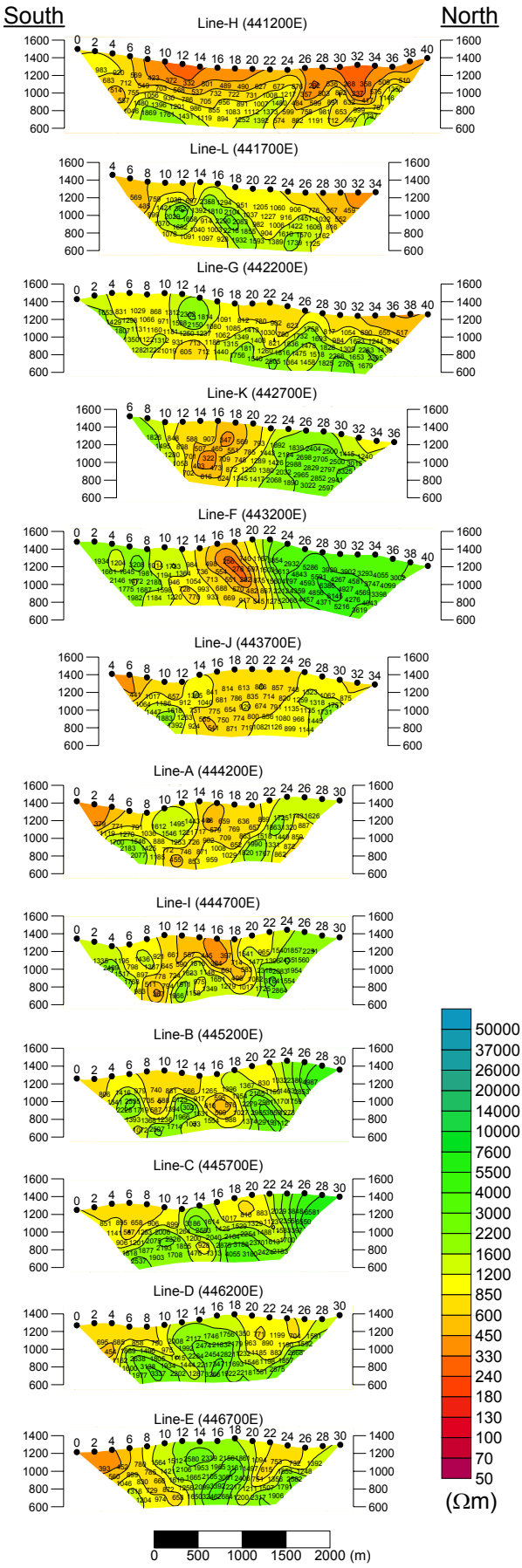

Fig. II-2-16 Apparent resistivity pseudo-sections in Zuukhiin gol area

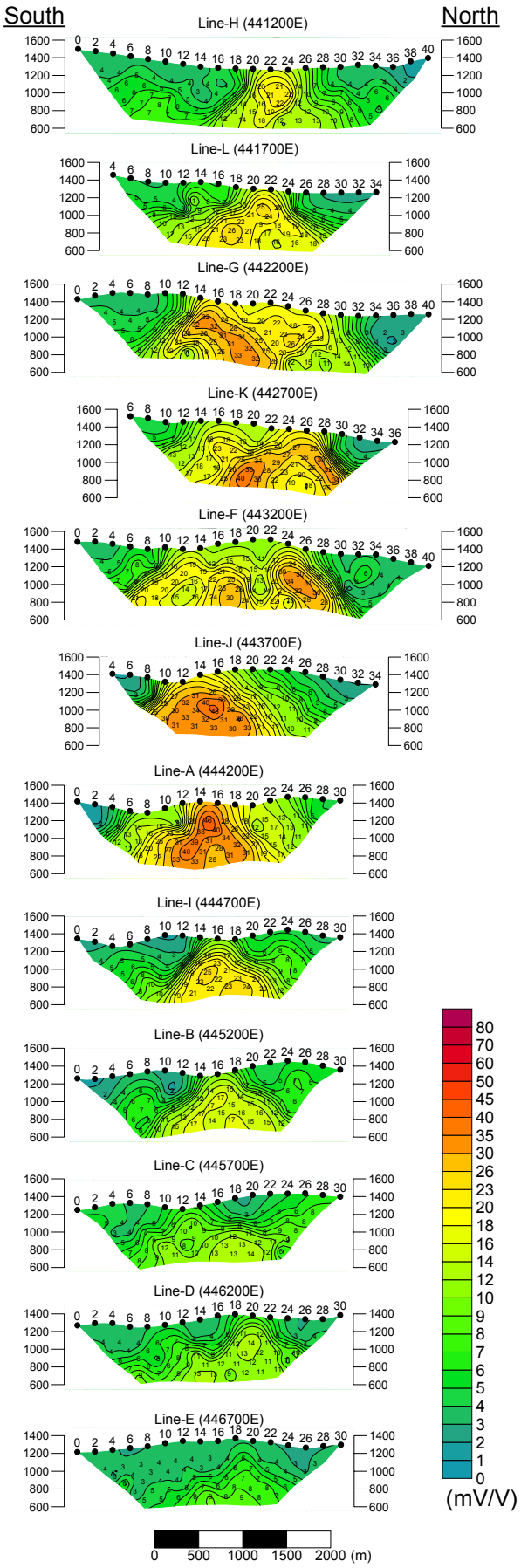

Fig. II-2-17 Chargeability pseudo-sections in Zuukhiin gol area

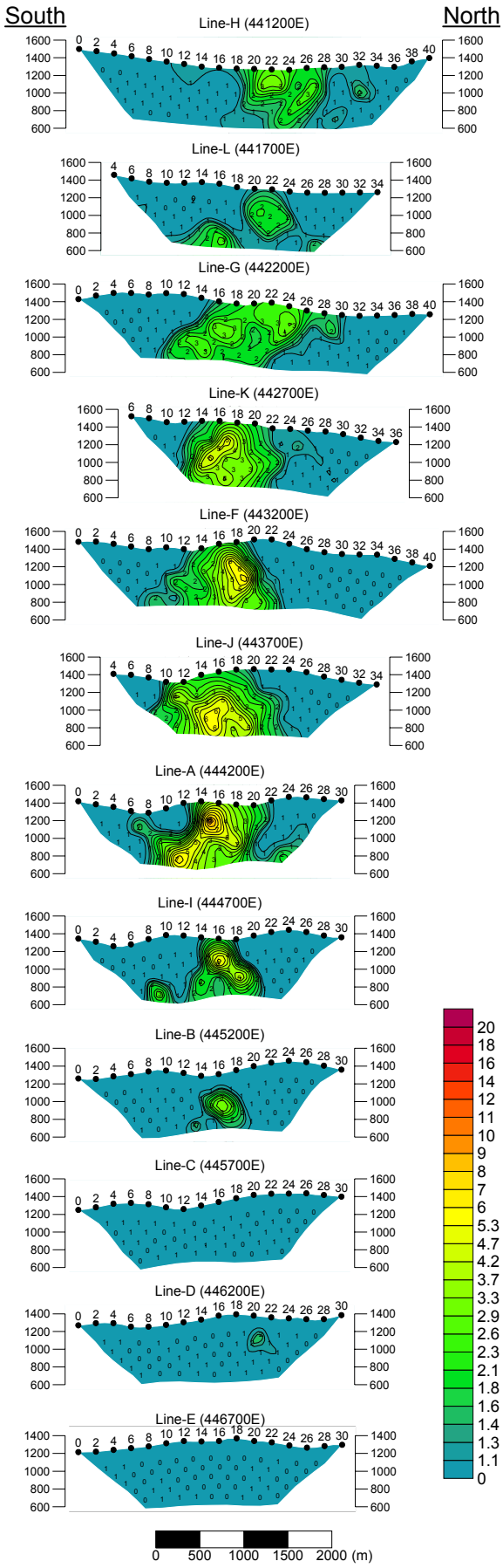

Fig. II-2-18 Metal factor pseudo-sections in Zuukhiin gol area

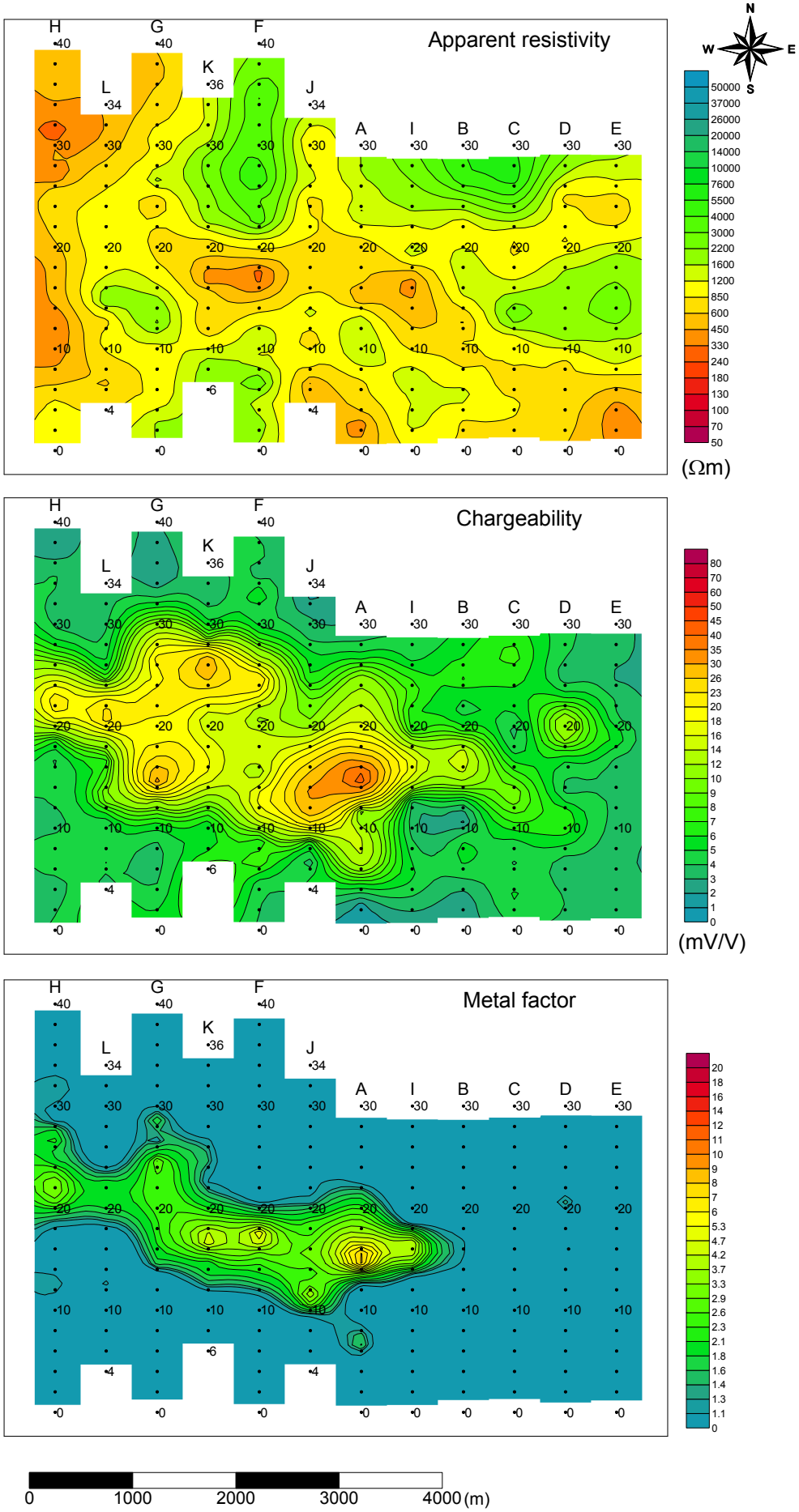

Fig. II-2-19 TDIP plane map for n=1 in Zuukhiin gol area

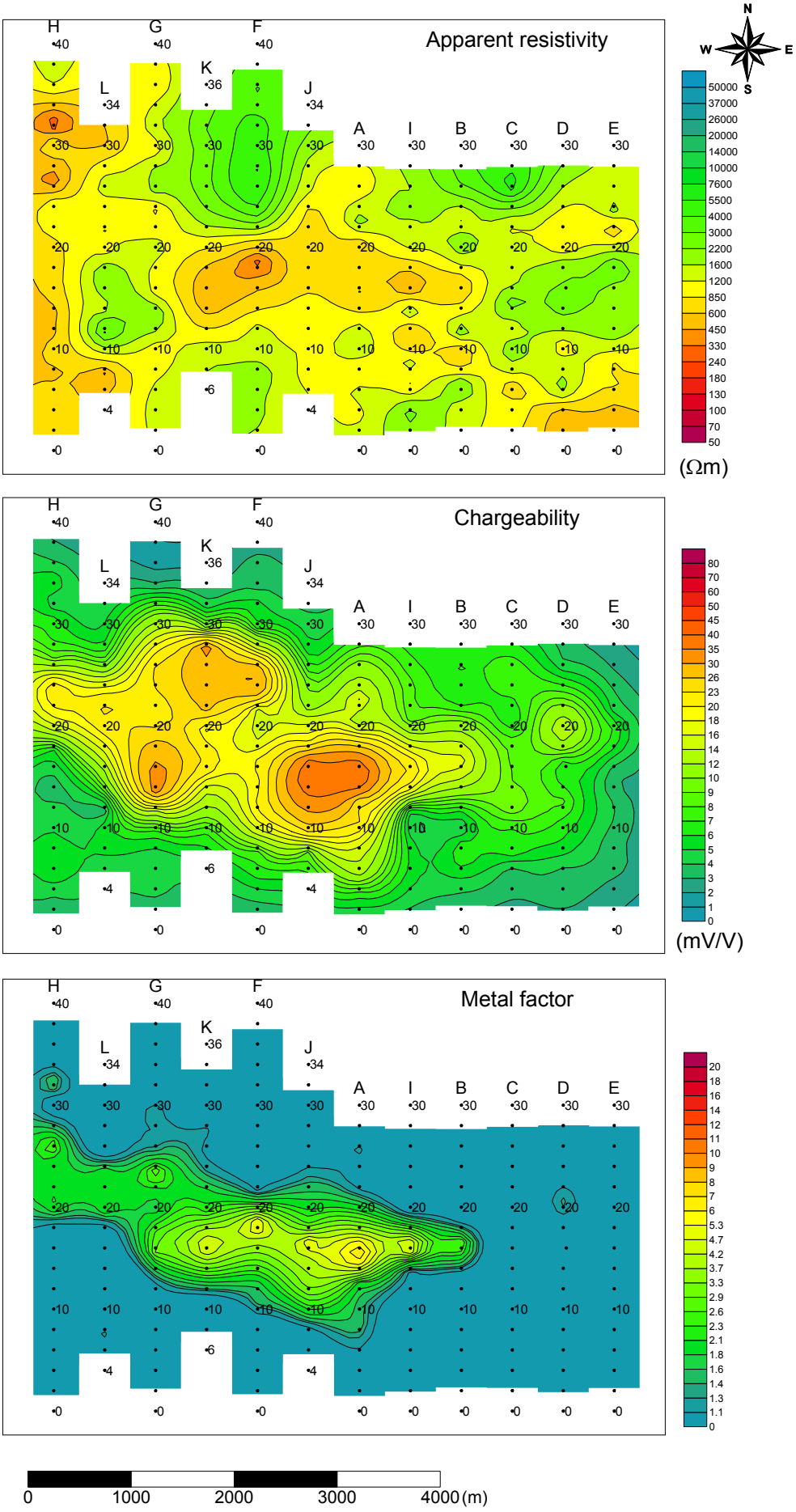

Fig. II-2-20 TDIP plane map for n=2 in Zuukhiin gol area

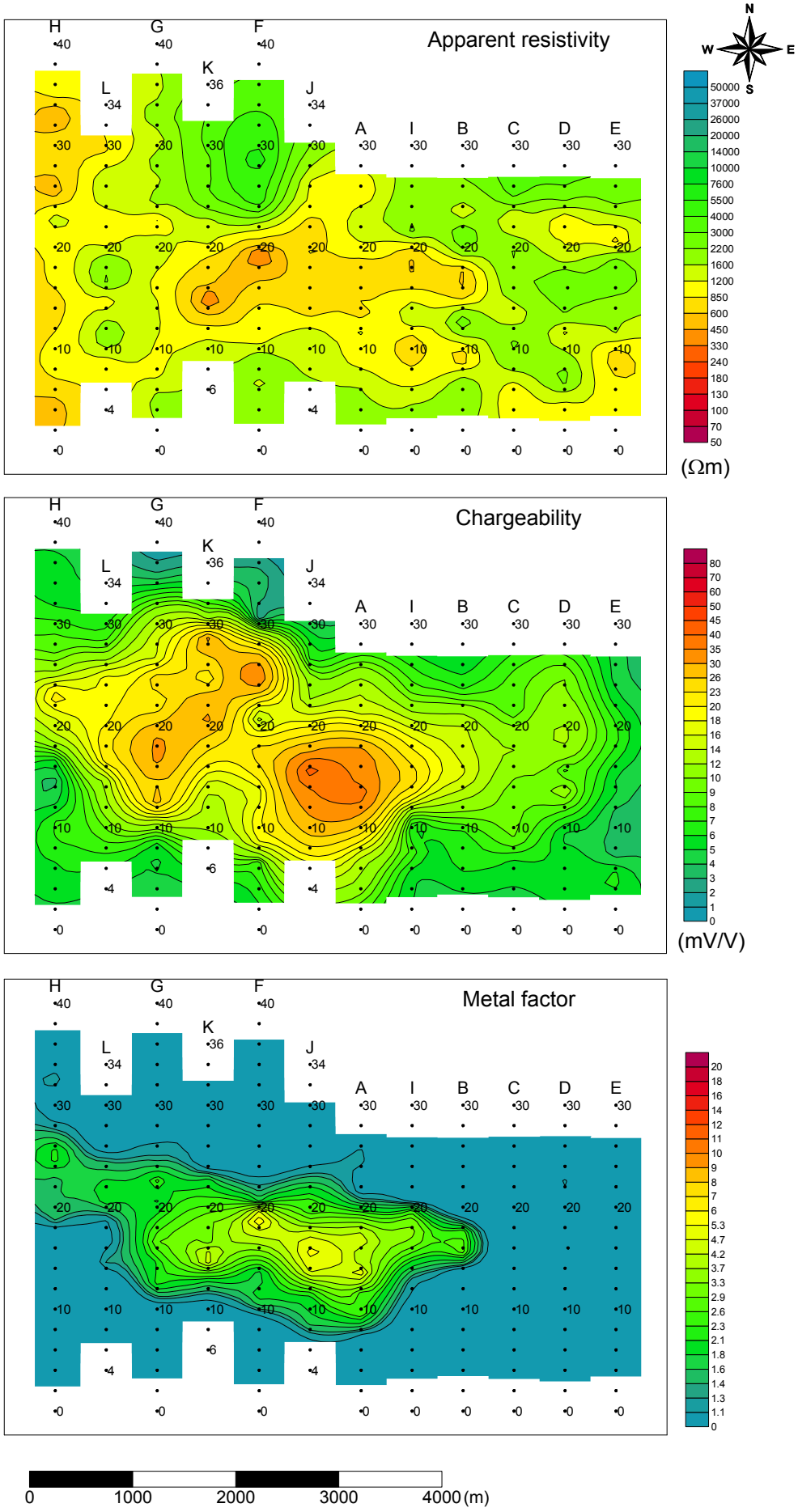

Fig. II-2-21 TDIP plane map for n=3 in Zuukhiin gol area

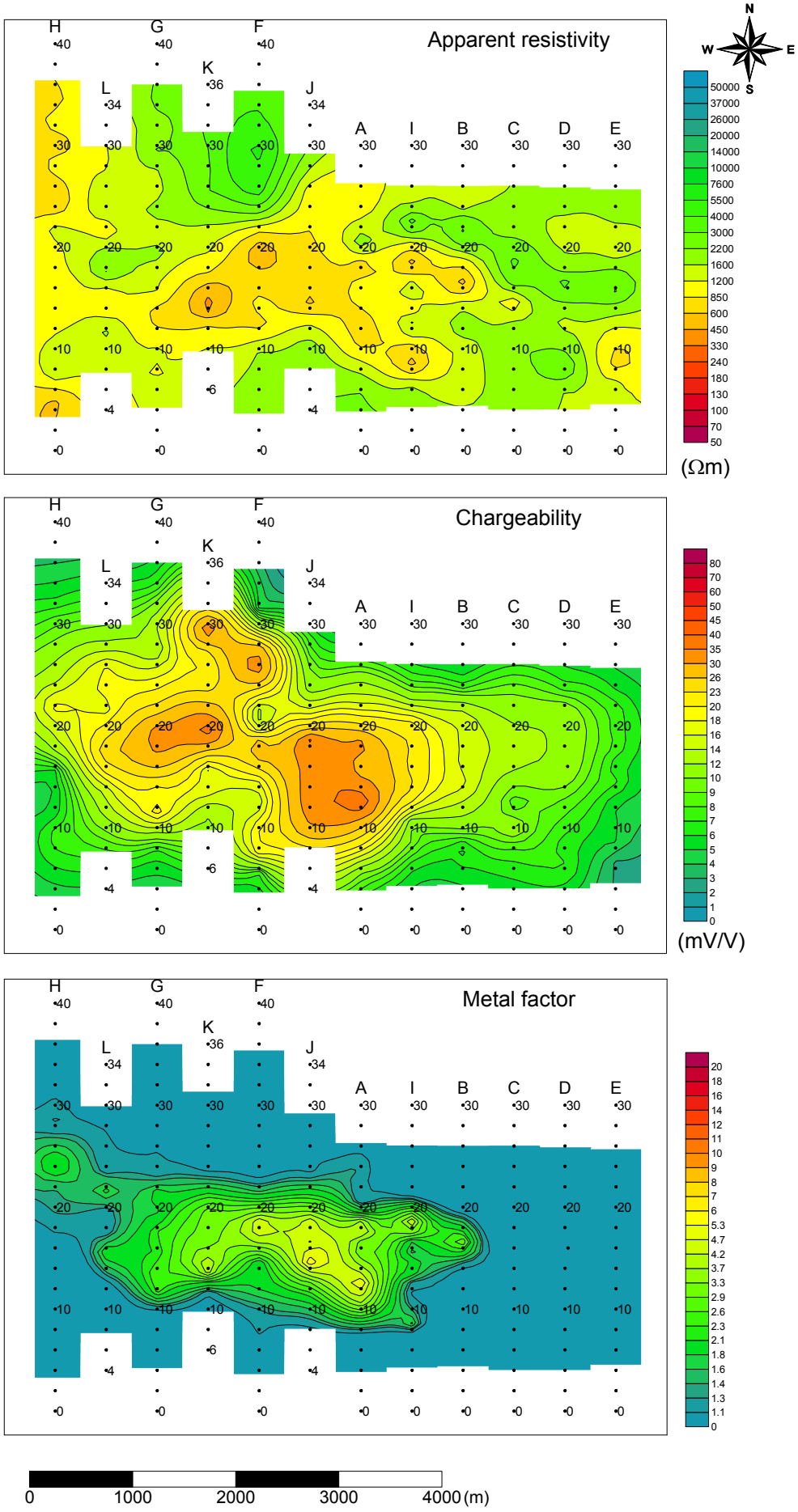

Fig. II-2-22 TDIP plane map for n=4 in Zuukhiin gol area

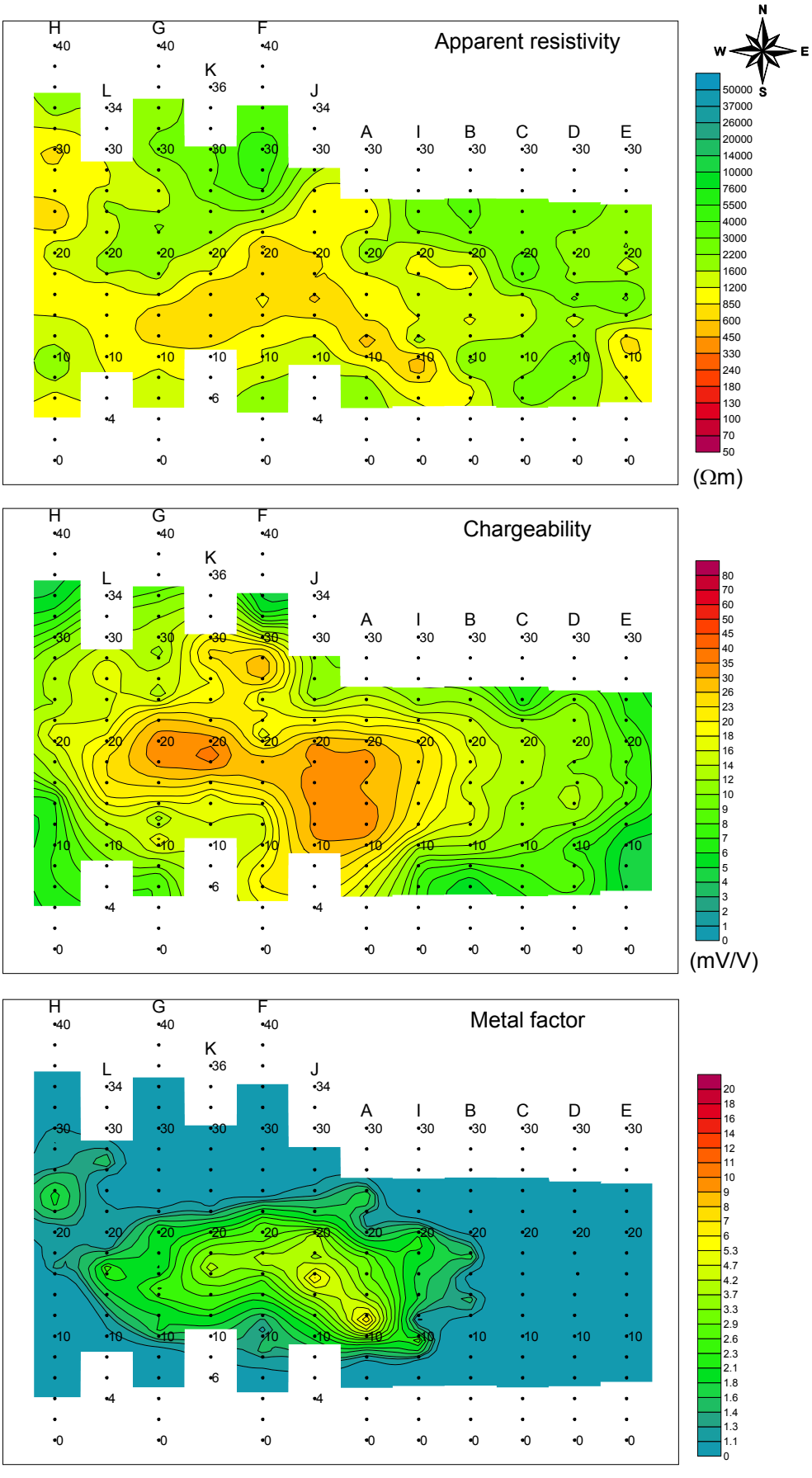

Fig. II-2-23 TDIP plane map for n=5 in Zuukhiin gol area

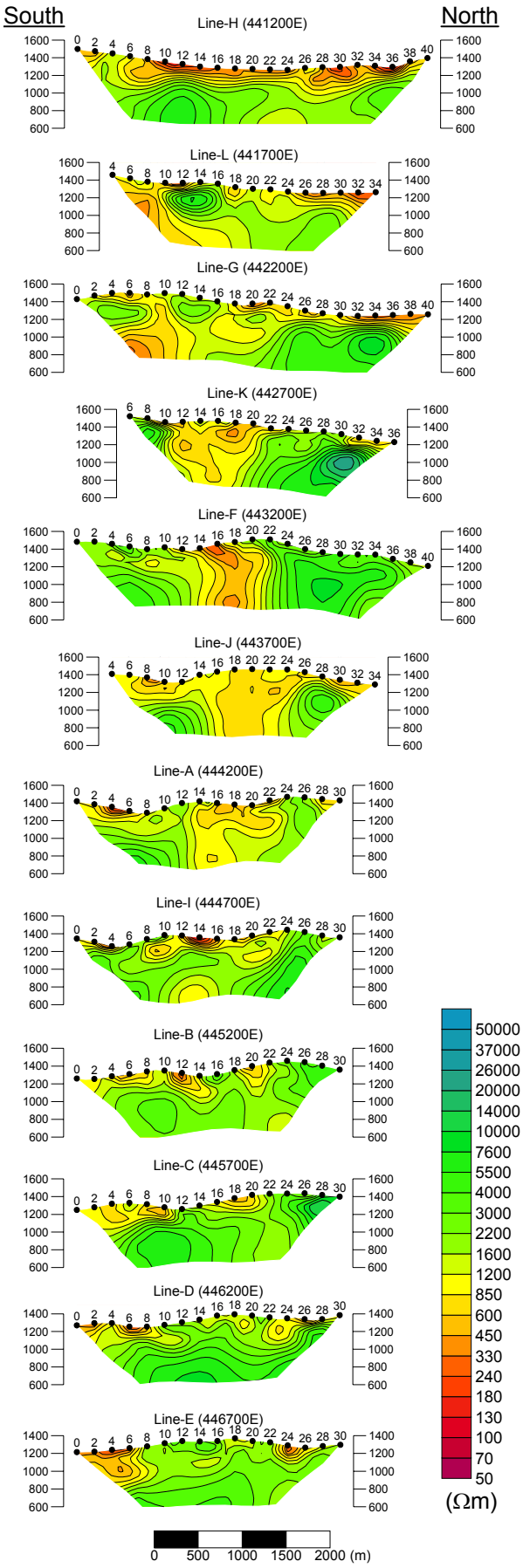

Fig. II-2-24 2D analysis sections for resistivity in Zuukhiin gol area

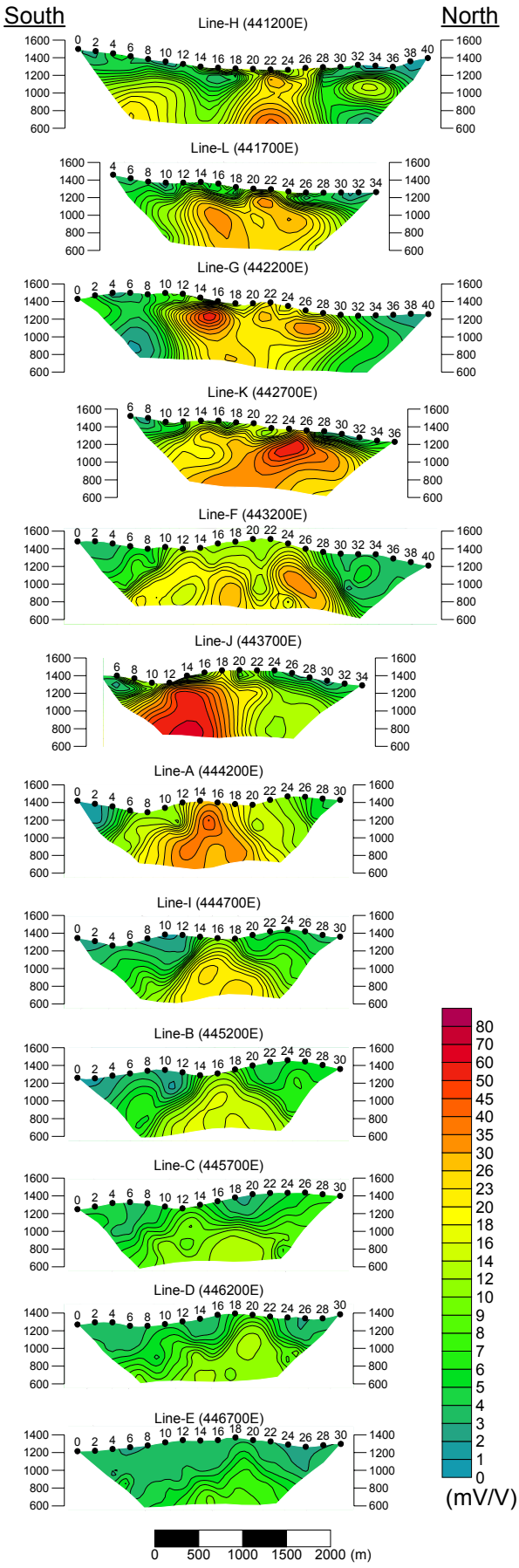

Fig. II-2-25 2D analysis sections for chargeability in Zuukhiin gol area

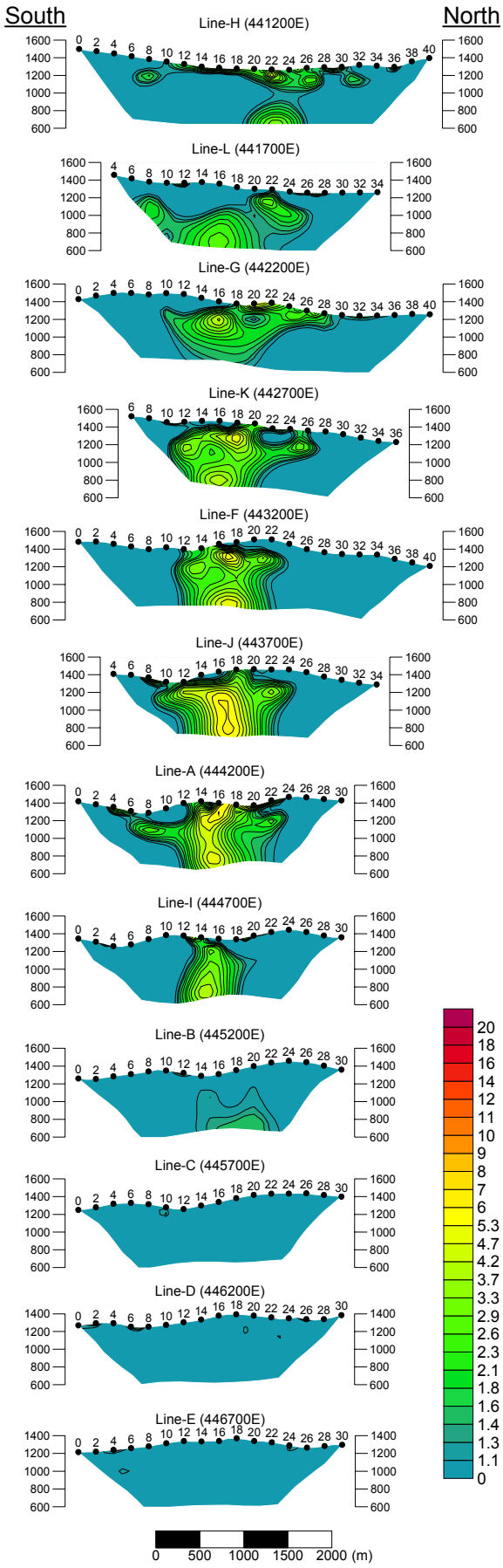

Fig. II-2-26 2D analysis sections for metal factor in Zuukhiin gol area

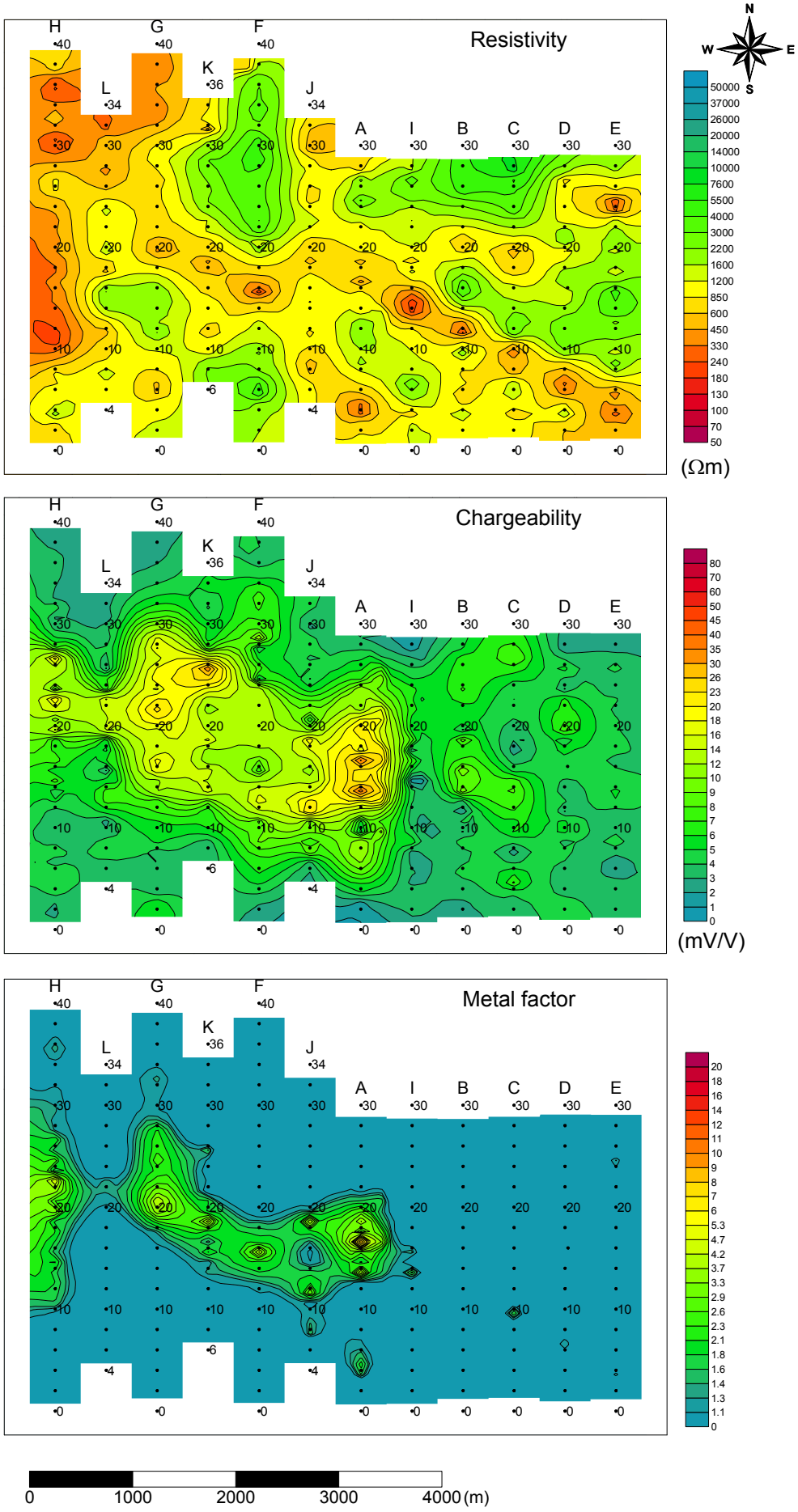

Fig. II-2-27 2D analysis plane map at the depth of 50m in Zuukhiin gol area

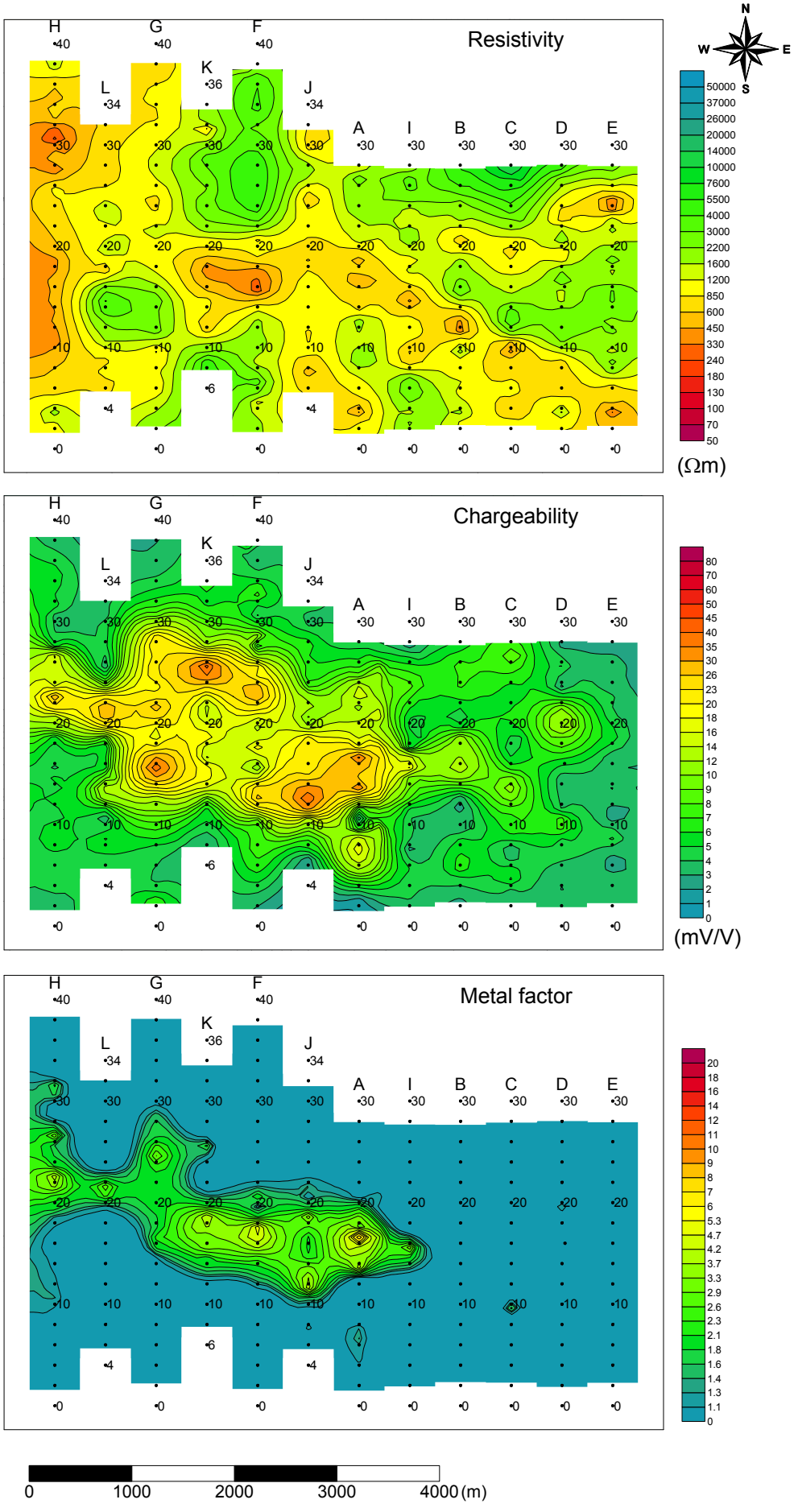

Fig. II-2-28 2D analysis plane map at the depth of 100m in Zuukhiin gol area

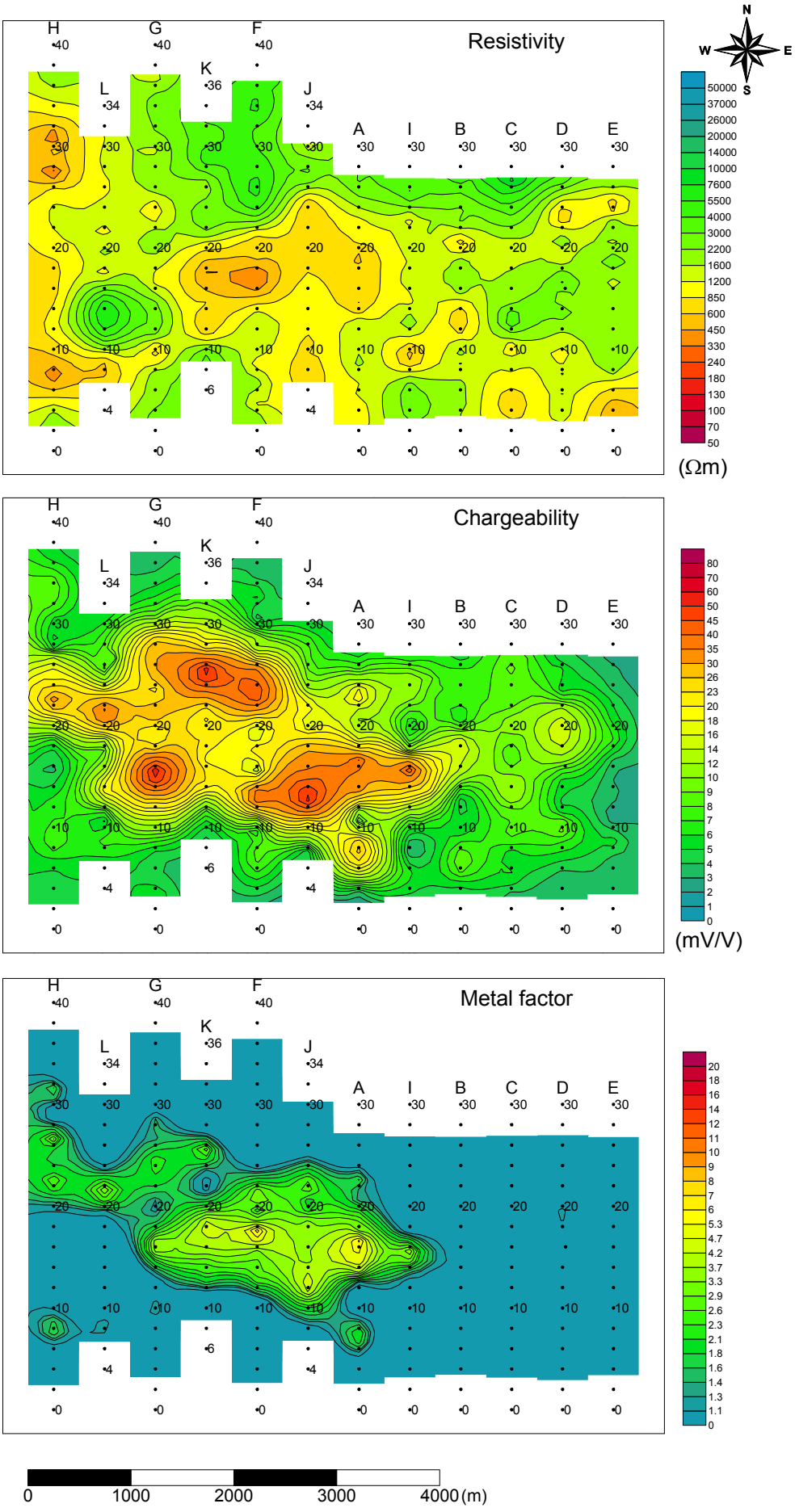

Fig. II-2-29　2D analysis plane map at the depth of 150m in Zuukhiin gol area

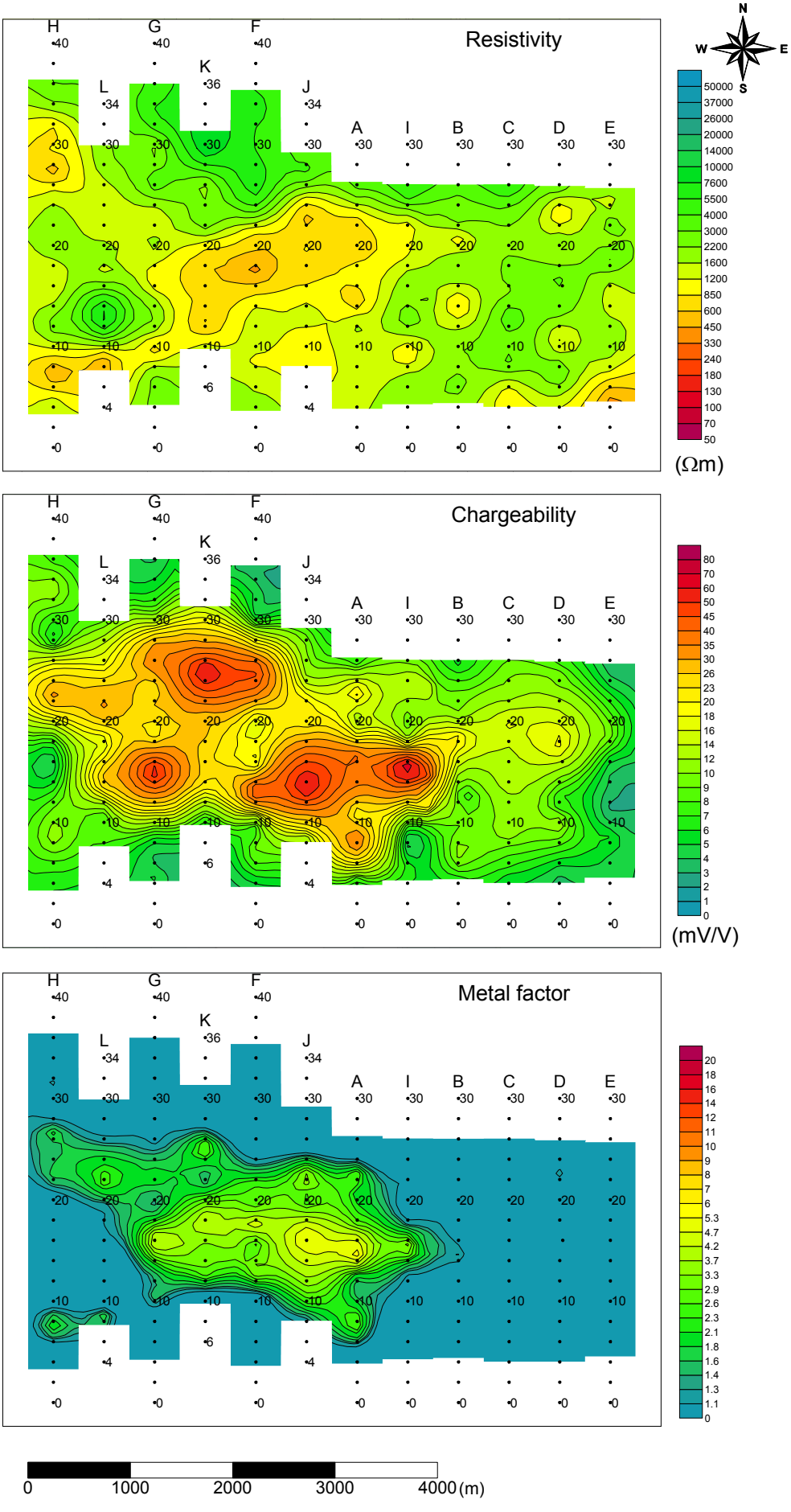

Fig. II-2-30 2D analysis plane map at the depth of 200m in Zuukhiin gol area

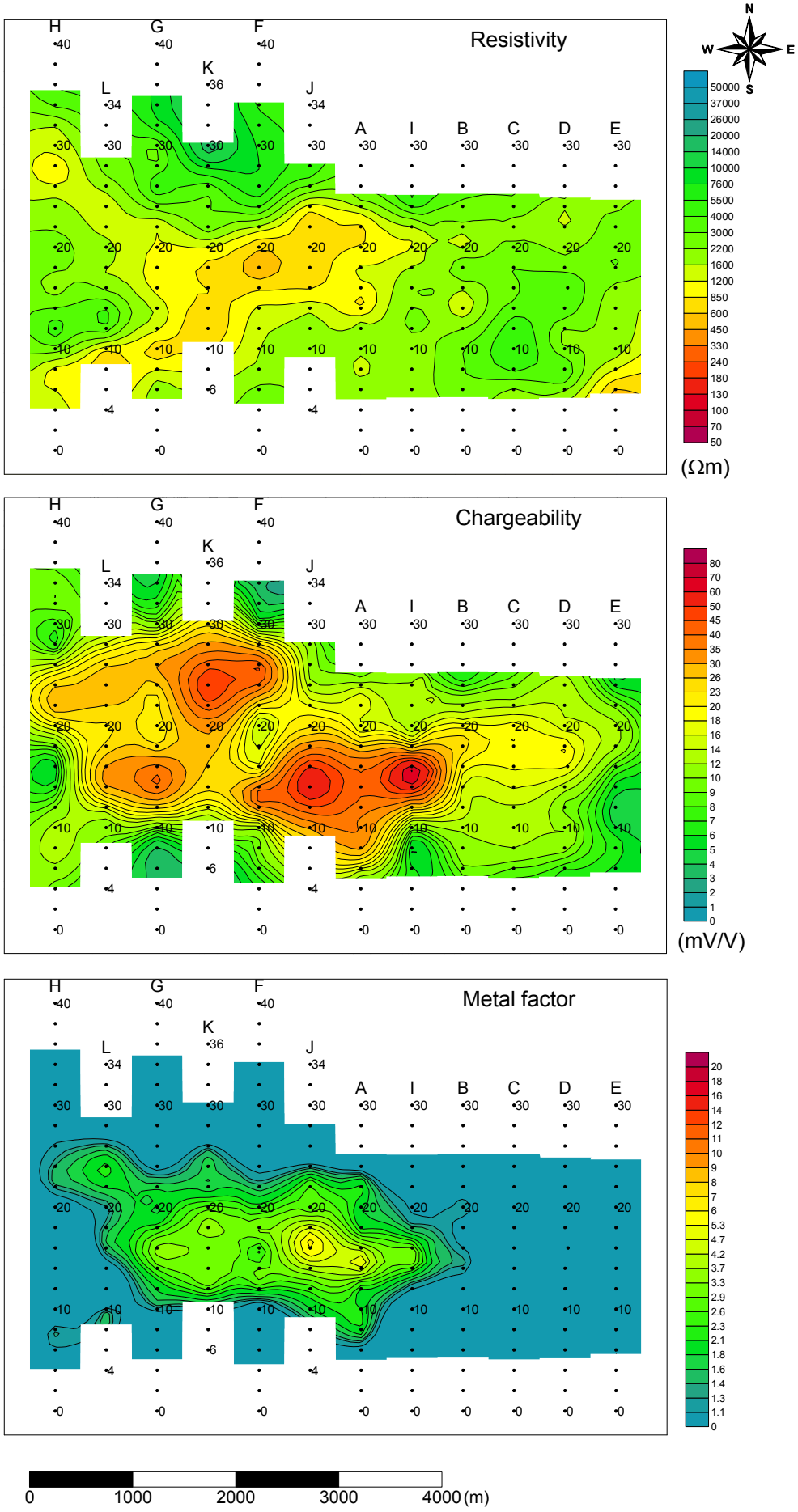

Fig. II-2-31 2D analysis plane map at the depth of 300m in Zuukhiin gol area

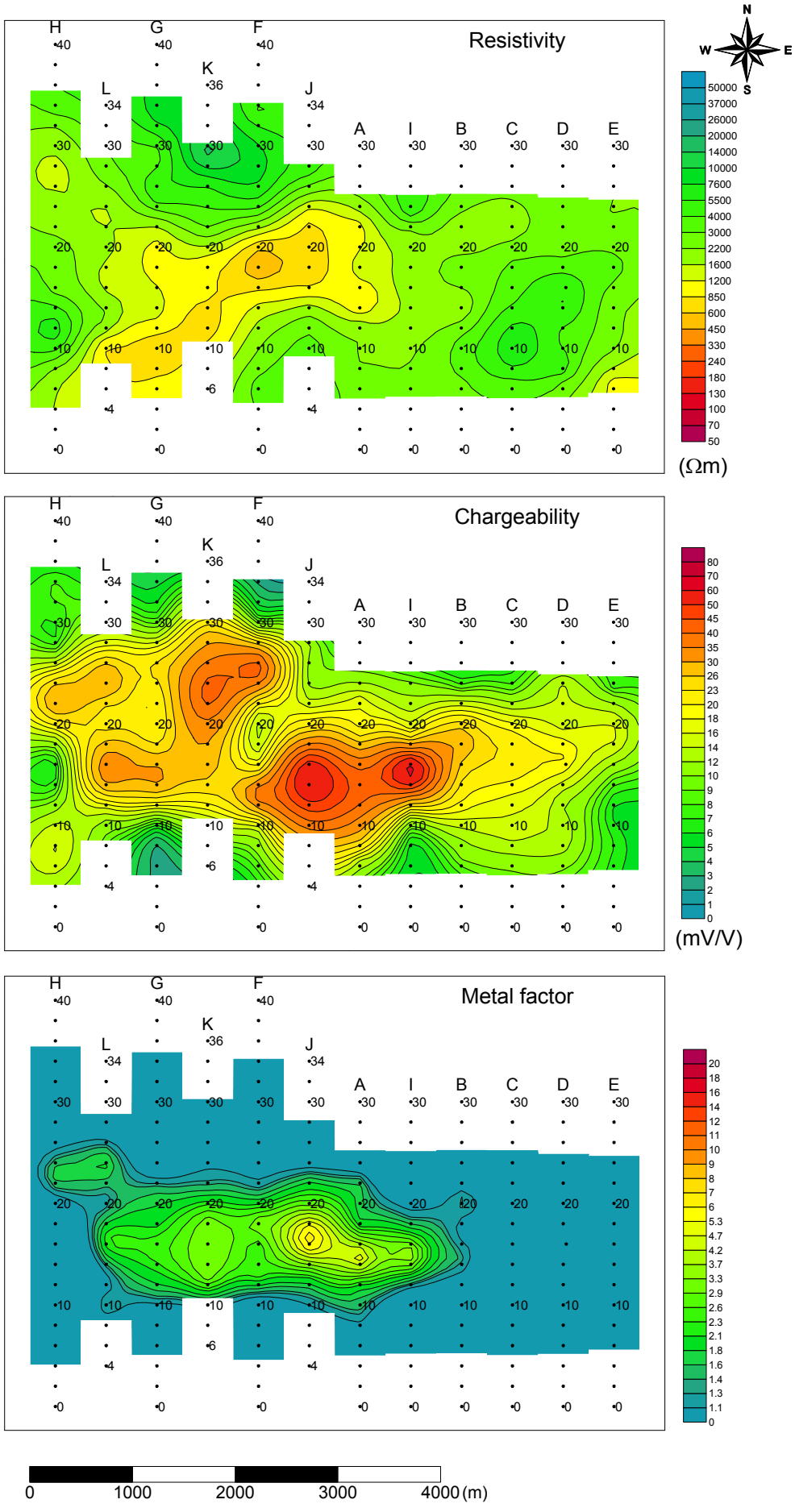

Fig. II-2-32 2D analysis plane map at the depth of 400m in Zuukhiin gol area

2-5-3 Danbatseren east-1 area

(1) Lines location

Fig.II-2-33 shows the location of TDIP lines. This area is located in the south of Danbatseren east area. 2 lines of 3.0km each were set up along N90°E.

(2) Results

Fig.II-2-34 shows the pseudo-sections.

In this area, the apparent resistivity value ranges between 100 ~ 3964Ωm, and average is 1121Ωm. Low resistivity is distributed at the shallow part around the stream running through the western part of the area from north to south, and it shows pant-legs shape at the deeper part.

The chargeability value ranges between 2.0 ~ 15.4mV/V and average is 7.1mV/V. Slightly high chargeability is distributed at n=2 and 3 around the stations 16 to 20 on the line A. High chargeability is also recognized on the line B, and its depth is deeper than that of the line A.

The maximum value of the metal factor is 4.3.

(3) 2-D analysis

Fig.II-2-35 shows the 2-D analysis sections.

The analyzed resistivity value ranges between 31 ~ 5185Ωm and average is 1625Ωm. Low resistivity caused by Quaternary sediments is distributed at the shallow part. Low resistivity is also recognized at the deep part around the stations 16 to 18 on the line A.

The analyzed chargeability value ranges between 1.2 ~ 26.0mV/V and average is 10.3mV/V. High chargeability is distributed at the deep part around the center of both lines. On the line A, 2 high charegeability zones surrounding low resistivity zone are distributed. It seems to indicate some mineralization accompanying sulfide, but its intensity is weak.

The maximum value of metal factor is 9

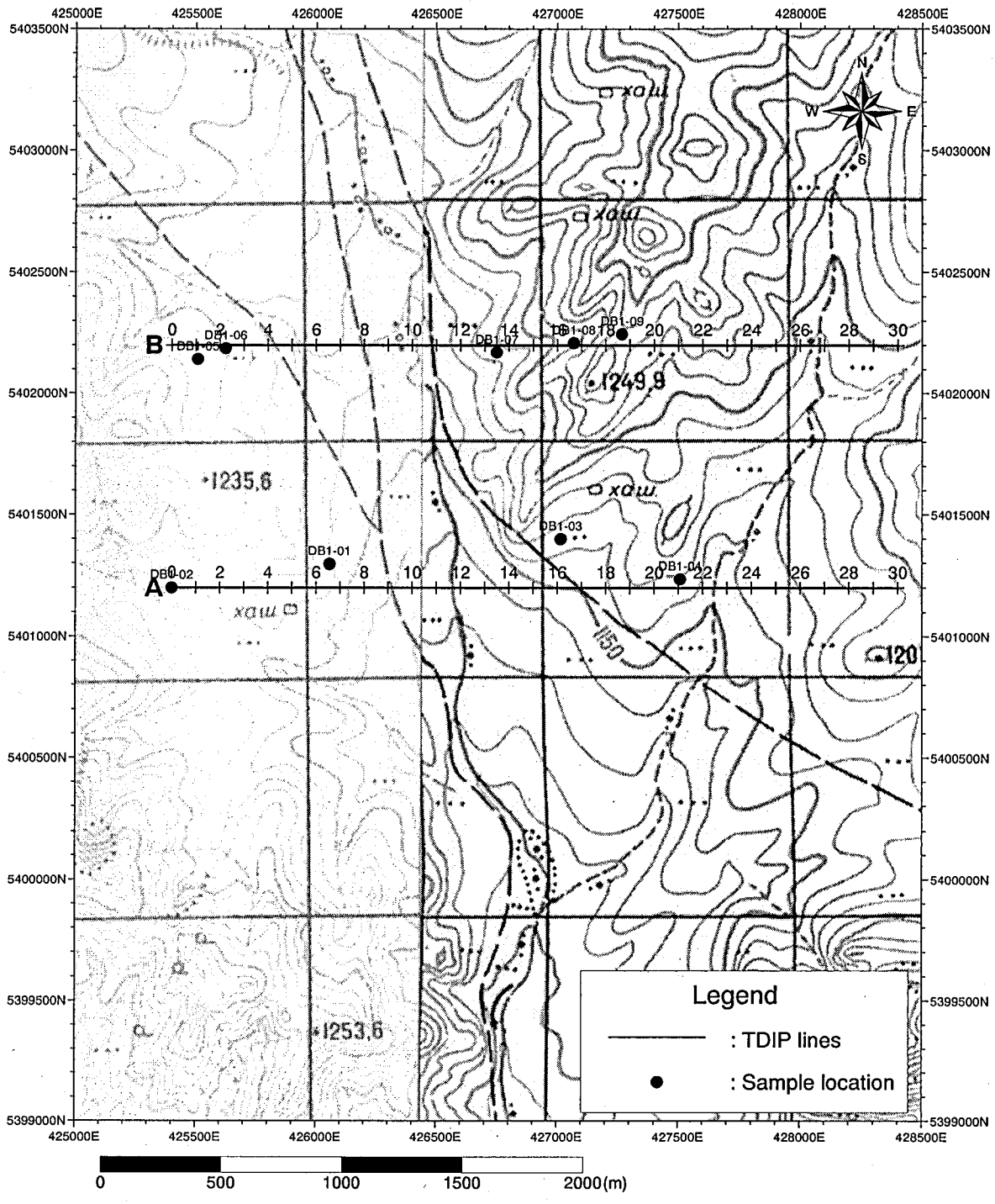

Fig. II-2-33 Geophysical survey location in Danbatseren east - 1 area

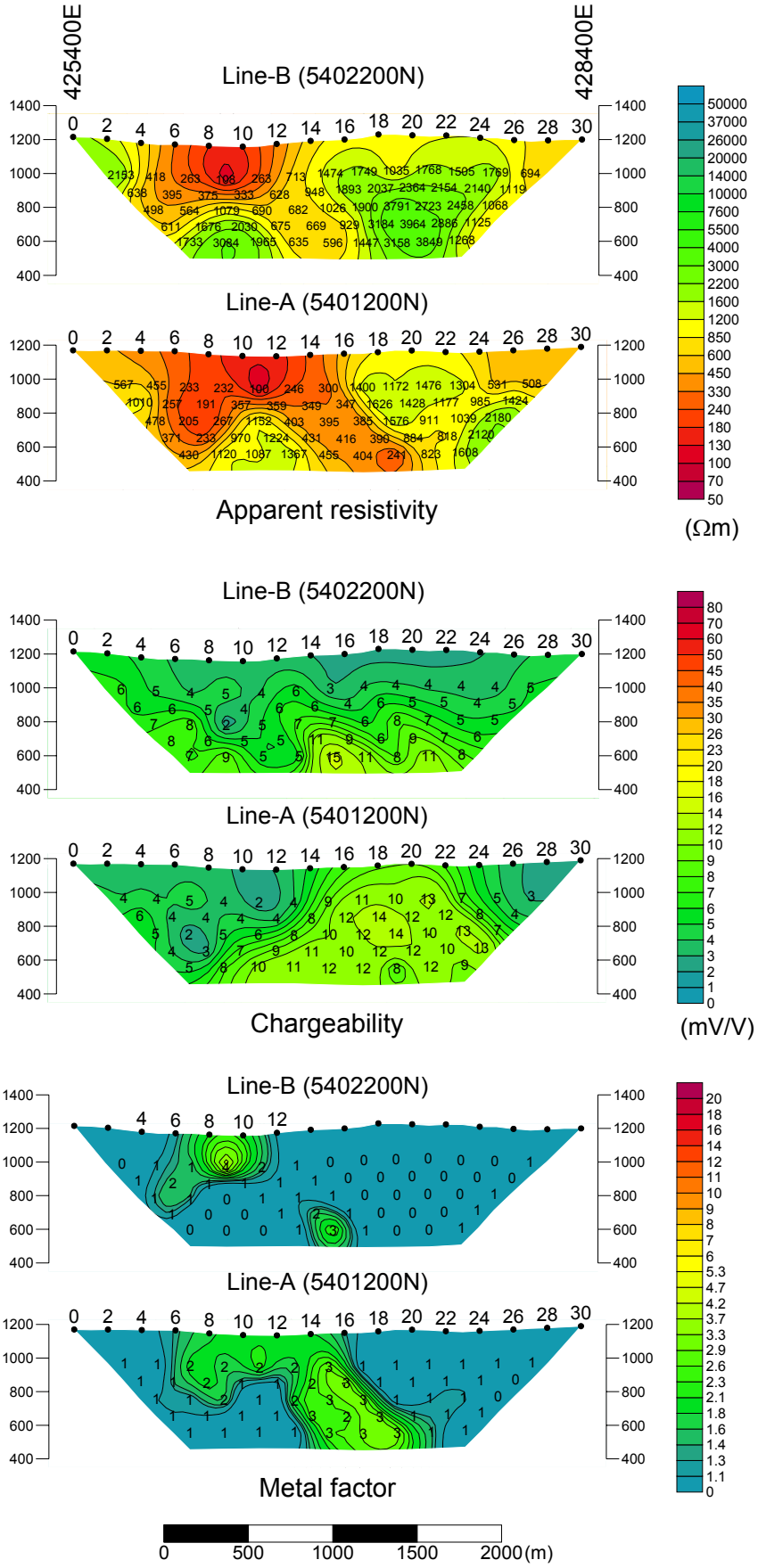

Fig. II-2-34 TDIP pseudo-sections in Danbatseren east - 1 area

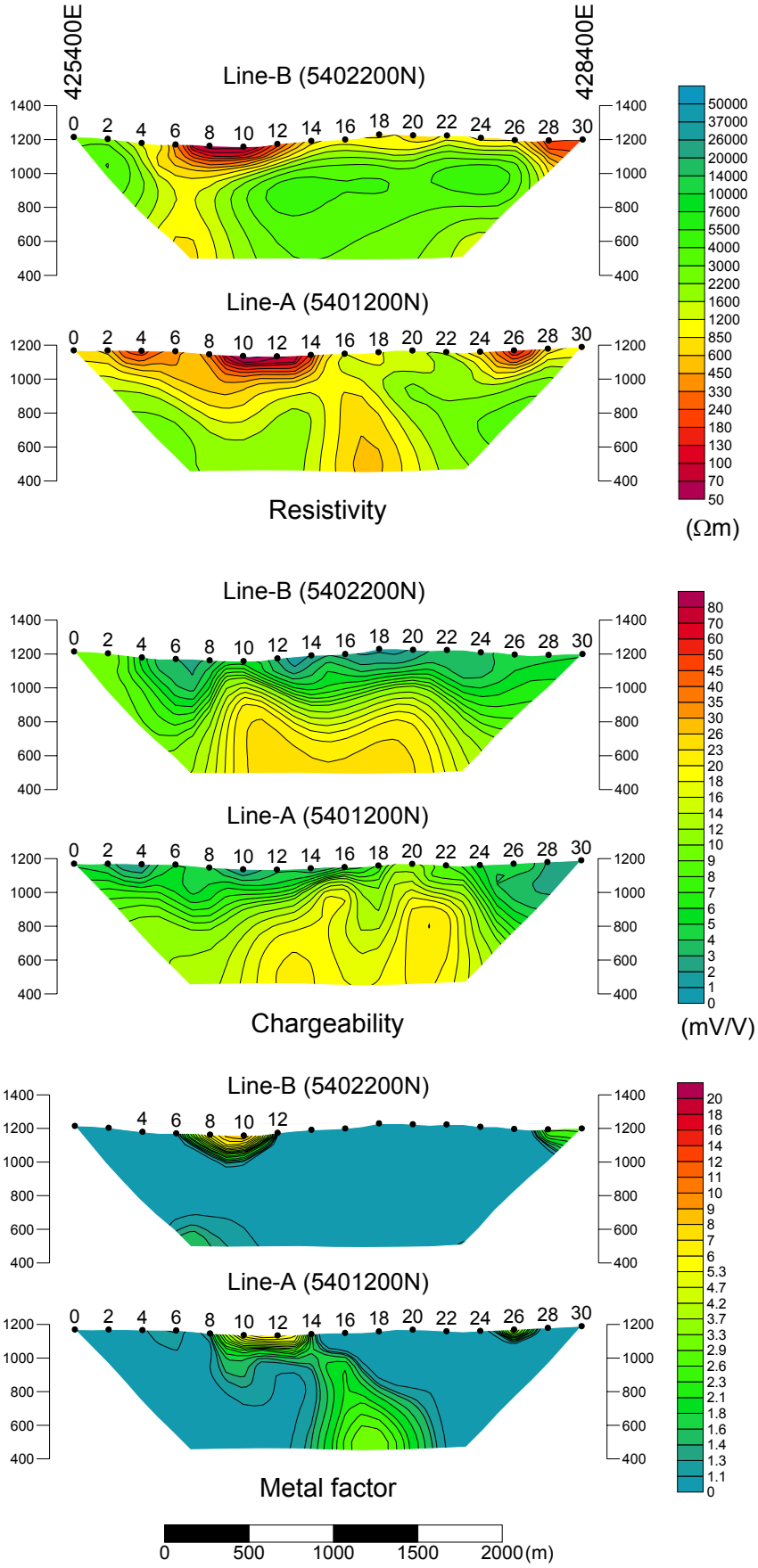

Fig. II-2-35 2D analysis sections in Danbatseren east - 1 area

2-5-4 Danbatseren east-3 area

(1) Lines location

Fig.II-2-36 shows the location of TDIP lines. In this area, 1 line of 5.0km was set up along the direction of NW-SE.

(2) Results

Fig.II-2-37 shows the pseudo-sections.

In this area, the apparent resistivity value ranges between 164 ~ 2550Ωm, and average is about 795Ωm. Low resistibity is distributed at the shallow part, and shows pants-legs shape at the deeper part. Resistivitiy shows slightly high value at the deep part in the southeast on the line. Low resistivity is recognized at the deep part of the center part on the line. The center of this anomaly is located at n=5 around the stations 26 to 30.

The chargeability value ranges between 3.1 ~ 9.6mV/V, and average is about 5.5mV/V. Slightly high chargeability is distributed around the stations 20 to 28.

The maximum value of metal factor is 3.

(3) 2-D analysis

Figs.II-2-38 shows the 2-D analysis sections.

The analyzed resistivity value ranges between 53 ~ 22kΩm, and average is 2080Ωm. Low resistivity zone corresponding to Quaternary sediments is distributed at the shallow part. Low resistivity is also recognized at the deep part around the stations 26 to 32.

The analyzed chargeability value ranges between 2.1 ~ 15.9mV/V, and average is 7.5mV/V. Slightly high chargeability is distributed at the deep part around the stations 8 to 14 and the stations 36 to 42.

The maximum value of metal factor is 9. No remarkable IP anomaly is recognized.

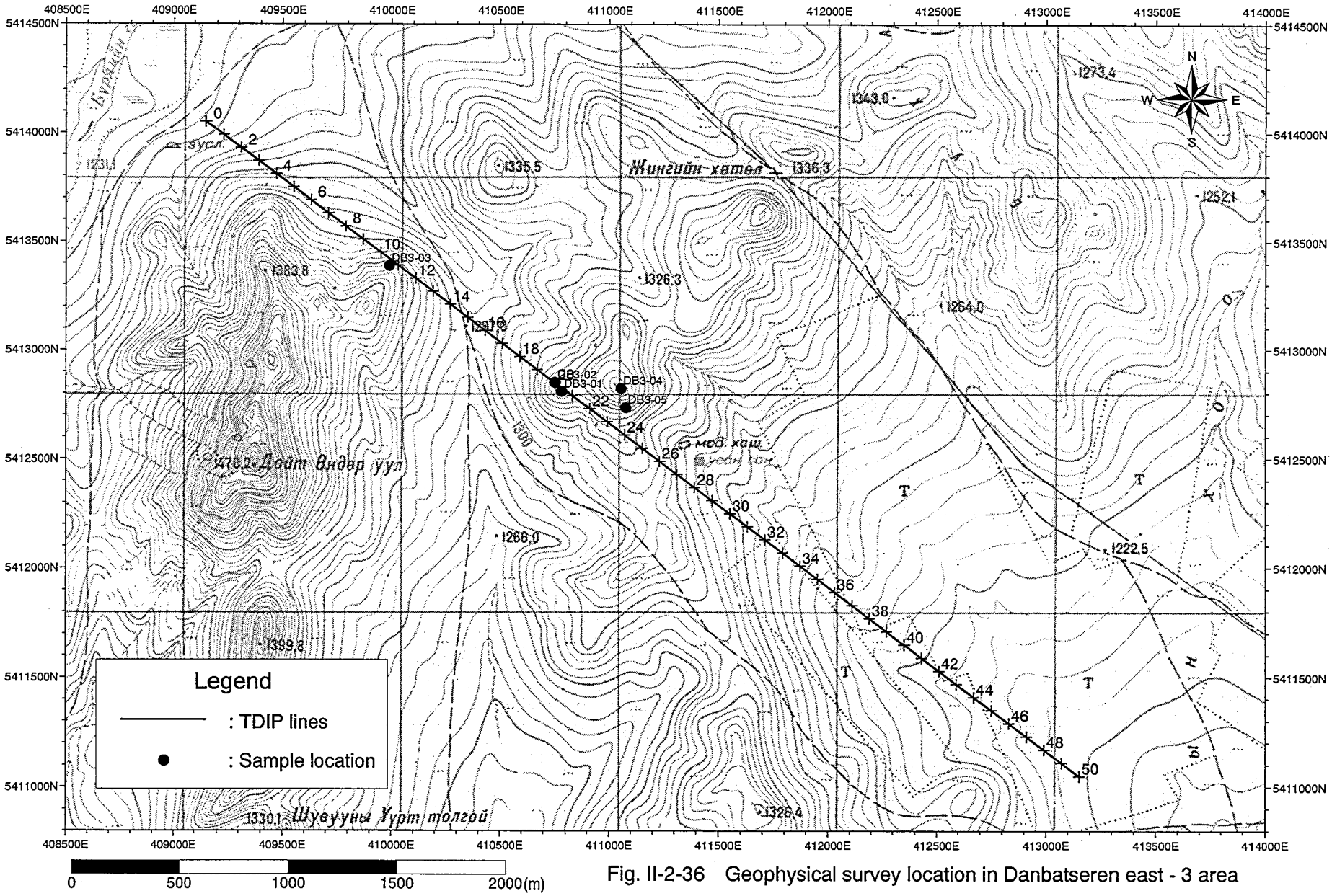

Fig. II-2-36 Geophysical survey location in Danbatseren east - 3 area

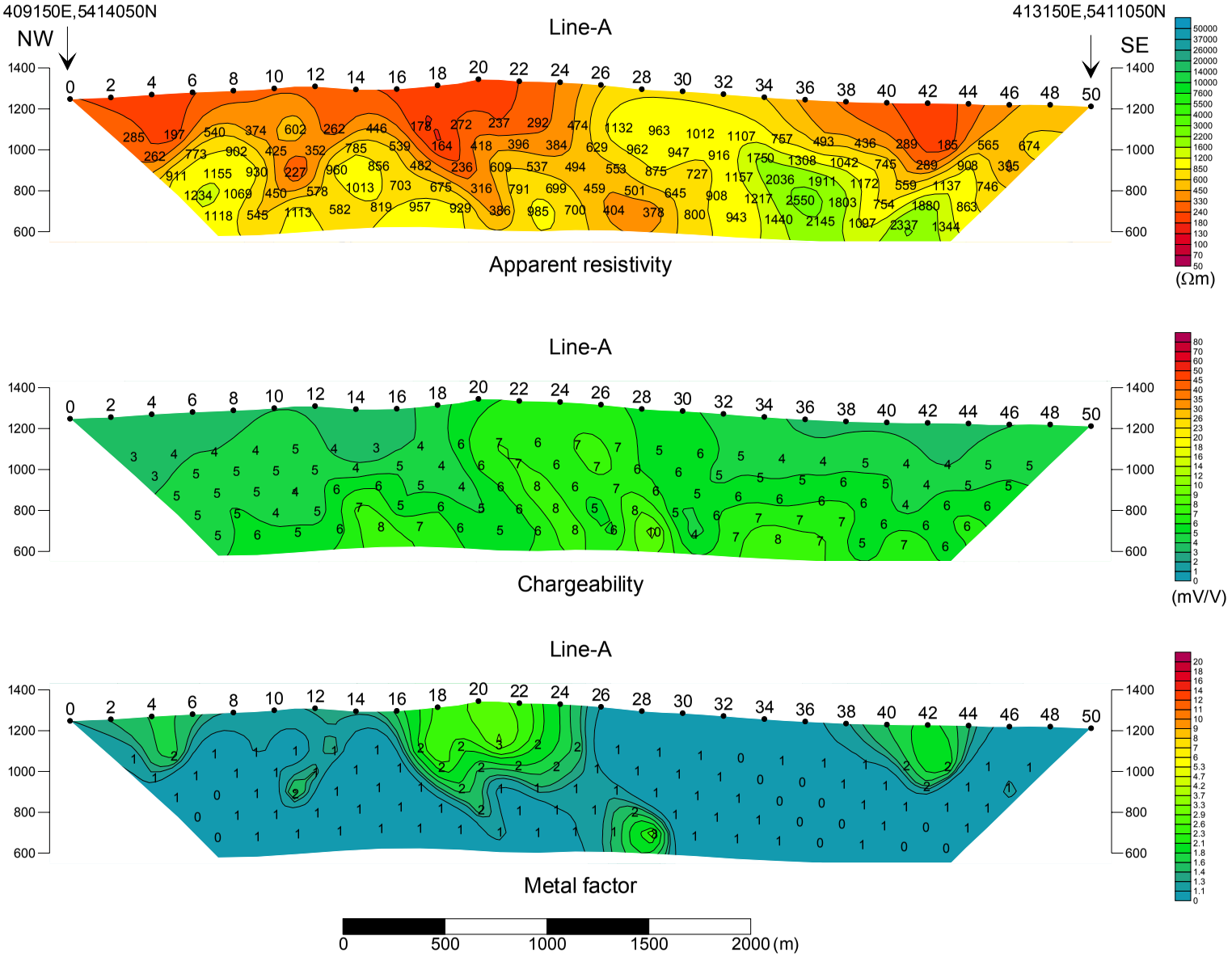

Fig. II-2-37 TDIP pseudo-sections in Danbatseren east - 3 area

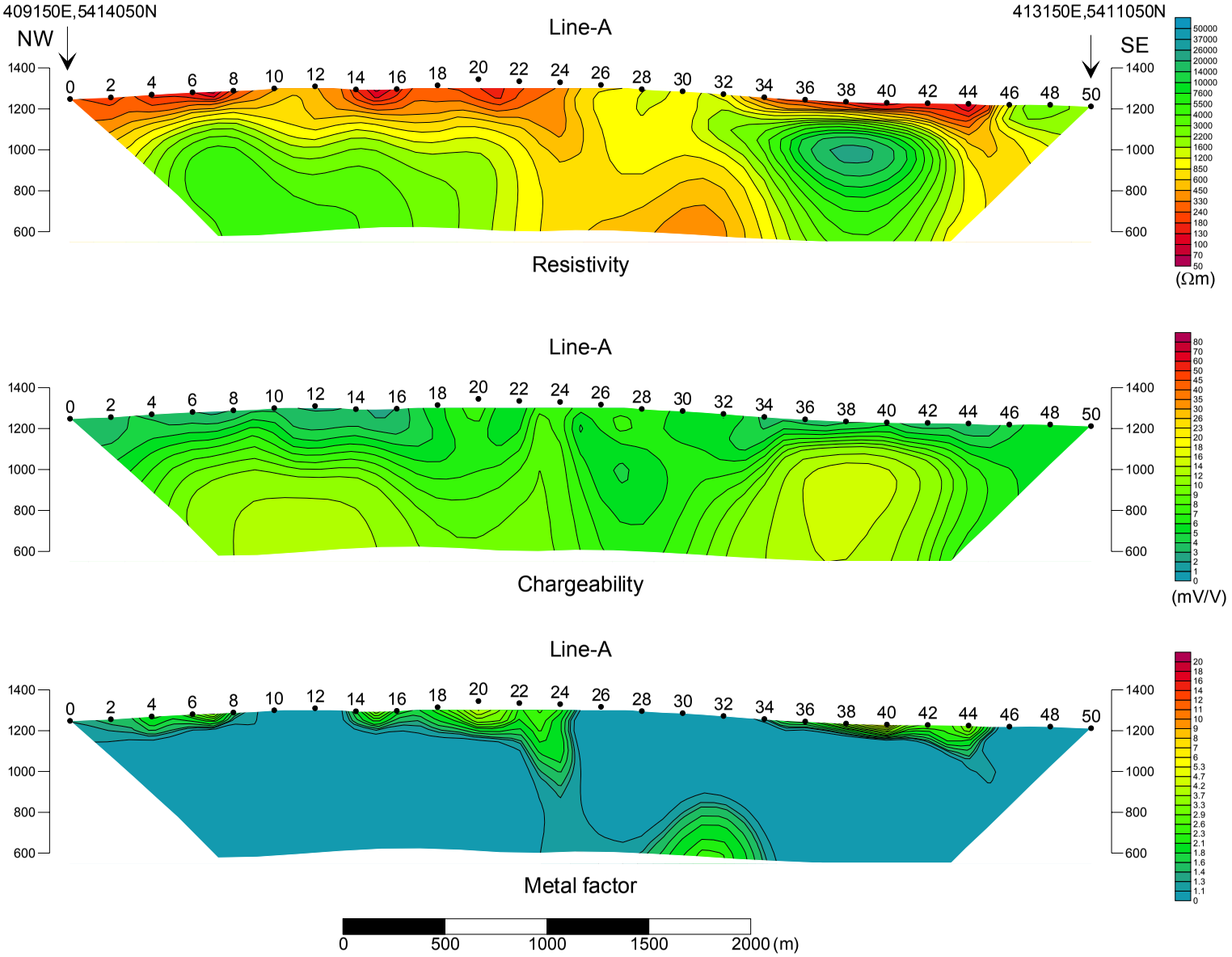

Fig. II-2-38　2D analysis sections in Danbatseren east - 3 area

2-5-5 Danbatseren east-4 area

(1) Lines location

Fig.II-2-39 shows the location of TDIP lines. In this area, 2 lines of 3.0km were set up along N90°E.

(2) Results

Fig.II-2-40 shows the pseudo-sections.

In this area, the apparent resistivity value ranges between 78 ~ 3034Ωm, and average is about 607Ωm. Low resistibity is distributed in the west of the line A and in allover the line B. High resistivity is recognized in the east of the line A.

The chargeability value ranges between 1.6 ~ 7.6mV/V, and average is about 4.0mV/V. No remarkable chargeability anomaly is recognized.

The maximum value of metal factor is 6.

(3) 2-D analysis

Fig.II-2-41 shows the 2-D analysis sections.

The analyzed resistivity value ranges between 13 ~ 16kΩm, and average is 2379Ωm. Low resistivity zone corresponding to Quaternary sediments is distributed at the shallow part. Most part of this area is occupied by a farm, therefore, the value of resistivity at the shallow part is less than that of the other area. Low resistivity is also recognized at the deep part in the west of the area.

The analyzed chargeability value ranges between 0.2 ~ 7.0mV/V and average is 4.0mV/V. No remarkable high chargeability such as to indicate mineralization is recognized.

The maximum value of metal factor is 18. High metal factor zone is distributed limitedly at the shallow part. It is considered to be caused by extremely low resistivity.

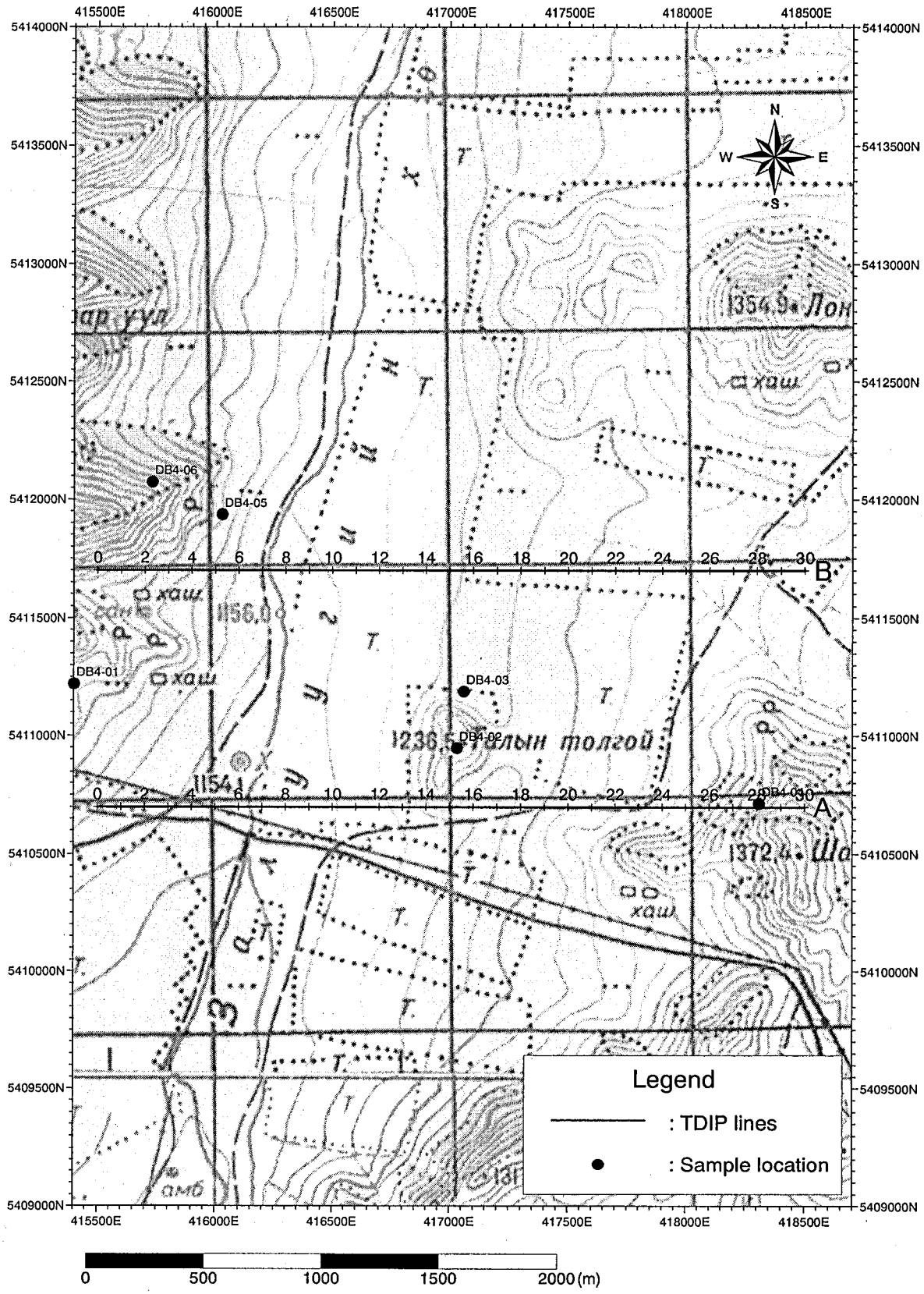
415500E
416000E
416500E
417000E
417500E
418000E
418500E
5414000N
5413500N
5413000N
5412500N
5412000N
5411500N
5411000N
5410500N
5410000N
5409500N
5409000N
N
W
E
S
DB4-06
DB4-05
DB4-01
DB4-03
DB4-02
DB4-04
A
B
0 2 4 6 8 10 12 14 16 18 20 22 24 26 28 30
Legend
: TDIP lines
: Sample location
0 500 1000 1500 2000 (m)

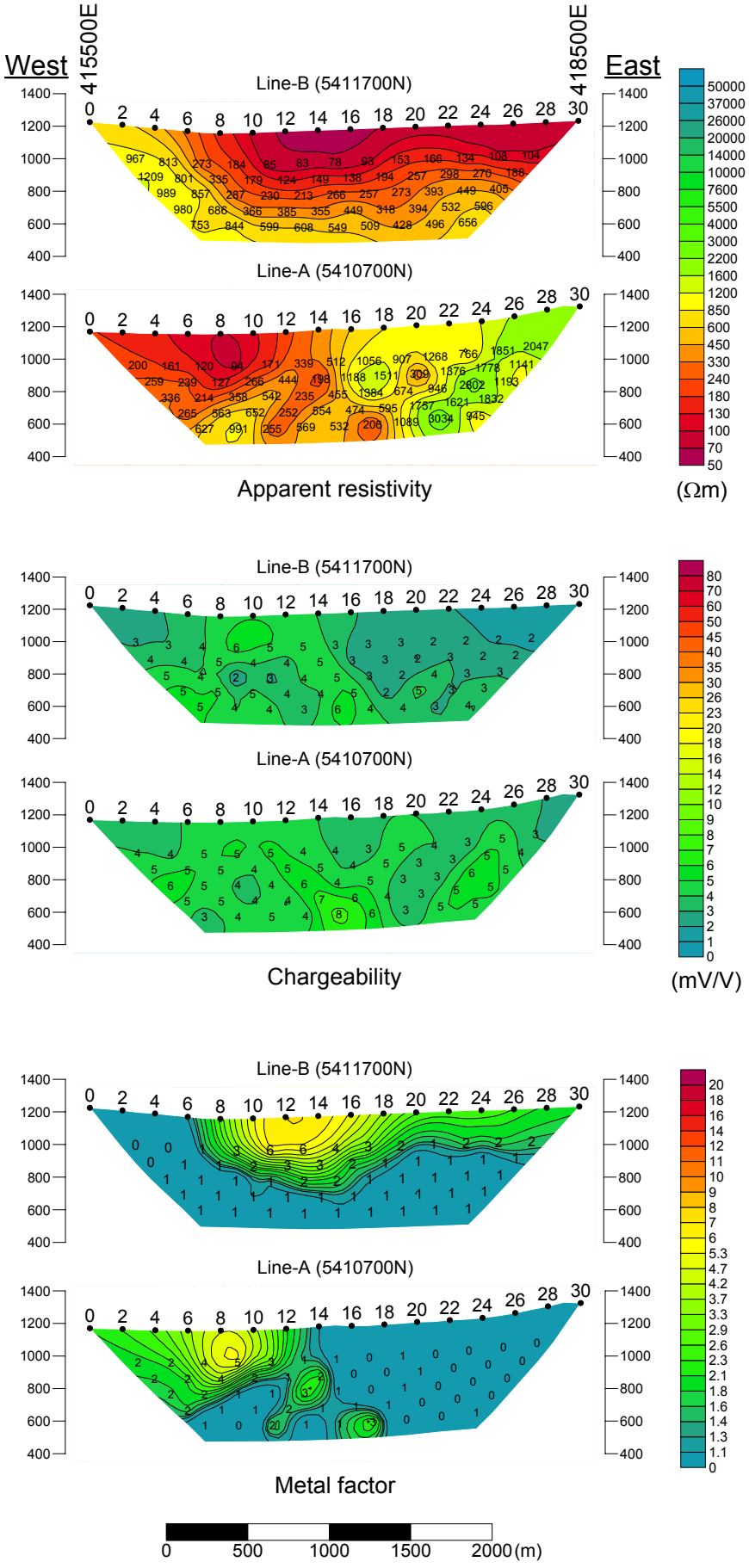

Fig. II-2-40 TDIP pseudo-sections in Danbatseren east - 4 area

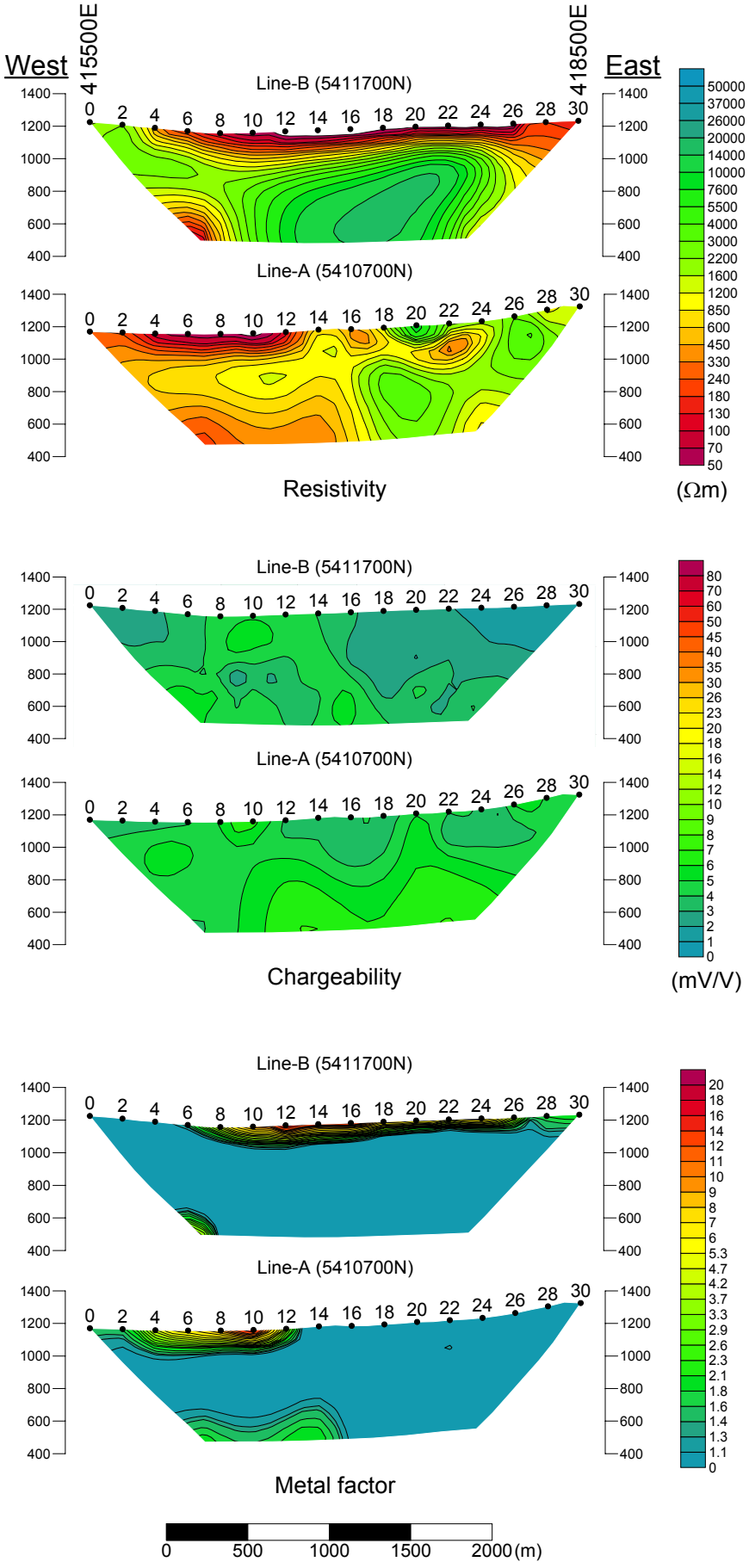

Fig. II-2-41 2D analysis sections in Danbatseren east - 4 area

2-5-6 Tsagaan chuluut west area

(1) Lines location

Fig.II-2-42 shows the location of TDIP lines. In this area, 1 line of 2.4km were set up along N0°E.

(2) Results

Fig.II-2-43 shows the pseudo-sections.

In this area, the apparent resistivity value ranges between 117 ~ 713Ωm, and average is about 276Ωm. Low resistibity is distributed allover.

The chargeability value ranges between 2.1 ~ 6.7mV/V, and average is about 4.2mV/V. No remarkable chargeability anomaly is recognized.

The maximum value of metal factor is 3.

(3) 2-D analysis

Fig.II-2-44 shows the 2-D analysis sections.

The analyzed resistivity value ranges between 52 ~ 945Ωm, and average is 348Ωm. Low resistivity is distributed allover. Extremely low resistivity is recognized at the shallow part. Around the stations 12 to 18, low resistivity zone continues to deeper part.

The analyzed chargeability value ranges between 2.0 ~ 8.8mV/V and average is 4.9mV/V. Slightly high chargeability is recognized at the depth of 300m around the center of the line.

The maximum value of metal factor is 6.3. Slightly high metal factor zone is distributed at the high chargeability zone. It is possible to reflect weak mineralization accompanied by intrusive rock.

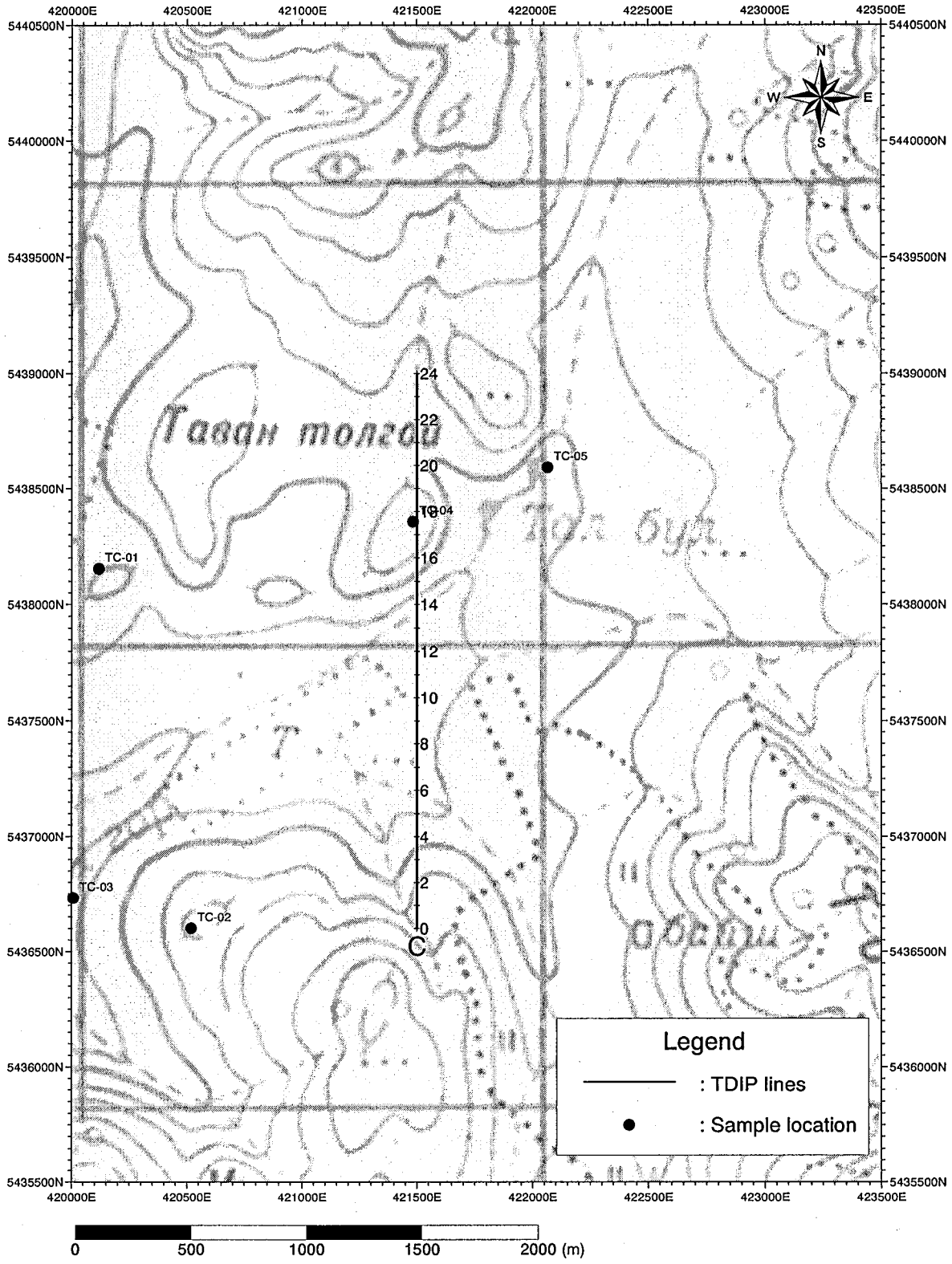

Fig. II-2-42 Geophysical survey location in Tsagaan chuluut west area

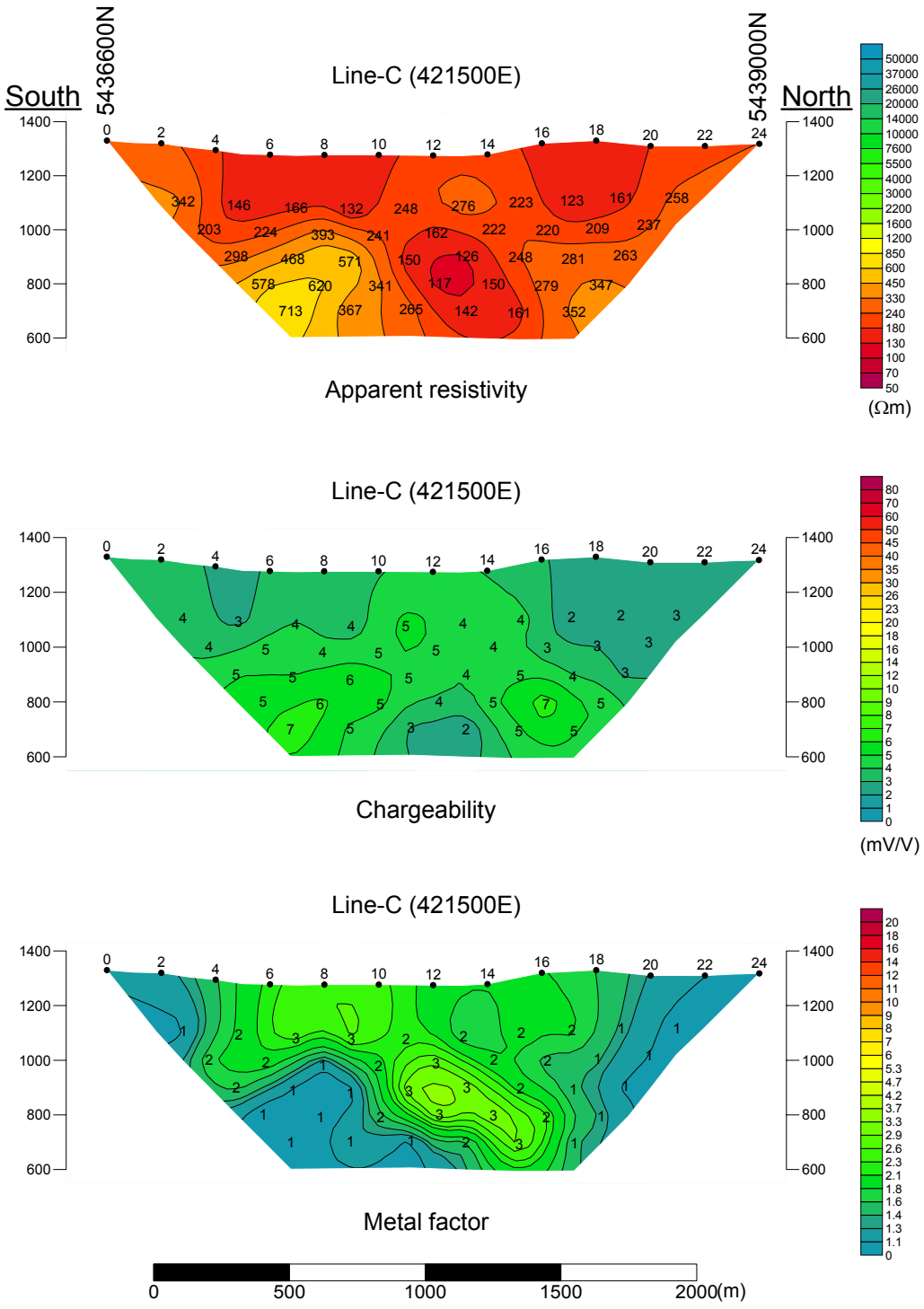

Fig. II-2-43　TDIP pseudo-sections in Tsagaan chuluut west area

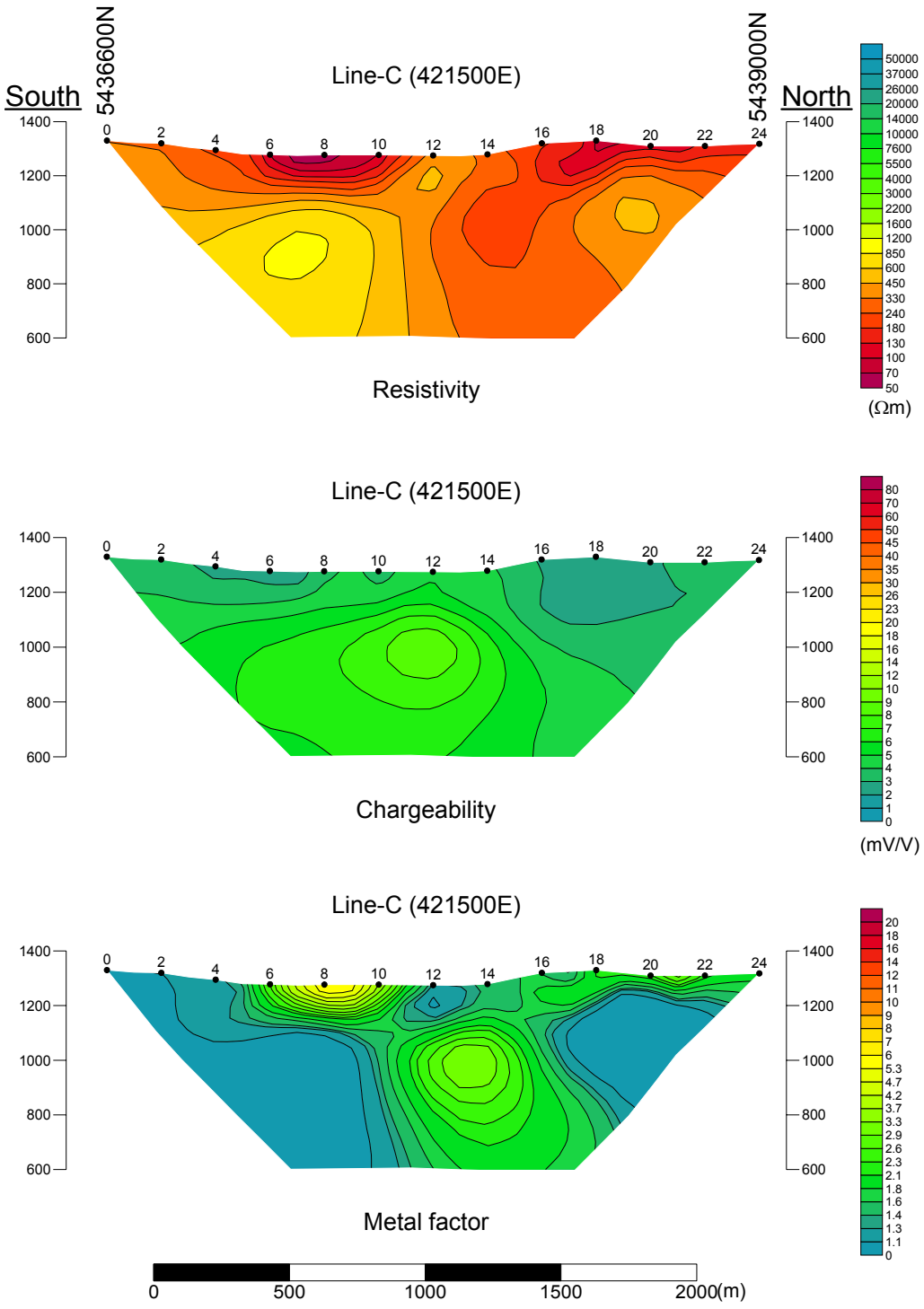

Fig. II-2-44　2D analysis sections in Tsagaan chuluut west area

2-5-7 Electrical measurements of rock samples

Representative rock samples from the survey area were analyzed. Samples are consist of 68 outcrops and 25 core samples.

In general, resistivity and IP measurements in rocks may not reflect in a direct way the intrinsic resistivity or chargeability because of different degree of alteration and water content over the survey area, however clear ideas can be obtained related to the relative variations between rocks units and mineralization.

(1) Measurement method

Measurement of the electrical properties of rock samples, such as resistivity and chargeability were carried out on some samples selected from the survey area. The rock samples were formed into cylindrical or cubic shape and thereafter, soaked into water for a reasonable amount of days but not less than 48 hours. Apparent resistivities as well as chargeability values were measured according to the IP time domain procedures in the laboratory. For this purpose, it was used a Lab Downhole Transmitter LDT-10 made by Zonge. During the determinations of the resistivity and chargeability values, the following formulas were utilized:

For Resistivity:

$$\rho = \frac{A}{L} \times \frac{V_p}{I},$$

where ρ is resistivity (Ωm), A the section of the sample (m^2), L the length of the rock sample (m), V_p the voltage (V) and I the current (A).

For Chargeability:

$$M = \frac{1.87}{V_p} \times \int_{t1}^{t2} V_s dT,$$

where M is the chargeability(mV/V), V_p the primary voltage (V), V_s the secondary voltage (mV), dT the sampling interval (sec), $t1$ the off-time voltage 450msec and $t2$ the off-time voltage 1,100msec.

(2) Results

Electrical properties of rock samples from outcroppings and core drillings were measured in the laboratory. Their results are indicated in Tables II-2-4 and II-2-5. Figs.II-2-45 and II-2-46 show correlation between chargeability and resistivity. Fig.II-2-47 shows comparison of the core sample measurement results with TDIP sections.

The resistivity value of core samples ranges from 195.9 to 14.5kΩm, and the average value is 3800Ωm. The chargeability value of core samples ranges from 1.3 to 135.6mV/V, and the average

value is 14.7mV/V. The resistivity of diorite and granodiorite show high value above 1000Ωm generally, while that of tuff shows wide range of value from 280 to 7000Ωm. The samples of No. 18 and 22 which are diorite and granodiorite respectively show low resistivity from 200 to 300Ωm. It's caused by veinlet of pyrite or chalcopyrite.

It is considered generally that chargeability is caused by sulfide. Sulfide is recognized in almost all samples, but the samples from Mogoin gol area show less chargeability than that from Zuukhiin gol area. According to Fig.II-2-47, chargeability of samples has a good correlation with the analyzed chargeability and also with the grade of sulfur, therefore chargeability of samples shows various value depending on the amount of sulfide. The sample of No.18 shows extremely high chargeability of 135.6mV/V caused by pyrite veinlet.

According to Fig.II-2-45, all rocks show negative correlation between chargeability and resistivity. Pyrite and chalcopyrite showing high chargeability are also good conductor, therfore if the amout of pyrite or chalcopyrite increase, chargeability becomes high and resistivity low.

The resistivity value of outcrop samples ranges from 120.6 to 10.9kΩm and the average value is 3100Ωm. The chargeability value of those ranges from 0.0 to 8.5mV/V and the average value is 3.0mV/V. Many samples show high resistivity over 1000Ωm, some samples of andesite, granodiorite and tuff show low resitivity. The range of resistivity of granodiorite and granodiorite porphyry is narrower than that of other rocks, limited from 500 to 2500Ωm. According to Fig.II-2-46, the data of andesite, granodiorite porphyry and syenite show positive correlation, and that of rhyolite and rhyolite porphyry show negative correlation.

Table II-2-4 Resistivity and chargeability of core samples

Ser. No.	Hole No.	Area	Sampling depth		Rock Name	Geological Unit	Description	Resistivity	Chargeability
			from	to				(Ωm)	(mV/V)
1	MJME-M3	Mogoin gol	99.80	99.90	oxidized crystalline tuff	αBtfP2	greenish grey, weakly pyrite-disseminated, oxidized, quartz-sericite alteration.	4302.9	4.0
2	MJME-M3	Mogoin gol	201.90	202.00	silicified tuff	αBtfP2	grey, pyrite-disseminated, quartz-sericite alteration.	1158.5	4.7
3	MJME-M3	Mogoin gol	288.00	288.10	silicified tuff	αBtfP2	grey, pyrite-disseminated and filmed, quartz-sericite alteration.	280.0	6.6
4	MJME-M3	Mogoin gol	381.60	381.80	silicified tuff	αBtfP2	grey, strong pyrite-dissemination and veinlets, strong quartz-sericite, chlorite film in fractures.	1262.4	30.0
5	MJME-M3	Mogoin gol	481.60	481.70	crystalline tuff	αBtfP2	grey, pyrite-dissemination and films.	634.4	3.3
6	MJME-M4	Mogoin gol	103.15	103.25	silicified tuff	αBtfP2	grey to dark grey, silicified vein, chlorite-epidote veinlets.	977.3	2.4
7	MJME-M4	Mogoin gol	200.00	200.10	silicified tuff	αBtfP2	dark brownish grey, pyrite-dissemination, epidote-calcite veins.	728.9	2.5
8	MJME-M4	Mogoin gol	300.00	300.10	silicified tuff	αBtfP2	dark grey, weak pyrite-dissemination, silicified veins.	7157.1	2.7
9	MJME-M4	Mogoin gol	403.00	403.10	silicified tuff	αBtfP2	grey, pyrite-dissemination and veinlets, quartz veinlets.	1276.6	3.1
10	MJME-M4	Mogoin gol	500.60	500.70	silicified tuff	αBtfP2	grey, pyrite-dissemination, quartz veinlets, silicified veinlets.	1623.6	1.6
11	MJME-Z1	Zuukhiin gol	100.70	100.80	altered granodiorite	γδ2T1s	quartz-sericite-chlorite, pyrite-cp-dissemination., quartz-pyrite-vein	1077.2	12.8
12	MJME-Z1	Zuukhiin gol	199.95	200.05	altered granodiorite	γδ2T1s	quartz-sericite-chlorite, pyrite-chalcopyrite-dissemination.	2052.4	12.7
13	MJME-Z1	Zuukhiin gol	302.05	302.15	granodiorite	γδ2T1s	light grey, chalcopyrite-vein	3916.3	6.8
14	MJME-Z1	Zuukhiin gol	400.10	400.20	granodiorite	γδ2T1s	light grey pyrite-chalcopyrite-vein, heterogeneous, porphyritic.	9379.2	6.2
15	MJME-Z1	Zuukhiin gol	500.00	500.10	granodiorite	γδ2T1s	grey, chalcopyrite-pyrite dissemination.	7919.2	2.5
16	MJME-Z2	Zuukhiin gol	100.45	100.55	pinkish altered granodiorite	γδ2T1s	pinkish brown, calcite-veinlets, chlorite, epidote veinlets.	1205.8	8.5
17	MJME-Z2	Zuukhiin gol	199.85	199.95	med. Gr. Diorite	δ3T1s	grey, chalcopyrite pyrite dissemination and spots, epidote veinlets.	6801.7	10.6
18	MJME-Z2	Zuukhiin gol	299.05	299.15	micro diorite	δ3T1s	dark grey, pyrite-vein, pyrite-chalcopyrite-dissemination.	312.4	135.6
19	MJME-Z2	Zuukhiin gol	400.00	400.10	micro diorite	δ3T1s	dark grey, pyrite-vein, pyrite-chalcopyrite-dissemination, pyrite-chalcopyrite veinlets.	5219.4	16.4
20	MJME-Z2	Zuukhiin gol	500.00	500.10	med. gr. Diorite	δ3T1s	grey, chalcopyrite-vein and dissemination	6447.7	12.4
21	MJME-Z3	Zuukhiin gol	100.25	100.35	silicified granodiorite	γδ2T1s	greenish grey, pyrite-chalcopyrite-dissemination, pyrite veinlets.	14450.6	4.3
22	MJME-Z3	Zuukhiin gol	199.30	199.40	altered granodiorite	γδ2T1s	light brownish grey, pyrite-chalcopyrite dissemination, calcite veinlets	195.9	66.9
23	MJME-Z3	Zuukhiin gol	500.50	500.60	altered granodiorite	γδ2T1s	grey, chalcopyrite-pyrite-dissemination.	10311.7	6.1
24	MJME-Z3	Zuukhiin gol	400.20	400.30	green altered granodiorite	γδ2T1s	greenish grey, pyrite-chalcopyrite-dissemination.	4949.4	1.3
25	MJME-Z3	Zuukhiin gol	499.80	499.90	green altered granodiorite	γδ2T1s	irregular-quartz-veins, pyrite-chalcopyrite-dissemination.	1050.7	3.6

Table II-2-5 Resistivity and chargeability of outcrop samples

Ser. No.	Sample No.	Area	Coordinates		Rock Name	Geological Unit	Description	Resistivity (Ωm)	Chargeability (mV/V)
			N	E					
26	TC-01	Tsagaan chuluut west	5438153	420117	andesite	T2-J1mg	brownish grey.	237.0	1.4
27	TC-02	Tsagaan chuluut west	5436601	420518	andesitic tuff	T2-J1mg	dark brownish grey, coarse tuff to lapilli tuff.	543.6	1.4
28	TC-03	Tsagaan chuluut west	5436733	420007	micro-syenite	λJ	brown.	410.8	1.5
29	TC-04	Tsagaan chuluut west	5438356	421483	andesite	T2-J1mg	brownish grey, plagioclase porphyritic.	8708.8	6.7
30	TC-05	Tsagaan chuluut west	5438592	422064	andesite	T2-J1mg	dark brownish grey, hornblende porphyritic.	120.6	1.0
31	KG-01	Khujiriin gol	5441690	394920	diorite porphyry	δ1Tis	grey, heterogeneous, plagioclase and hornblende porphyritic.	1829.0	5.6
32	KG-02	Khujiriin gol	5441821	394847	syenite porphyry	ξ3Tis	pink, plagioclase and biotite porphyritic.	2828.3	4.9
33	KG-03	Khujiriin gol	5442052	394918	micro diorite	δ1Tis	grey, weak chloritization.	7950.1	4.8
34	KG-04	Khujiriin gol	5443412	394921	granite	γ2Tis	light brown, fine grained, pyrite dissemination.	1719.9	4.8
35	KG-05	Khujiriin gol	5442500	394900	quartz vein	γιι3Tis	with druse.	4591.8	0.7
36	ZG-01	Zuukhiin gol	5450500	445215	aprite	γιι3Tis	alaskite? Fine grained, biotite granite? Light pinkish grey, chlorite films.	5917.2	1.7
37	ZG-02	Zuukhiin gol	5450648	445209	granite	T2-J1mg	light brownish grey, fine grained.	2620.8	1.0
38	ZG-03	Zuukhiin gol	5450878	445200	andesitic fine tuff	dyke	light brownish grey, fine grained, pyrite dissemination.	1166.3	4.6
39	ZG-04	Zuukhiin gol	5451766	445207	andesite	γδ2Tis	greenish grey.	1871.7	3.9
40	ZG-05	Zuukhiin gol	5452015	445147	granodiorite	δ1Tis	light brownish grey.	2537.6	5.0
41	ZG-06	Zuukhiin gol	5452490	445238	micro diorite porphyry	γδ3Tis	brown, fine grained.	891.7	3.7
42	ZG-07	Zuukhiin gol	5450275	444232	diorite porphyry	δ1Tis	grey, heterogeneous, porphyritic.	2841.7	3.5
43	ZG-08	Zuukhiin gol	5451056	444206	aprite	γιι3Tis	greenish white, strong epidotization.	8841.4	2.2
44	ZG-09	Zuukhiin gol	5451084	444195	aprite	ξ3Tis	pink, fine grained, syenitic.	7497.1	2.1
45	ZG-10	Zuukhiin gol	5451257	444240	aprite	ξ3Tis	light greenish grey, fine grained.	524.1	1.9
46	ZG-11	Zuukhiin gol	5450572	445692	aprite	ξ3Tis	light brown, fine grained, syenitic.	2150.4	3.2
47	ZG-12	Zuukhiin gol	5450672	445710	micro diorite	δ1Tis	light grey, heterogeneous.	568.6	2.8
48	ZG-13	Zuukhiin gol	5451421	445707	micro diorite	δ1Tis	grey, fine grained.	3030.3	4.7
49	ZG-14	Zuukhiin gol	5452999	445703	syenite	ξ3Tis	light brown, epidotization.	4526.8	2.8
50	ZG-15	Zuukhiin gol	5450252	446178	andesite	dyke	greenish grey, plagioclase porphyritic.	631.1	1.3
51	ZG-16	Zuukhiin gol	5452216	442226	granodiorite	γδ2Tis	light grey, medium grained, malachite films.	521.4	3.5
52	ZG-17	Zuukhiin gol	5452234	442234	granodiorite	γδ2Tis	pinkish grey, weak chlorite.	1755.4	2.3
53	ZG-18	Zuukhiin gol	5452299	442237	diorite porphyry	δ1Tis	dark grey, fine grained, heterogeneous, malachite spots.	1221.2	3.4
54	ZG-19	Zuukhiin gol	5452318	442215	granodiorite	γδ2Tis	pinkish grey, medium grained, malachite films and spots.	827.0	2.9
55	ZG-20	Zuukhiin gol	5453426	441097	syenite porphyry	ξ3Tis	pinkish brown, potassic feldspar porphyritic.	4897.2	2.6
56	ZG-21	Zuukhiin gol	5452840	441200	syenite porphyry	ξ3Tis	pinkish brown, potassic feldspar porphyritic.	2137.8	2.9
57	ZG-22	Zuukhiin gol	5452993	441205	syenite porphyry	ξ3Tis	pinkish brown, potassic feldspar porphyritic, malachite spots and films in quartz-hematite vein.	5792.6	2.8
58	ZG-23	Zuukhiin gol	5451040	444700	syenite and quartz vein	ξ3Tis	quartz vein in syenite, epidotization.	4407.9	1.9
59	ZG-24	Zuukhiin gol	5451040	444700	andesitic tuff and quartz vein	T2-J1mg	greenish grey, fine tuff.	674.3	1.8
60	ZG-25	Zuukhiin gol	5451543	443693	granodiorite	γδ2Tis	grey, medium grained, hornblende-biotite, sericite alteration.	1218.0	2.9
61	ZG-26	Zuukhiin gol	5451566	443666	granodiorite porphyry	γδ2Tis	pinkish grey, heterogeneous, sericite.	1246.2	3.7
62	ZG-27	Zuukhiin gol	5451587	443646	granodiorite	γδ2Tis	light grey, medium grained.	671.8	4.1
63	ZG-28	Zuukhiin gol	5451798	443660	granodiorite	γδ2Tis	light greenish grey, medium grained, heterogeneous.	1024.0	3.2
64	ZG-29	Zuukhiin gol	5453493	443712	diorite porphyry	γδ2Tis	grey, porphyritic.	1840.7	2.5
65	ZG-30	Zuukhiin gol	5451594	442827	granodiorite porphyry	γδ2Tis	light brown, porphyritic, biotite-hornblende.	1358.9	4.0
66	ZG-31	Zuukhiin gol	5451643	442831	granodiorite	γδ2Tis	light brown, medium grained, chloritization, malachite spots.	1846.7	3.2
67	ZG-32	Zuukhiin gol	5451828	442834	granodiorite porphyry	γδ2Tis	light brown, biotite-hornblende, quartz vein.	1548.3	4.3
68	ZG-33	Zuukhiin gol	5452062	442857	granodiorite porphyry	γδ2Tis	light greenish brown, hornblende-biotite, malachite vein and spots.	751.4	1.5
69	ZG-34	Zuukhiin gol	5452665	442680	granodiorite porphyry	γδ2Tis	light greenish brown, hornblende-biotite.	1225.9	2.9
70	DB1-01	Danbatseren east 1	5401297	426056	granodiorite porphyry	γδ2Tis	light greenish brown, hornblende-biotite, epidotization.	2426.2	3.3

continued to next page

Ser.	Sample	Area	Coordinates	Rock Name	Geological	Description	Resistivity	Chargeability

No.	No.		N	E		Unit		(Ωm)	(mV/V)
71	DB1-02	Danbatseren east 1	5401200	425400	rhyolite porphyry	αλtP1-2	light brownish white, quartz-potassic feldspar porphyritic.	4300.5	2.0
72	DB1-03	Danbatseren east 1	5401400	427014	rhyolite porphyry	αλtP1-2	light brownish white, quartz-potassic feldspar porphyritic.	2372.8	5.2
73	DB1-04	Danbatseren east 1	5401236	427507	rhyolite porphyry	αλtP1-2	light brownish white, quartz-potassic feldspar porphyritic.	1531.9	1.9
74	DB1-05	Danbatseren east 1	5402142	425508	rhyolite	αλtP1-2	pinkish brown.	910.9	6.6
75	DB1-06	Danbatseren east 1	5402187	425624	micro diorite	γδ2PZ1	grey, fine grained.	4706.6	4.7
76	DB1-07	Danbatseren east 1	5402171	426749	andesite	dyke	black grey, plagioclase porphyritic.	6559.0	3.6
77	DB1-08	Danbatseren east 1	5402210	427068	syenite porphyry	γδ2PZ1	brown, potassic feldspar porphyritic.	1611.8	5.1
78	DB1-09	Danbatseren east 1	5402246	427267	rhyolite porphyry	γδ2PZ1	light brown, sericitization, hematite.	935.1	8.5
79	DB3-01	Danbatseren east 3	5412810	410781	silicified rock	λJ	light brown, sericite-quartz, hematite, pyrite holes.	8018.6	1.8
80	DB3-02	Danbatseren east 3	5412851	410752	silicified rock	λJ	light brown, sericite-quartz, hematite, pyrite holes.	1644.7	1.3
81	DB3-03	Danbatseren east 3	5413388	409989	andesite	αλtP1-2	pinkish grey, plagioclase porphyritic.	4197.6	2.0
82	DB3-04	Danbatseren east 3	5412823	411053	silicified rock	λJ	light brown, sericite-quartz, hematite, pyrite holes.	6924.6	1.5
83	DB3-05	Danbatseren east 3	5412735	411075	silicified rock	λJ	light brown, sericite-quartz, hematite, pyrite holes.	8813.0	0.0
84	DB4-01	Danbatseren east 4	5411221	415401	sandy tuff	αλtP1-2	dark grey, clastic texture.	6651.7	1.2
85	DB4-02	Danbatseren east 4	5410948	417031	rhyolite	λJ	brown, potassic feldspar porphyritic.	2837.4	4.2
86	DB4-03	Danbatseren east 4	5411189	417060	rhyolite	λJ	brown, potassic feldspar porphyritic.	10869.6	1.5
87	DB4-04	Danbatseren east 4	5410715	418309	diorite	δ1Tis	grey, fine grained.	9330.2	1.5
88	DB4-05	Danbatseren east 4	5411936	416029	andesite	αλtP1-2	dark grey, aphanitic.	5624.8	1.0
89	DB4-06	Danbatseren east 4	5412075	415731	fine tuff	αλtP1-2	greenish grey.	2035.9	1.6
90	KG-6	Khujiriin gol	5442025	396428	granodiorite	γδ2Tis	grey, fractured, quartz veinlets with malachite films and spots.	832.8	3.1
91	KG-7	Khujiriin gol	5442025	396428	silicified rock	γδ2Tis	light brown, quartz veinlets with malachite spots.	1035.2	2.3
92	KG-8	Khujiriin gol	5442025	396428	silicified rock	γδ2Tis	light brown, strong silicified, granodiorite with malachite spots.	2781.0	3.8
93	KG-9	Khujiriin gol	5442025	396428	silicified rock	γδ2Tis	light brown, strong silicified, granodiorite with malachite spots.	6898.5	3.0

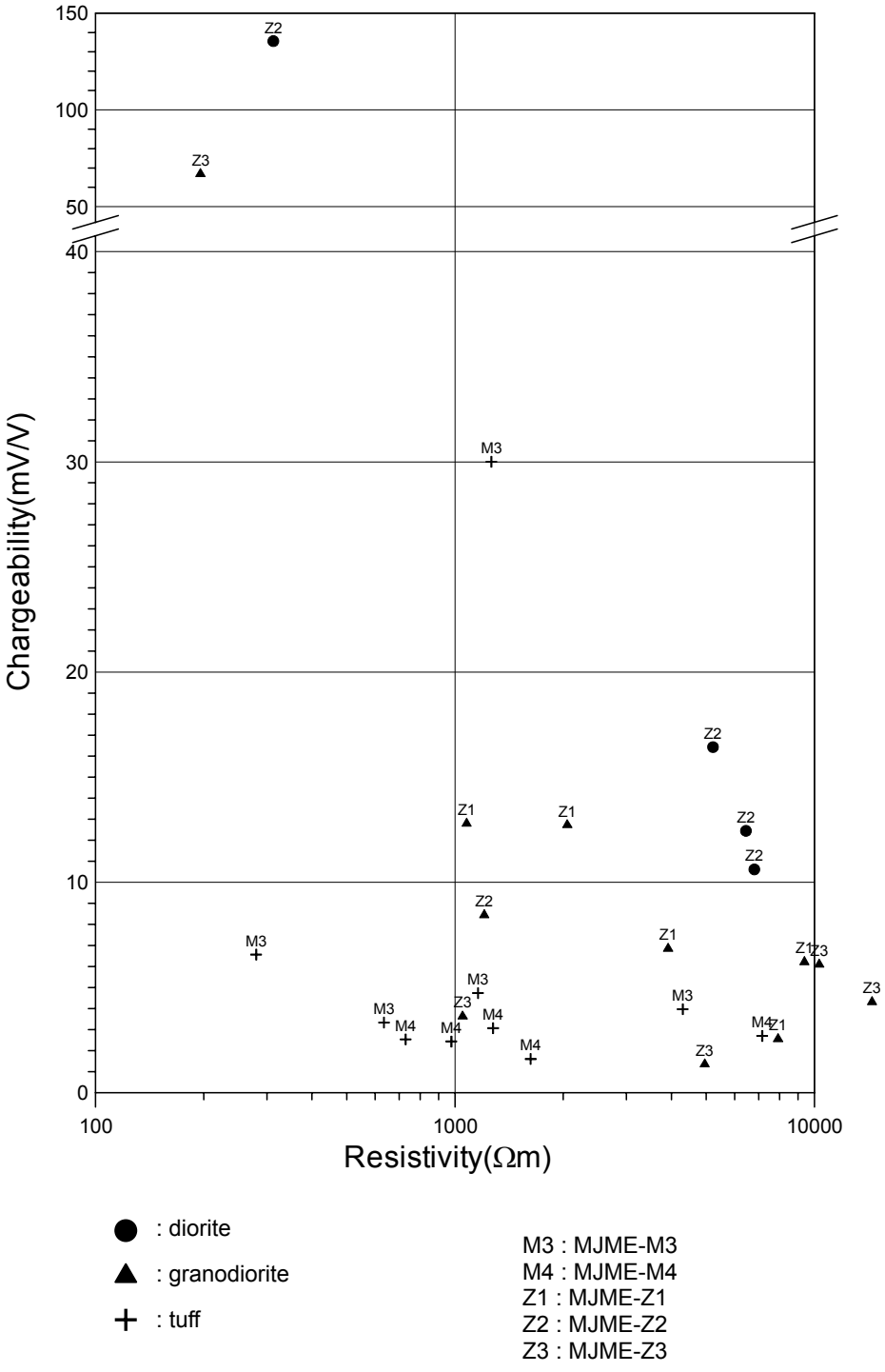

Fig. II-2-45　Correlation between chargeability and resistivity for core samples

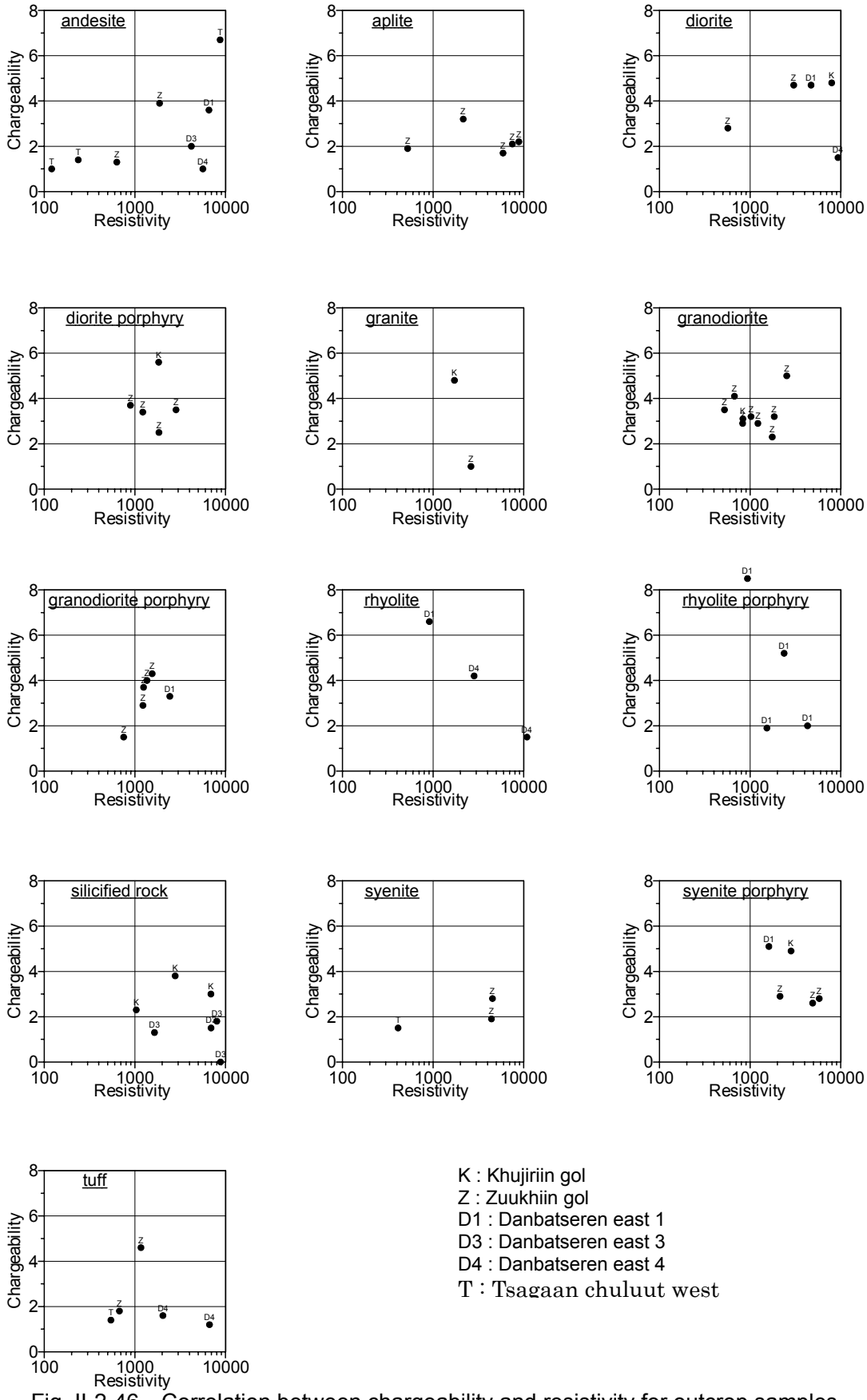

Fig. II-2-46 Correlation between chargeability and resistivity for outcrop samples

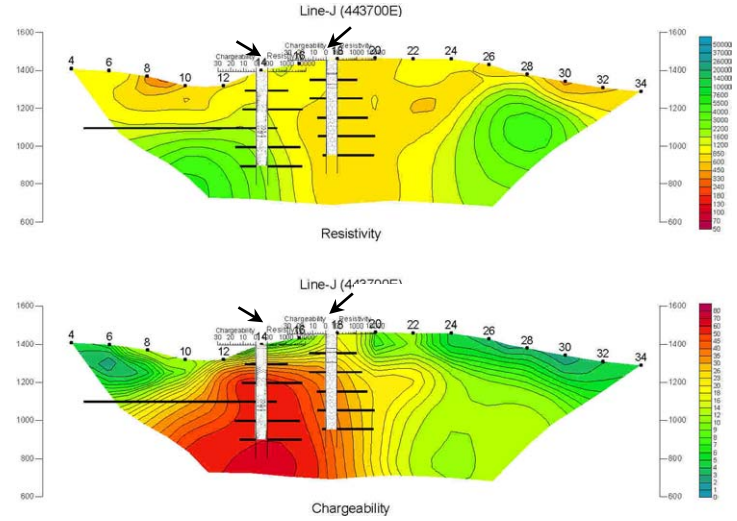

TDIP sections on the Line-J in Zuukhiin gol area

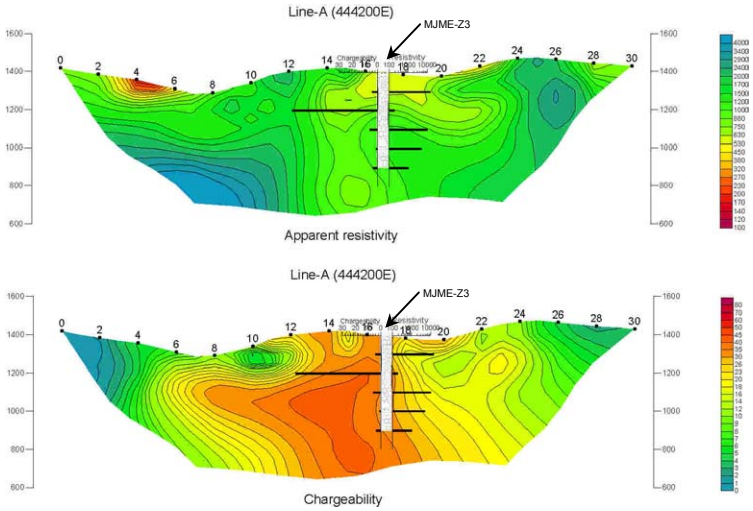

TDIP sections on the Line-A in Zuukhiin gol area

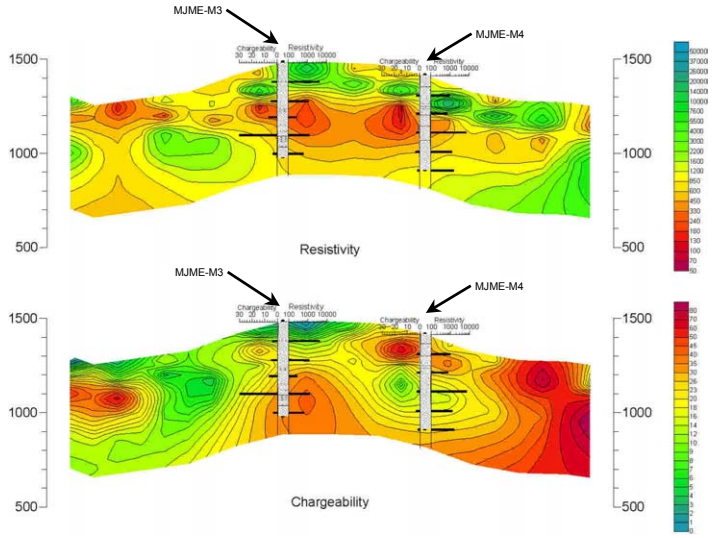

TDIP sections on the Line-4800N in Mogoin gol area

Fig.II-2-47 Comparison of the core sample measurement results with TDIP sections

2-6 Further Considerations

The results of the geophysical survey at Khujiriin gol area and Zuukhiin gol area are considered as follows.

2-6-1 Khujiriin gol area

Fig.II-2-48 shows compiled map of geophysical survey in Khujiriin gol area, indicating high resistivity zone over 1000Ωm, high chargeability zone over 6mV/V at the depth of 100m and low magnetic anomaly zone under 59700nT detected by the airborne magnetic survey. Judging from the chargeability value, there is little possibility of existence of porphyry copper ore in this area. According to fig.II-2-48, high resistivity is distributed around the quartz veinlet with copper recognized in the southern part of the area. Slightly high chargeability is distributed partially in this high resistivity zone. It is considered to reflect that some sulfide is accompanied by the quartz veinlet. This high resistibity zone shifts to north in deeper part, therefore the quartz veinlet is estimated to incline northward. High resistivity and high chargeability is also recognized in the northwestern part (northern edge of the line E) and in the northeastern part (station 22 to 24 on the line C).

The IP anomaly corresponding to the quartz veinlet is not clear because the dipole length is too long to detect veinlet with suitable resolution. It is considered generally that a range of anomaly distribution caused by veinlet is smaller than that by porphyry copper ore. Therefore, a detailed survey using shorter length dipole is effective to detect veinlet clearly.

Below the depth of 150m, high resistivity is dominant in the eastern part of the area, and resistivity structure changes on the east and west of the stream running through the eastern part of the area from north to south along the line B.

There is no clear relation between the IP anomaly and the low magnetic anomaly zone.

2-6-2 Zuukhiin gol area

Fig.II-2-49 shows compiled map of geophysical survey in Zuukhiin gol area, indicating low resistivity zone under 700Ωm, high chargeability zone over 20mV/V at the depth of 200m and low magnetic anomaly zone under 59400nT detected by the airborne magnetic survey.

In this area, geological, geophysical and drilling survey had been conducted previous to this project, and IP anomaly and mineralization had been recognized. In this survey, TDIP survey was carried out on 12 lines set up inside and outside of previous survey area in order to grasp the whole feature of the IP anomaly.

As the result of the survey, it was found that the IP anomaly extends eastward widely. At the depth of 200m, the range of high chargeability zone over 20mV/V extends 4km in E-W direction and 2km in N-S, and it is considered to reflect large scale mineralization. It seems that this high chargeability zone consists of three parts. According to the plane map at the depth of 200m, high chargeability zones over 30mV/V are recognized around the stations 10 to 18 on the lines F to I, the stations 20 to 28 on the lines G to F and the stations 12 to 18 on the lines L to K. Low resistivity zone is recognized surrounded by these high chargeability zones. According to the 2D analysis sections of lines K, F, J and A, low

resistivity is distributed continuously from shallow to deep part. Outcrop samples for electrical measurements gathered within this low resistivity zone are granodiorite and granodiorite porphyry, and some samples show low resistivity below 1000Ωm. The high chargeability zone corresponds to the area underlain by granite of Selenge Complex.

Drilling survey was conducted at the stations 14 and 18 on the line J and the station 17 on the line A. Fig.II-2-50 shows S, Fe and Cu grade of core samples corresponding to 2D analysis sections. There is a positive correlation between the grade of sulfur and chargeability, and it is considered that high chargeability reflects large amount of sulfide in this area. Metallic mineral such as iron and copper is thought to be a factor to decrease resistivity, but there is no remarkable correlation between the grade of iron or copper and resistivity. Not only metallic mineral but also water content, argillization and alteration can be a factor to decrease resistivity. Therefore, it is difficult to compare resistivity with the amount of metallic mineral simply.

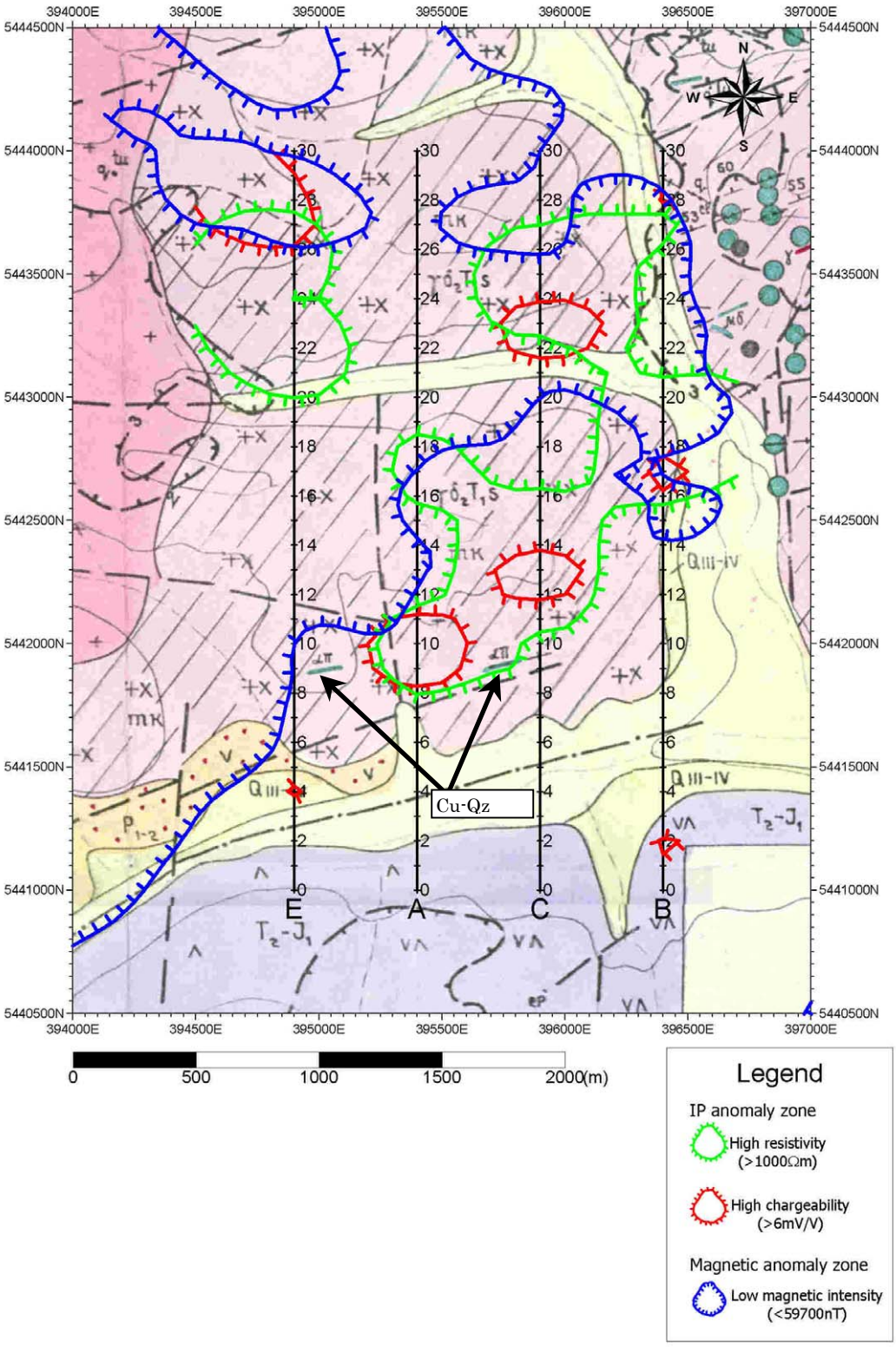

Fig. II-2-48 Compiled map of geophysical survey in Khujiriin gol area

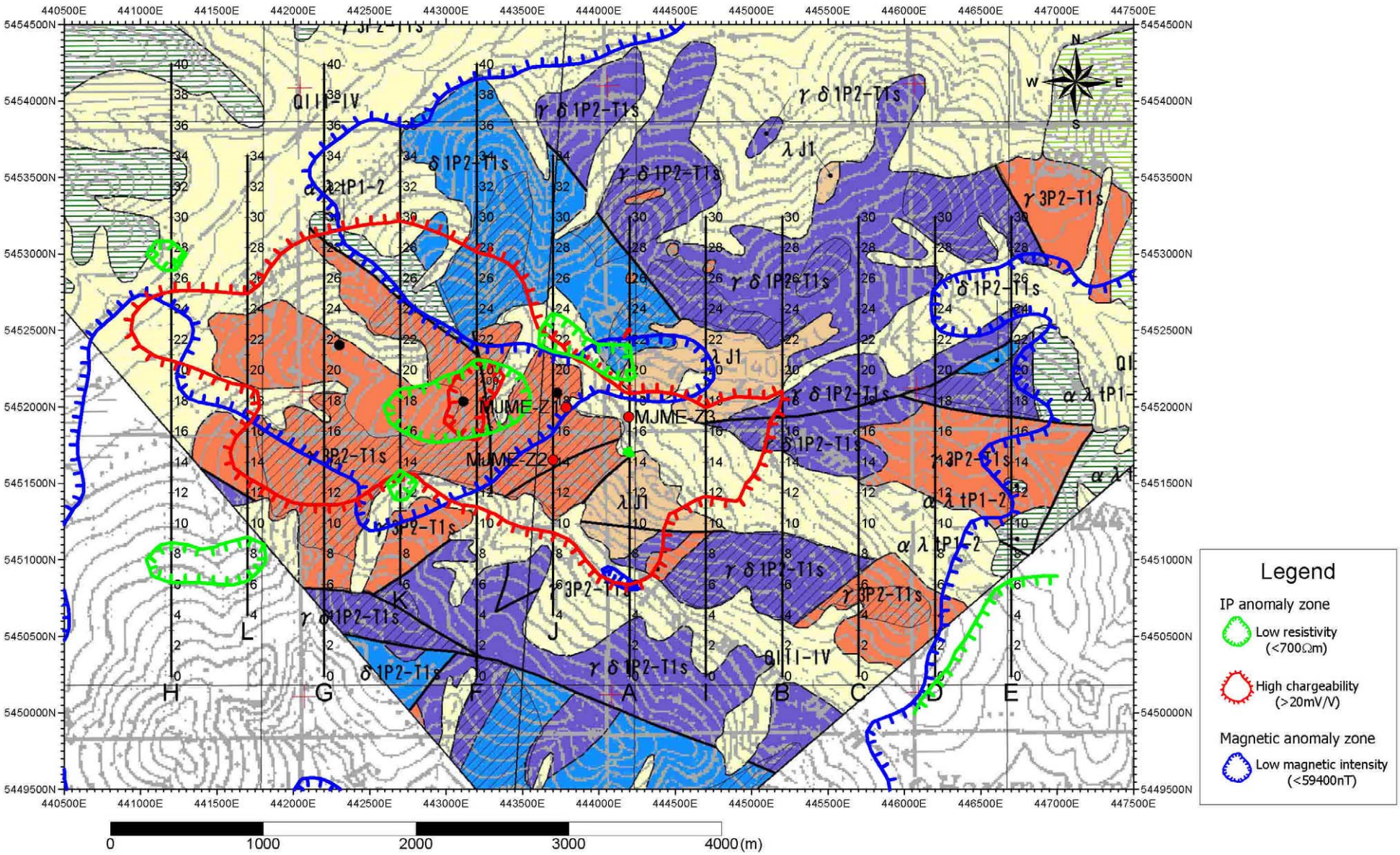

Fig. II-2-49 Compiled map of geophysical survey in Zuukhiin gol area

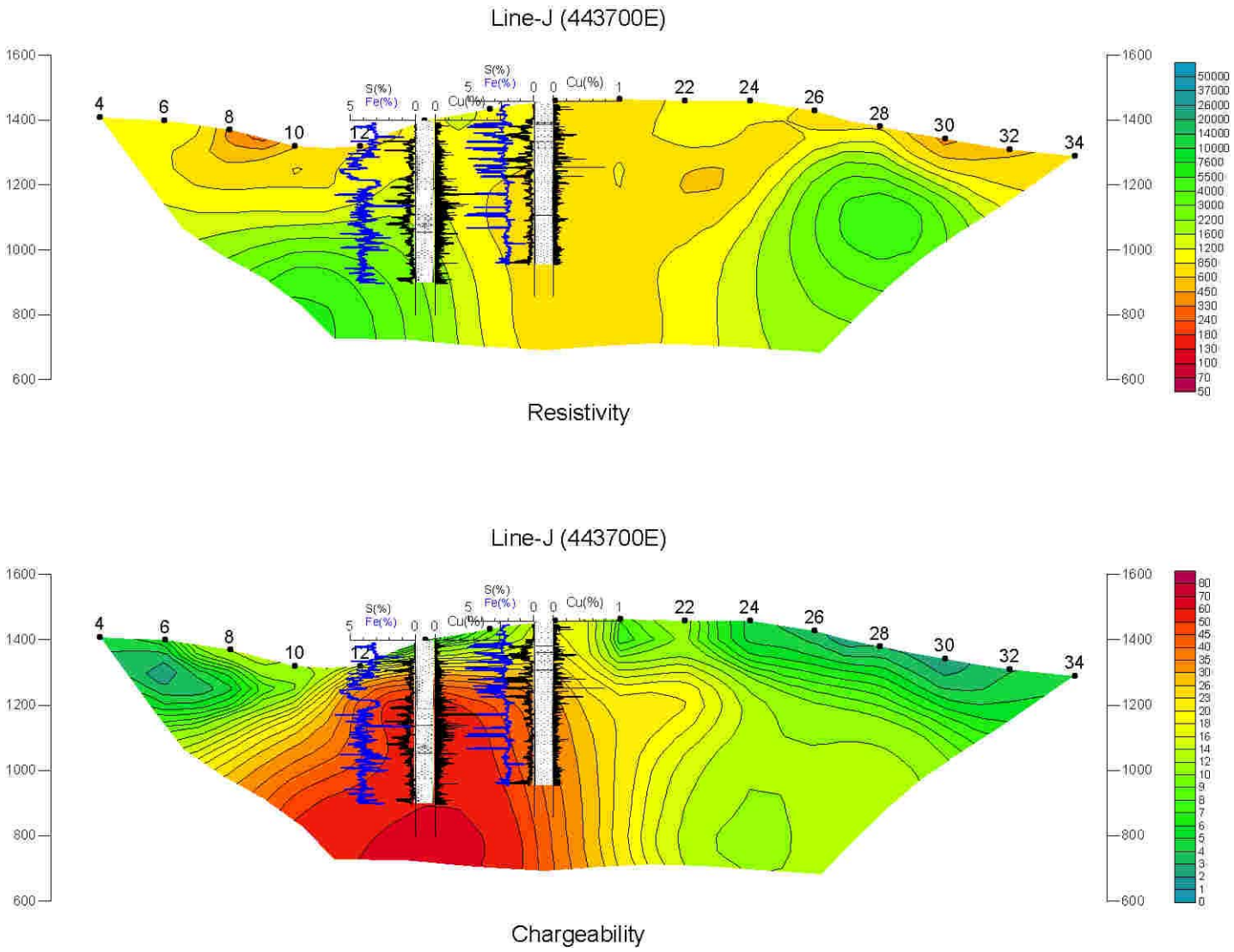

Fig. II-2-51 S, Fe and Cu grade of core samples corresponding to TDIP sections on the line A in Zuukhiin gol area

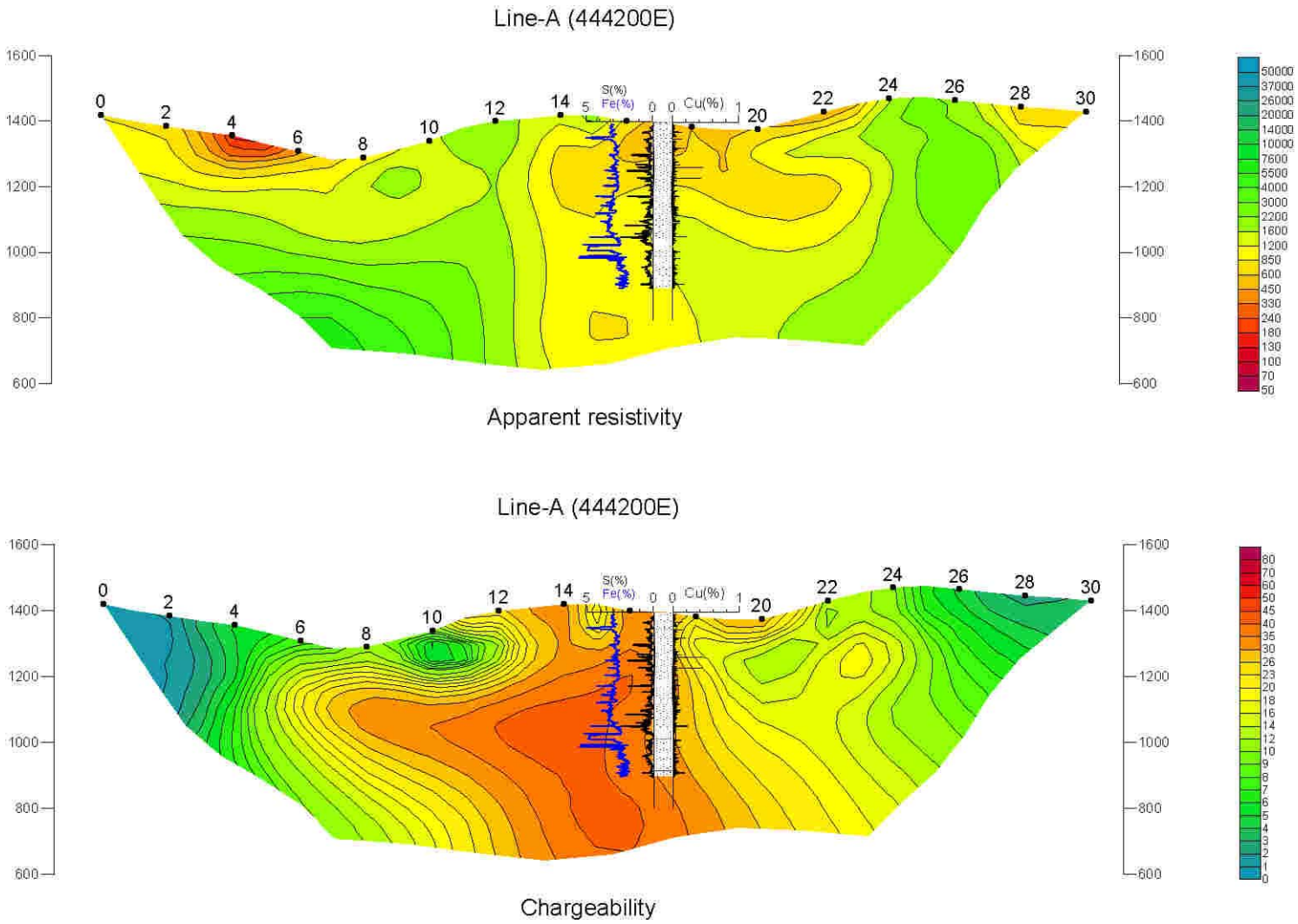

Fig. II-2-51 S, Fe and Cu grade of core samples corresponding to TDIP sections on the line A in Zuukhiin gol area